

LOCALIZED DEFECTS IN PBTE

VIA A

$\vec{k} \cdot \vec{\pi}$ -APW ENERGY BAND CALCULATION

by

NELSON DE JESUS PARADA

S.B., Instituto Tecnológico de Aeronáutica-Brazil
(1963)

M.S., Instituto Tecnológico de Aeronáutica-Brazil
(1965)

SUBMITTED IN PARTIAL FULFILLMENT OF THE
REQUIREMENTS FOR THE DEGREE OF
DOCTOR OF PHILOSOPHY

at the

MASSACHUSETTS INSTITUTE OF TECHNOLOGY

November, 1968, *i. e. Feb. 1969*

Signature redacted

Signature of Author

Department of Electrical Engineering, November 8, 1968

Signature redacted

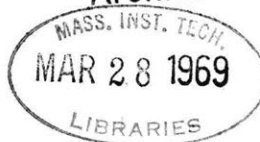
Certified by

Signature redacted

Accepted by

Chairman, Departmental Committee on Graduate Students

Archives





77 Massachusetts Avenue
Cambridge, MA 02139
<http://libraries.mit.edu/ask>

DISCLAIMER NOTICE

Due to the condition of the original material, there are unavoidable flaws in this reproduction. We have made every effort possible to provide you with the best copy available.

Thank you.

Some pages in the original document contain text that runs off the edge of the page.

LOCALIZED DEFECTS IN PBTE
VIA A
 $\vec{K} \cdot \vec{\pi}$ -APW ENERGY BAND CALCULATION

by

NELSON DE JESUS PARADA

Submitted to the Department of Electrical Engineering on November 8, 1968, in partial fulfillment of the requirements for the degree of Doctor of Philosophy.

ABSTRACT

This thesis is a study of the electronic energy levels associated with vacancies in PbTe using the Green's function method of Koster and Slater, and using unperturbed Bloch functions obtained from a relativistic $\vec{K} \cdot \vec{\pi}$ -APW energy band calculation.

APW one electron energies were obtained at Γ and the corresponding eigenfunctions were used to obtain matrix elements of the relativistic momentum operator $\vec{\pi}$ between states at Γ . These energies and matrix elements were used in a $\vec{K} \cdot \vec{\pi}$ secular equation to obtain energies and wavefunctions at approximately 4300 points in the Brillouin zone. With 11 relativistic bands at Γ , excellent results were obtained.

Localized Wannier functions were then constructed by taking suitable linear combinations of the unperturbed Bloch functions, and these Wannier functions provided the basis in which the energy levels in the presence of the perturbing impurity potential were found. We have solved the vacancy problem using Wannier functions from 9 bands (5 valence and 4 conduction) and 13 lattice sites.

The results obtained from this calculation show that Pb vacancies produce p-type PbTe, whereas Te vacancies produce n-type PbTe, and in both cases, carriers are present at all temperatures. If it is assumed that Pb vacancies are the major defect in Te-rich material and Te vacancies are the major defect in Pb-rich material, our results are in agreement with the experimental observations and explain why carriers in PbTe cannot be "frozen out" even at low temperatures.

Thesis Supervisor: George W. Pratt, Jr.
Title: Professor of Electrical Engineering

ACKNOWLEDGEMENTS

The author is deeply grateful to Professor George W. Pratt, Jr. for suggesting this research and for his stimulating supervision throughout the course of this work. He is also indebted to the thesis readers, Professors Mildred S. Dresselhaus and Keith H. Johnson for their advice in preparing this report. Appreciations are due to Dr. Dennis D. Buss, Dr. Sohrab Rabi and Dr. Jose E. Ripper Filho for their helpful discussions, and to Dr. Paul Bailey and Dr. Sergio M. Rezende for the much needed encouragement and moral support. Thanks are extended to Mrs. Colleen Keough and Miss Susan M. Johnson for the excellent typing of this report.

The author wishes to express his love and gratitude to his wife, Maria Ines, and son, Rogerio, for helping him realize his dreams and for bringing happiness to his sad world.

The author is grateful to the Conselho Nacional de Pesquisas (C.N.Pq.-Brasil) for supporting his graduate work at M.I.T.

The present research was supported by the Army Research Office in Durham, to which appreciations are rendered.

TABLE OF CONTENTS

	page
ABSTRACT	
ACKNOWLEDGEMENTS	4
TABLE OF CONTENTS	5
LIST OF FIGURES	6
LIST OF TABLES	8
CHAPTER I INTRODUCTION	9
CHAPTER II APW ENERGY BAND CALCULATION FOR PBTE	15
CHAPTER III $\vec{K}\cdot\vec{\pi}$ SCHEME	24
3.1 Introduction	24
3.2 General Theory	28
3.3 Transformation Properties of Bloch Functions and the $\vec{K}\cdot\vec{\pi}$ scheme	32
3.4 $\vec{K}\cdot\vec{\pi}$ - APW Results for PbTe	45
CHAPTER IV LOCALIZED DEFECTS IN THE $\vec{K}\cdot\vec{\pi}$ - APW SCHEME	81
4.1 Introduction	81
4.2 The U Matrix in the $\vec{K}\cdot\vec{\pi}$ - APW Scheme	99
4.3 Vacancies in PbTe	114
CHAPTER V RESULTS AND CONCLUSIONS	147
APPENDIX	150
BIBLIOGRAPHY	158

LIST OF FIGURES

	page
Figure 2.1. Calculated Energy Bands for the $\langle 100 \rangle$ direction (after Conklin).	20
Figure 2.2. Calculated Energy Bands for the $\langle 110 \rangle$ direction (after Conklin).	21
Figure 2.3. Calculated Energy Bands for the $\langle 111 \rangle$ direction (after Conklin).	22
Figure 3.1. Schematic representation of the energy levels at Γ for PbTe (after Conklin).	46
Figure 3.2. Momentum matrix elements at Γ obtained with the non-relativistic bands of Conklin's APW calculation plotted against the number of SAPW's constituting the wave-functions. The dashed-line parts of the curves correspond to the matrix elements calculated considering the variation of the number of SAPW's of only one of the wave-functions (the wave-functions have been calculated with different number of SAPW's).	56
Figure 3.3. Schematic representation of the energy levels at Γ^* for PbTe (new calculation).	62
Figure 3.4. Momentum matrix elements at Γ obtained with the non-relativistic bands of the new APW calculation (15 SAPW's) plotted against the number of SAPW's.	63
Figure 3.5. Variation of the energy gap at L as a function of $M_{1;15}^{2;2}$.	65
Figure 3.6. First Brillouin zone for a f.c.c. lattice.	65
Figure 3.7. $\vec{K} \cdot \vec{\pi}$ Energy Bands for the $\langle 100 \rangle$ direction.	67
Figure 3.8. $\vec{K} \cdot \vec{\pi}$ Energy Bands for the $\langle 110 \rangle$ direction.	68
Figure 3.9. $\vec{K} \cdot \vec{\pi}$ Energy Bands for the $\langle 111 \rangle$ direction.	69
Figure 3.10.a. $\vec{K} \cdot \vec{\pi}$ Coefficients for the lowest conduction and the highest valence bands along the $\langle 100 \rangle$ direction. The curves are labeled by the corresponding bands at Γ .	70
Figure 3.10.b. $\vec{K} \cdot \vec{\pi}$ Coefficients for the lowest conduction and the highest valence bands along the $\langle 110 \rangle$ direction. The curves are labeled by the corresponding bands at Γ .	71

Figure 3.10.c.	$\vec{k} \cdot \vec{\pi}$ Coefficients for the lowest conduction and the highest valence bands along the $\langle 111 \rangle$ direction. The curves are labeled by the corresponding bands at Γ .	72
Figure 3.11.	$\vec{k} \cdot \vec{\pi}$ Energy Bands for the line $\vec{k} = \frac{\pi}{a}(x, 0.2, 0.2)$ where x varies from 0.0 to 2.0.	74
Figure 3.12.	Real part of the optical dielectric constant $\epsilon_1(q=0, \omega)$ (after Buss).	75
Figure 3.13.	Matrix element of p_x between the lowest conduction band and the highest valence band along the $\langle 100 \rangle$ direction.	77
Figure 3.14.	Matrix elements of momentum between the lowest conduction and the highest valence bands along the $\langle 110 \rangle$ axis. In the figures, // and \perp denote parallel and perpendicular, respectively.	78
Figure 3.15.	Matrix elements of momentum between the lowest conduction and the highest valence bands along the $\langle 111 \rangle$ axis.	80
Figure 4.1.	Example of band-crossing in a symmetry axis (a) and how the bands are in a general axis adjacent to it (b).	105
Figure 4.2.	Radius r times the crystal and vacancy potentials in the sphere where the Pb-vacancy is located.	117
Figure 4.3.	Radius r times the crystal and vacancy potentials in the sphere where the Te-vacancy is located.	118
Figure 4.4.	Matrix elements of $e^{i \Delta \vec{k} \cdot \vec{r}} U(\vec{r})$ between non-relativistic single-group functions at Γ as a function of t (see also Table 4.2).	122
Figure 4.5.	$G_{n,n}^{i,i}(0, E)$ as a function of E for the valence bands number 3, 4 and 5 and conduction band number 1.	132
Figure 4.6.	Symmetric bound states produced by a Pb- and Te-vacancy in the single-band approximation for valence bands number 1 and 2 of PbTe.	138
Figure 4.7.	Symmetric bound states produced by a Pb- and a Te-vacancy in the single-band approximation for valence bands number 3, 4 and 5.	139
Figure 4.8.	Schematic representation of the effect of a Pb- and a Te-vacancy in PbTe.	144

LIST OF TABLES

	page
Table 3.1. Transformation properties of the single-group irreducible representations at Γ .	47
Table 3.2. Relations between partners of the double-group and single-group irreducible representations at Γ .	48
Table 3.3. Mixing between the non-relativistic bands due to the relativistic corrections, in Conklin's calculation.	49
Table 3.4. Momentum matrix elements between single-group irreducible representations at Γ .	52
Table 3.5. Momentum matrix elements between double-group representations at Γ . ($a=1/\sqrt{3}$; $b=1/\sqrt{2}$; $c=1/\sqrt{6}$; $d=1/3$).	53
Table 3.6. Matrix elements of $\frac{\hbar}{m} \vec{p}$ between basis functions at Γ . In this table we represent $\langle n_{\Gamma_i} \frac{\hbar}{m} \vec{p} m_{\Gamma_j} \rangle$ by $\frac{\hbar}{m} M_{i;j}^{n;m}$. The calculated values refer to the values calculated with the maximum number of SAPW's available.	55
Table 3.7. Compatibility relations between the interesting irreducible representations of the group of Γ , and the groups of Δ , Σ and Λ , respectively.	57
Table 3.8. Mixing between the non-relativistic bands due to the relativistic corrections in the new calculation.	62
Table 4.1. Crystal potential and vacancy potentials due to a Pb- and a Te-vacancy. Radius r refers to the center of the spheres. ($R_{Te}=2.9958$ a.u.; $R_{Pb}=3.1005$ a.u.).	116
Table 4.2. Matrix elements of $e^{i\Delta\vec{k}\cdot\vec{r}} U(\vec{r})$ between non-relativistic single group wave-functions at Γ .	120
Table 4.3. Matrix elements of $U(\vec{r})$ and $ixU(\vec{r})$ between non-relativistic bands at Γ , for Pb- and Te-vacancies.	125
Table 4.4. Phase factors for the 24 proper rotations.	129
Table 4.5. Symmetric and antisymmetric states obtained in the single-band approximation for the valence bands of PbTe. The zero of energy is taken at the top of the band.	137
Table 4.6. Symmetric and antisymmetric states appearing between the top of valence band 5 ($E_{top}=-0.56395$ Ry) and the highest energy ($E_{max}=-0.56218$ Ry) in the Conroy's mesh of 1000 points corresponding to this band (single band approximation). The zero of energy in this table	145

CHAPTER I

INTRODUCTION

The purpose of this work is to study the electronic energy levels associated with vacancies in PbTe using the Green's function method of Koster and Slater.¹ In this scheme the perturbed wave-function is expanded in terms of Wannier functions of the unperturbed case, which are written in terms of the unperturbed Bloch functions. In our case, the latter functions are obtained from a relativistic $\vec{K} \cdot \vec{\pi}$ - APW energy band calculation.* The importance of this study is that it explains some of the very interesting properties of PbTe to be discussed below.

Lead Telluride has been the subject of considerable experimental and theoretical investigations for several years. It is known to have a NaCl crystal structure with a lattice constant of 6.452 \AA (12.193 atomic units)² and to be a semiconductor with a direct gap of about 0.3 eV at room temperature.³ The gap is located at the point L in the Brillouin zone. The measured and calculated electronic properties of the lead salts have been recently reviewed by Prakash,⁴ in his work on the measurements of the optical absorption edge of these salts and its variation with temperature and pressure.

* \vec{k} is not to be confused with the magnetic momentum $(\vec{p} + \frac{e\vec{A}}{c})$, where \vec{p} is the linear momentum and \vec{A} is the vector potential. In the case of non-relativistic bands $\vec{\pi}$ is equal to the linear momentum and the method is called the $\vec{K} \cdot \vec{P}$ method.

A very interesting property of the lead chalcogenide group of semiconductors is that they have ranges of non-stoichiometry, the lattice incorporating either excess lead or chalcogen with the corresponding defects. While excess lead produces a n-type semiconductor, excess chalcogen gives rise to a p-type material. Both cases are characterized by high mobilities at liquid helium temperatures and it is not possible to freeze out the carriers at low temperatures.⁵ The concentration of the excess component can be controlled by equilibrating the solid with the vapour pressure of that component and the variation of this equilibrium with the vapour pressure has been carried out for all lead salts. It has been found out that for excess chalcogen the principal defect is a singly ionized lead vacancy while for excess Pb, the situation is not yet clear: for PbSe it seems that the principal defect is a doubly-ionized interstitial Pb,^{6,7} while for PbS, a singly ionized sulfur vacancy appears to be the primary donor defect, although an appreciable concentration of doubly ionized interstitial Pb also exists.⁸ On the other hand, a singly ionized tellurium vacancy is probably the most important defect in PbTe.⁹ The theoretical study of vacancies in PbTe, therefore, presents the possibility of explaining the behavior described above.

The defect problem associated with a Pb- and a Te-vacancy is solved here in a manner similar to that used by Callaway and Hughes¹⁰ for single and di-vacancies in silicon, that is, by applying the Green's function method of Koster and Slater, which has also been successfully used in connection with the study of impurities in metals.¹¹ The

effect of the vacancy is treated as a time-independent localized potential and the perturbed wave-functions are expanded in terms of Wannier functions of the unperturbed lattice. Because the latter functions are defined as linear combinations of Bloch functions, the knowledge of those wave-functions, on a reasonable mesh of points in the Brillouin zone, is necessary.

The one-electron energy bands of PbTe were obtained by Conklin,¹² through a first principle relativistic APW calculation, and by Lin and Kleinman,¹³ using a pseudopotential approach. Conklin's calculation is briefly discussed in Chapter II, in conjunction with the APW method. Some experimental results can be very well explained by his bands¹² and the effective-masses¹⁴ and deformation potentials¹⁵ obtained with these bands are in good agreement with the experimental values.

In principle, we can use the APW method to calculate the eigenfunctions and eigenvalues of the one-electron Hamiltonian at every point in the Brillouin zone, although the program for a low symmetry point will not fit our computer systems. Even if this were not the case, the computation time involved would make these calculations prohibitive. As shown in Chapter II, the eigenfunctions of the one-electron Hamiltonian are expanded in terms of symmetrized APW (SAPW), and the number of SAPW necessary to obtain a good energy convergence increases rapidly as the number of symmetry operations of the group of

the wave-vector decreases.* The energy levels and wave-functions are calculated only for the high symmetry points and for one or two points in the symmetry axes of the Brillouin zone. The energy bands are then sketched along these axes using the compatibility relations between the groups of the wave-vector at these different points.

As we mention before, in order to explain and calculate many of the experimentally observable properties of the material it is desirable to know the eigenvalues and eigenfunctions of the one-electron Hamiltonian at every point in the Brillouin zone. In Chapter III we show how to do this by a first principles $\vec{K} \cdot \vec{\pi}$ interpolation scheme. In this method, if the energies, wave-functions and momentum matrix elements between these functions are known at a particular point in k-space, \vec{k}_0 say, the energies and wave-functions can be obtained at every other point. This method involves no approximation if all energy bands at \vec{k}_0 are included in the calculations. For a semiconductor, however, we are mainly interested in the conduction and valence bands, and we expect that bands with energy far away from these bands will give a small contribution in the calculations. Thus, if a reasonable number of bands around the conduction and valence bands is used in the $\vec{K} \cdot \vec{\pi}$ calculation, we expect good results for bands near the Fermi level.

The choice of \vec{k}_0 is based on the following considerations. If we choose \vec{k}_0 to be a point of low symmetry, two difficulties arise: first,

* For more information in the convergence of the energy and momentum matrix elements in PbTe-APW calculation, see reference 16.

it is difficult to calculate momentum matrix elements at points of low symmetry, and second, when going from \vec{k}_0 to a point of higher symmetry, the symmetry enforced degeneracies are not built in the calculations. It is wise, therefore, to choose as \vec{k}_0 the point of highest symmetry in the Brillouin zone, because there we can perform a very good energy band calculation and the symmetry properties of each point in the B.Z. (except the zone faces) are automatically satisfied. In Chapter III we also discuss how such a calculation was performed by us for PbTe, using 11 relativistic bands at Γ , obtained from a relativistic APW calculation.

The $\vec{K} \cdot \vec{\pi}$ method was first used by Cardona and Pollack¹⁷ for germanium and silicon. The values for some of the energy gaps and momentum matrix elements were obtained from the experimental data on cyclotron resonance and optical measurements. The remaining parameters were assigned values suggested by the OPW calculation of Herman¹⁸ and pseudo-potential calculation of Brust¹⁹ and were then adjusted until the calculated energy bands agreed with the ultraviolet reflection data. Our calculation, however, differs from that of Cardona and Pollack in that in ours the relativistic bands at Γ and all momentum matrix elements between these bands were calculated. The information was used in a $\vec{K} \cdot \vec{\pi}$ secular matrix and the bands were obtained in a mesh of points in the Brillouin zone. The results were surprising: it was necessary to change only one of the non-relativistic momentum matrix elements by 2.5% in order to fit the experimental gap, and at the points where Conklin performed his calculations, our results differ little from his.

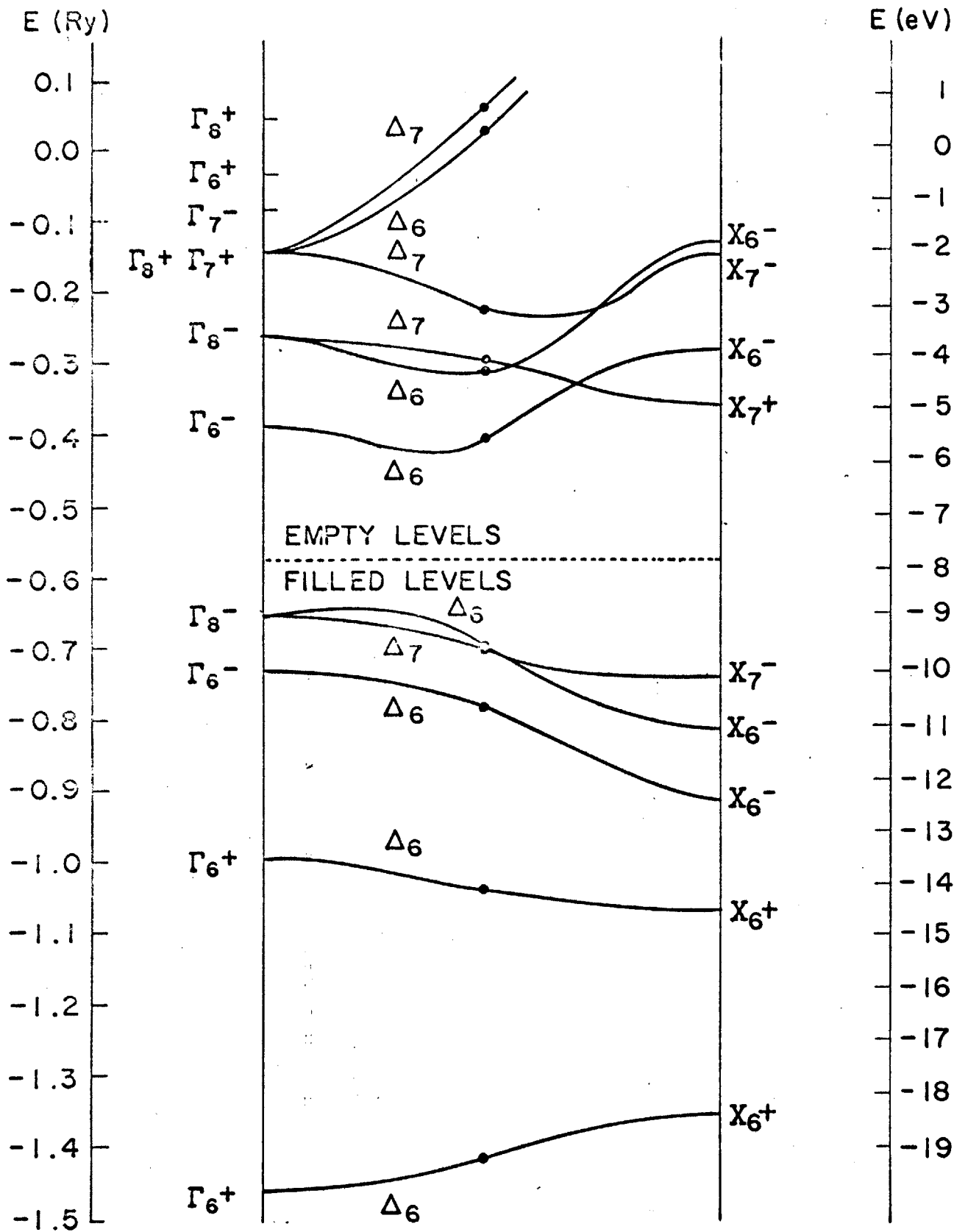


FIGURE 2.1 - Calculated Energy Bands for the <100> direction (after Conklin)

CHAPTER II

APW ENERGY BAND CALCULATION FOR PBTE

The APW energy band calculation of PbTe was performed by Conklin in 1964 as a Ph.D. dissertation at MIT.¹² In order to present his results, let us briefly discuss the APW method.

In the APW method the periodic potential in the crystal is assumed to be of the muffin-tin type which is obtained by placing touching spheres around the atoms in the lattice. The potential is taken to be spherically symmetric inside the spheres and constant in the region outside them. The spherically symmetric part of the potential is made of the atomic potential at the site under consideration plus the spherically averaged contribution of the neighboring atoms. The constant potential is chosen by linearly averaging the spherically symmetric potential in the region outside the spheres. The construction of the potential will be discussed in more detail in Chapter IV.

The solution of the Schrodinger equation can be broken up into two separate parts. In the region outside the spheres, where the potential is constant, the solutions are plane waves. Since the potential is spherically symmetric inside the spheres, the solutions in this region can be expanded as the sum of the products of radial wave-

functions $u_{\ell,E}(r)$ and spherical harmonics $Y_{\ell}^m(\theta,\phi)$, i.e.

$$\psi(\vec{r}) = \sum_{\ell,m} A_{\ell,m} u_{\ell,E}(r) Y_{\ell}^m(\theta,\phi) \quad (2.1)$$

where $u_{\ell,E}(\vec{r})$ must satisfy the following radial equation

$$\left[-\frac{d^2}{dr^2} + V(r) + \frac{\ell(\ell+1)}{r^2} \right] r u_{\ell,E}(r) = E r u_{\ell,E}(r) \quad (2.2)$$

The coefficients $A_{\ell,m}$ are chosen so that $\psi(\vec{r})$ be continuous with the plane wave at the surface of the spheres. The resulting function is called an augmented plane wave (APW) and can be written in the following fashion

$$\psi^{APW}(\vec{k}, \vec{r}) = \delta e^{i\vec{k}\cdot\vec{r}} + \rho e^{i\vec{k}\cdot\vec{R}_p} \sum_{\ell=0}^{\infty} \sum_{m=-\ell}^{\ell} 4\pi i^{\ell} j_{\ell}(|\vec{k}| R_p) \times \frac{u_{p,\ell,E}(r')}{u_{p,\ell,E}(R_p)} [Y_{\ell}^m(\theta_k, \phi_k)]^* Y_{\ell}^m(\theta', \phi') \quad (2.3)$$

where

$$\begin{aligned} \delta &= \begin{array}{l} 1 \text{ outside the sphere} \\ 0 \text{ inside the sphere} \end{array} \\ \rho &= \begin{array}{l} 1 \text{ inside the sphere} \\ 0 \text{ outside the sphere} \end{array} \end{aligned}$$

In (2.3), θ_k and ϕ_k are the spherical coordinates of the k -vector; $j_{\ell}(r)$ are spherical Bessel functions and the primed coordinates refer to a coordinate system having its origin at the center of the sphere situated at \vec{R}_p . The radial functions $u_{p,\ell,E}$ are subscripted by the additional index p because the crystal potential may differ in different spheres if the solid contains more than one kind of atom.

It is easy to prove¹² that the APW functions satisfy the Bloch condition, i.e.

$$\psi^{\text{APW}}(\vec{k}, \vec{r} + \vec{R}_n) = e^{i\vec{k} \cdot \vec{R}_n} \psi^{\text{APW}}(\vec{k}, \vec{r}) \quad (2.4)$$

where \vec{R}_n is a lattice translation.

In setting up the secular equation for the eigenvalues and eigenfunctions at a particular point \vec{k}_0 of the first Brillouin zone only APW functions corresponding to $\vec{k}_0 + \vec{K}_1$, where \vec{K}_1 are the various reciprocal lattice vectors, need be considered. A sufficient number of reciprocal lattice vectors must be used to adequately approximate the eigenfunction. The number of reciprocal lattice vectors necessary depends on the desired accuracy and can be determined empirically.

Computation is simplified by considering the group of the wave vector which describes the rotational properties of the wave-functions. Under the operation R of this group, these functions transform like the partners of one of its irreducible representations, i.e.,

$$R \psi_j^{\Gamma_\alpha}(\vec{k}, \vec{r}) = \sum_i \Gamma_\alpha(R)_{i,j} \psi_i^{\Gamma_\alpha}(\vec{k}, \vec{r}) \quad (2.5)$$

where $\psi_j^{\Gamma_\alpha}(\vec{k}, \vec{r})$ is said to transform like the j^{th} partner (or column) of the Γ_α irreducible representation of the group of the k-vector. In (2.5) $\Gamma_\alpha(R)_{i,j}$ is the (i,j) element of the matrix that represents R in the Γ_α irreducible representation. The transformation properties of the wave-functions will be considered in some detail in Chapter III.

To accomplish the objective expressed by (2.5), projection operators are formed for each irreducible representation and these

operators are used to project out of the augmented plane waves, functions that transform according to that representation. These functions are referred to as symmetrized augmented plane waves (SAPW), and have the form

$$\psi_{j,\ell}^{\Gamma_{\alpha}}(\vec{k}+\vec{K}_i, \vec{r}) = \sum_R \Gamma_{\alpha}(R)_{j,\ell}^* R\psi^{\text{APW}}(\vec{k}+\vec{K}_i, \vec{r}) \quad (2.6)$$

where R are the operations of the group of \vec{k} . The SAPW in (2.6) is said to transform as the j^{th} partner of the Γ_{α} irreducible representation. Because for the same j and different ℓ , different functions may be obtained, the column index ℓ is used as a subscripted index in the SAPW. The Bloch functions are then written as a linear combination of SAPW with different \vec{K}_i .

Let us consider now the one-electron relativistic Hamiltonian derived from the Dirac equation by decoupling large and small components of the four component wave-function by means of successive applications of the Foldy-Wouthuysen unitary transformation.²⁰ In the absence of a magnetic field, and for coupling terms between the large and small components of the order of $(v/c)^5$, where v and c are, respectively, the velocities of the electron and of light, we obtain:

$$H_0 = \frac{p^2}{2m} + V(\vec{r}) + \frac{\hbar}{4m^2 c^2} (\nabla V \times \vec{p}) \cdot \vec{\sigma} + \frac{\hbar^2}{8m^2 c^2} (\nabla^2 V) - \frac{\hbar^4}{8m^3 c^2} \quad (2.7)$$

The first two terms are the kinetic and potential energies; the third is the spin-orbit coupling and the two last are the Darwin and mass-velocity corrections.

In Conklin's relativistic APW calculation^{*}, the solution for the non-relativistic bands, i.e., the eigenvalues and eigenfunctions of $\frac{p^2}{2m} + V(\vec{r})$, are first obtained. The Darwin and the mass-velocity corrections are then considered as perturbations and new energies and wave-functions are obtained. These corrections do not lead to splitting of the single group levels because they have the same symmetry as the non-relativistic Hamiltonian. They will, however, mix levels with the same symmetry and will impart an unequal shift to them.

The last step in the calculations involves the inclusion of the spin-orbit term. At this point, spin must be introduced in the wave-functions, which then will transform as basis functions for the double-group irreducible representations.

Figures (2.1), (2.2) and (2.3) show the relativistic energy bands obtained by Conklin along the three major symmetry directions. These results show a small band gap occurring at L which is responsible for most of the observed electronic properties of Pbte.

Since the two levels which mark the forbidden gap at L are very close together, the calculated gap is the difference of two very large numbers and is therefore very sensitive to slight changes in the position of these levels. Since the L_2' non-relativistic band which is the major contributor to the bottom of the conduction band

^{*} Another way of including the relativistic effects in the APW formalism has been carried out by Loucks²¹. In this case we solve directly the Dirac equation based on the muffin-tin potential.

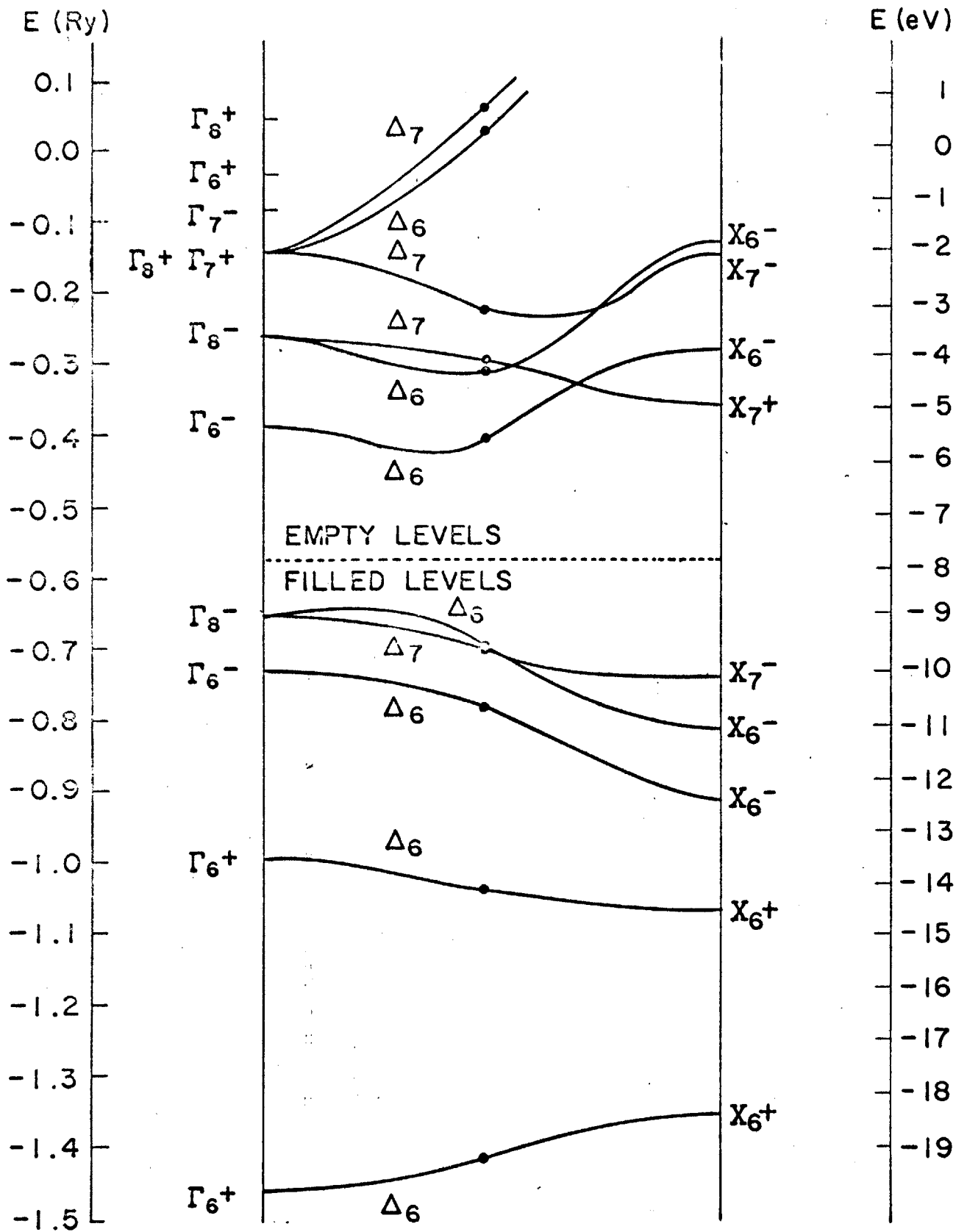


FIGURE 2.1 - Calculated Energy Bands for the <100> direction (after Conklin)

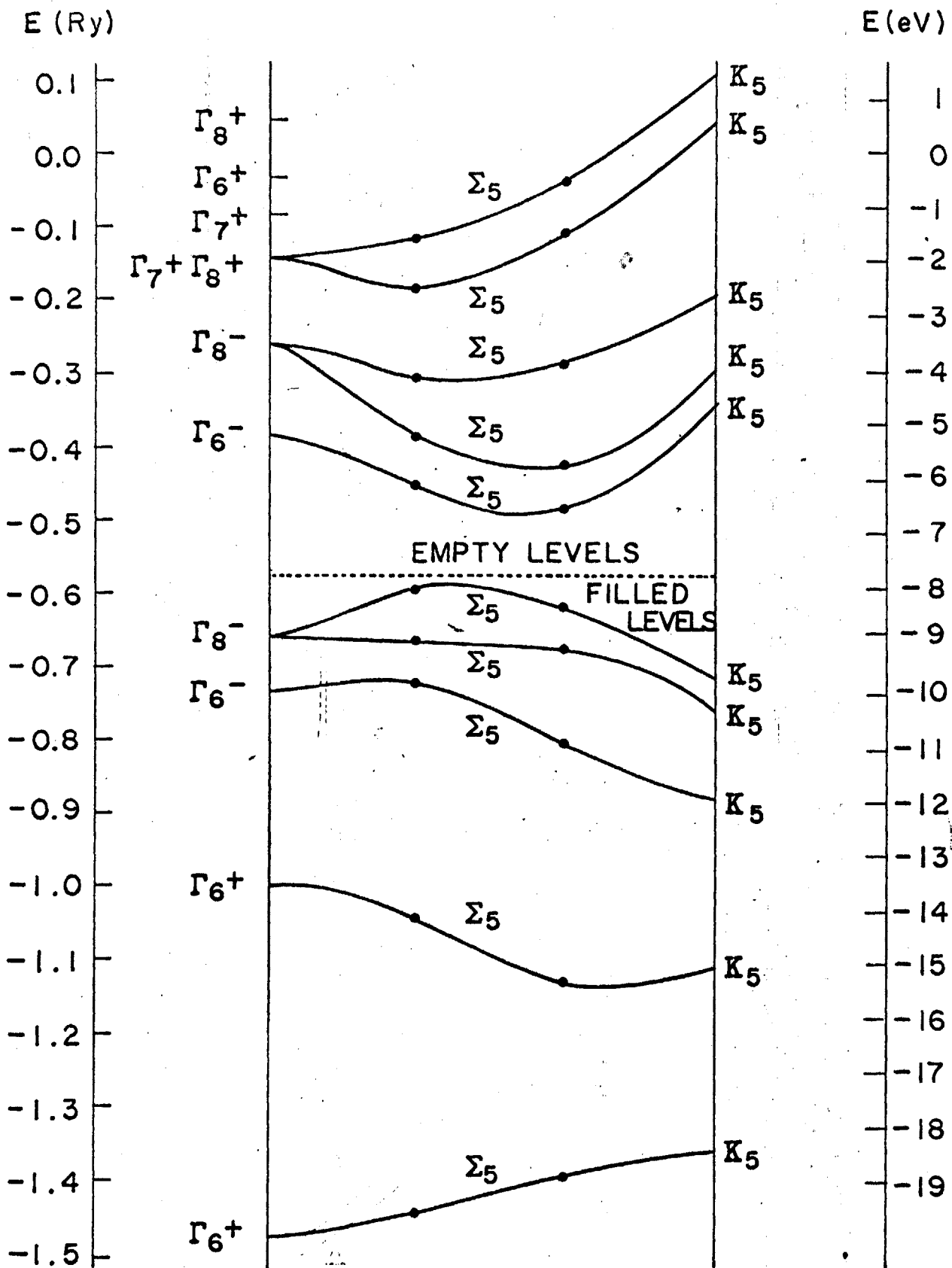


FIGURE 2.2 - Calculated Energy Bands for the <110> direction (after Conklin)

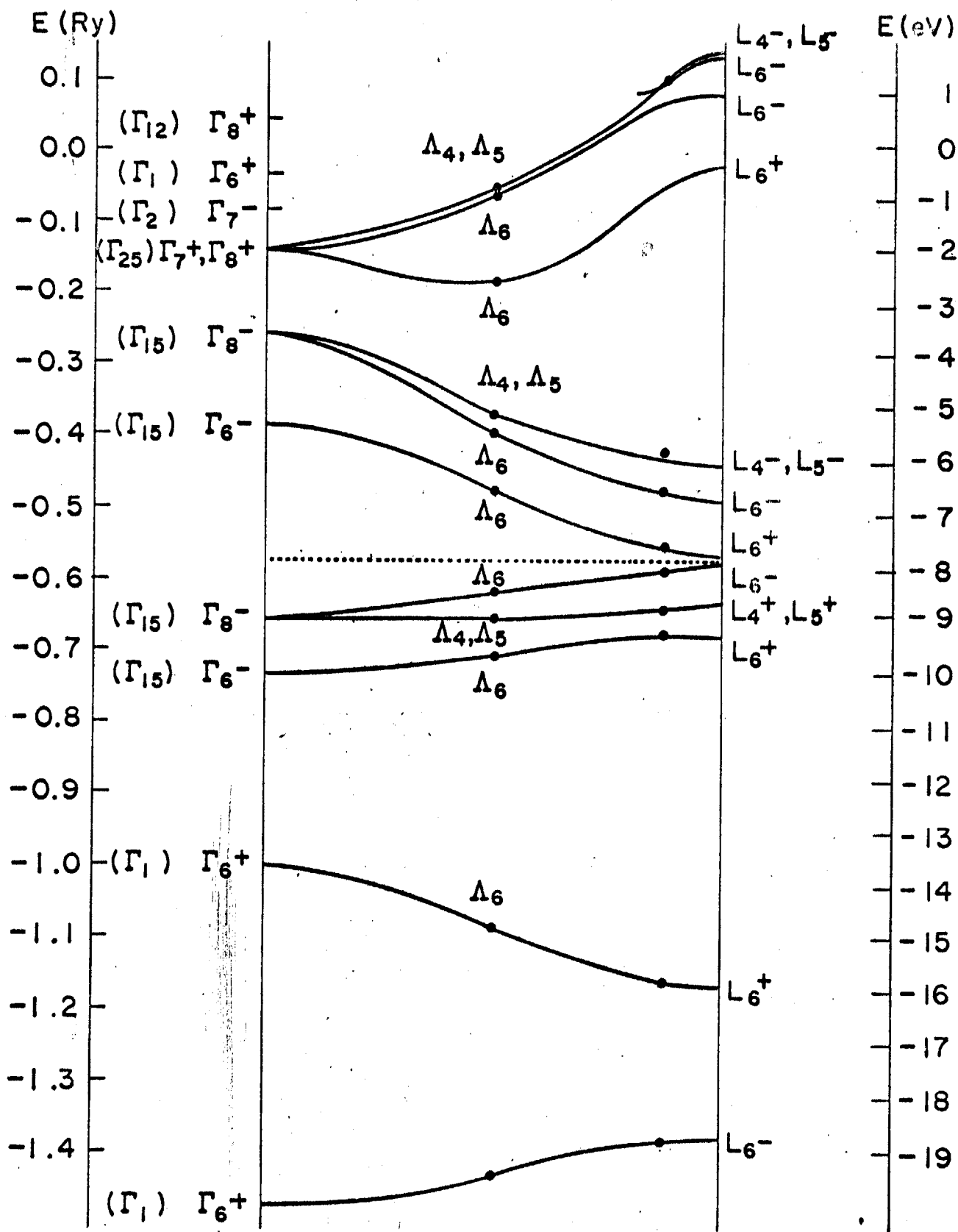


FIGURE 2.3 - Calculated Energy Bands for the $\langle 111 \rangle$ direction (after Conklin)

has a large part of its charge density concentrated in the plane wave region, the position of this level is very sensitive to the value of the constant potential in this region. Then, a slight change in this value results in a large relative change in the size of the energy gap, and can even lead to a reversing of the order of the conduction and valence bands at L. This reversing was indeed obtained by Conklin and a perturbation analysis performed by him showed that a small variation in the constant potential leads to the right gap.

CHAPTER III

THE $\vec{k} \cdot \vec{\pi}$ SCHEME

3.1 - INTRODUCTION

Before 1955, two complete sets of orthonormal functions were largely used for solving problems connected with the behavior of electrons in solids: the Bloch functions, eigenfunctions of the one-electron Hamiltonian, and characterized by a band index n^* and wave vector \vec{k} , and the Wannier functions defined in terms of the Bloch set and characterized by a band index n and a lattice site \vec{R}_m . The representations generated by these two sets, namely the crystal momentum representation (CMR) and crystal coordinate representation (CCR), will be discussed later, in Chapter IV, in connection with the study of localized defects in solids.

In 1955, however, a new complete set was introduced. Luttinger and Kohn²² showed that if the Bloch functions are known at a particular point in \vec{k} -space, \vec{k}_0 say, it is possible to construct a new complete set of functions, characterized by a band index n and wave vector \vec{k} , but different from the Bloch set. These functions, which we shall call Kohn-Luttinger functions, have been used in the establishment of the expressions for the effective-mass and g-factor tensors in solids. The effective-mass tensor is normally obtained

* If the energy band is degenerate, n also includes the partner index.

by constructing the so called $\vec{k}\cdot\vec{p}$ -effective Hamiltonian through Brillouin-Wigner perturbation theory and, in this scheme, the g-factor tensor can be obtained using the method introduced by Roth.²³

Assume that the eigenfunctions and eigenvalues of the one-electron Hamiltonian are known at \vec{k}_0 . We can construct the Kohn-Luttinger set and expand the Bloch functions at every \vec{k} in terms of this set. The coefficients in the expansion are determined by solving a secular equation and if all bands at \vec{k}_0 are included in the secular matrix the result is exact. In practice we are limited to a finite number of bands at \vec{k}_0 which limits the accuracy of the calculation. However, reasonably accurate calculations can be made for the conduction and valence bands using a manageable number of bands at \vec{k}_0 on either side of the gap.

In the case of non-relativistic bands, the off-diagonal terms in the secular matrix are given by the matrix elements of the operator $\frac{\hbar}{m} \vec{K}\cdot\vec{p}$ between the Bloch functions at \vec{k}_0 , \vec{p} being the linear momentum and $\vec{K}=(\vec{k}-\vec{k}_0)$. However, when relativistic corrections are taken into account, the appropriate operator is $\frac{\hbar}{m} \vec{K}\cdot\vec{\pi}$, where $\vec{\pi}$ is equal to \vec{p} plus other terms due to the relativistic corrections. This method of obtaining energy bands will be referred to as the $\vec{K}\cdot\vec{\pi}$ method.

The idea of using the $\vec{K}\cdot\vec{\pi}$ scheme for the calculation of energy bands at every point in the Brillouin zone was first put in practice by Cardona and Pollack¹⁷, for germanium and silicon. We will see later that to determine the energy levels at any point in

k-space it is necessary to know only the energy levels at \vec{k}_0 and the momentum matrix elements between states at \vec{k}_0 . As we mentioned in Chapter I, Cardona and Pollack treated the energy gaps and momentum matrix elements as adjustable parameters. The values for some of them were obtained from the experimental data on cyclotron resonance and optical measurements. The remaining parameters were assigned values suggested by the OPW calculation of Herman¹⁸ and the pseudopotential calculation of Brust¹⁹ and were then adjusted until the calculated energy bands agreed with the ultraviolet reflection data. Although this empirical method can in principle be used for any material, it requires the knowledge of sufficient experimental data to choose at least the initial trial values for the energy gaps and momentum matrix elements and does not provide the wave-functions at \vec{k} , unless the wave-functions at \vec{k}_0 are known.

However, the success of Cardona and Pollack in obtaining the energy levels suggested to us that perhaps the $\vec{K} \cdot \vec{\pi}$ scheme could be used as a reliable first principles method for determining the energy levels and wave-functions in a solid. Suppose, for a certain material, the energies and wave-functions are known at certain points in k-space through a first principles energy band calculation such as the APW or OPW schemes. Suppose that the energy levels and momentum matrix elements calculated at a particular point \vec{k}_0 are used in the $\vec{K} \cdot \vec{\pi}$ secular matrix to evaluate the energy levels at other points in the zone. If the $\vec{K} \cdot \vec{\pi}$ results at those

other points are compared with the first principles results how good is the agreement? In the following sections, this question is answered for PbTe, where the energies and wave-functions at \vec{k}_0 were obtained by a relativistic APW calculation.

Section 3.2 is devoted to the general theory of the $\vec{K} \cdot \vec{\pi}$ scheme in the case where relativistic corrections are taken into account. There, an expression for the $\vec{\pi}$ operator is derived and the difference between this expression and that obtained for the corresponding operator in the $\vec{K} \cdot \vec{p}$ perturbation theory is discussed.

Due to the reciprocal lattice symmetries, the electronic energy levels and wave-functions are calculated only in a small region A of the Brillouin zone, every \vec{k} in A being associated with a set of \vec{k}' 's in the remaining region. This set is called "star of \vec{k} " and the wave-functions in the star are defined in terms of the wave-functions at \vec{k} . In section 3.3 we present the transformations properties of Bloch functions and derive, in the $\vec{K} \cdot \vec{\pi}$ scheme, the expressions for the wave-functions in the star. The Bloch functions obtained in this case, however, do not vary smoothly in the Brillouin zone and the resulting Wannier functions will not be properly localized. In that section we also show how to obtain smooth Bloch functions near \vec{k}_0 for degenerate bands and in the case of non-degenerate bands our results are identical to that obtained by Callaway²⁴.

In section 3.4 we apply the $\vec{K} \cdot \vec{\pi}$ scheme to PbTe. The results are compared with Conklin's results at symmetry points and with

some of the experimental data available for PbTe.

3.2 - GENERAL THEORY

Let us consider the one-electron relativistic Hamiltonian (2.7), which is rewritten below.

$$H_0 = \frac{p^2}{2m} + V(\vec{r}) + \frac{\hbar}{4m^2 c^2} (\nabla V \times \vec{p}) \cdot \vec{\sigma} + \frac{\hbar^2}{8m^2 c^2} (\nabla^2 V) - \frac{p^4}{8m^3 c^2} \quad (3.1)$$

The eigenfunctions of H_0 are Bloch functions $b_{n,i}^{\Gamma_\alpha(\vec{k})}(\vec{k}, \vec{r})$,

which transforms like the i -partner of the double-group irreducible representation $\Gamma_\alpha(\vec{k})$ of the group of the wave vector \vec{k} . They form a complete set of orthonormal functions for every \vec{k} , band index n and partner i .

$$H_0 b_{n,i}^{\Gamma_\alpha(\vec{k})}(\vec{k}, \vec{r}) = E_n(\vec{k}) b_{n,i}^{\Gamma_\alpha(\vec{k})}(\vec{k}, \vec{r}) \quad (3.2)$$

According to Bloch's theorem, $b_{n,i}^{\Gamma_\alpha(\vec{k})}(\vec{k}, \vec{r})$ can be written as

$$b_{n,i}^{\Gamma_\alpha(\vec{k})}(\vec{k}, \vec{r}) = e^{i\vec{k} \cdot \vec{r}} u_{n,i}(\vec{k}, \vec{r}) \quad (3.3)$$

where $u_{n,i}(\vec{k}, \vec{r})$ is a periodic function with the periodicity of the lattice.

Any eigenfunction which belongs to the Hilbert space of eigenfunctions that characterize the one-electron states of the crystal can be expanded in terms of this complete set. Two other complete sets can be obtained from Bloch functions, namely the Wannier and the Kohn-Luttinger sets. In this section we are particularly interested in the last one.

The Kohn-Luttinger functions are of the form

$$\chi_{n,i}(\vec{k}-\vec{k}_0, \vec{r}) = e^{i(\vec{k}-\vec{k}_0) \cdot \vec{r}} b_{n,i}^{\Gamma_\alpha(\vec{k}_0)}(\vec{k}_0, \vec{r}) \quad (3.4)$$

where \vec{k}_0 is any particular point in k-space.

Now suppose that the Bloch functions and energy levels are known at \vec{k}_0 (i.e., $b_{m',j}^{\Gamma_\beta(\vec{k}_0)}(\vec{k}_0, \vec{r})$ and $E_m(\vec{k}_0)$), which are solutions of the Schrodinger equation

$$H_0 b_{m',j}^{\Gamma_\beta(\vec{k}_0)}(\vec{k}_0, \vec{r}) = E_m(\vec{k}_0) b_{m',j}^{\Gamma_\beta(\vec{k}_0)}(\vec{k}_0, \vec{r}) \quad (3.5)$$

are known). Suppose now that we wish to solve the stationary Schrodinger equation (3.6) at another point, \vec{k} .

$$H_0 b_{n,i}^{\Gamma_\alpha(\vec{k})}(\vec{k}, \vec{r}) = E_n(\vec{k}) b_{n,i}^{\Gamma_\alpha(\vec{k})}(\vec{k}, \vec{r}) \quad (3.6)$$

As the Kohn-Luttinger set is complete, it can be used as a basis

for expanding $b_{n,i}^{\Gamma_\alpha(\vec{k})}(\vec{k}, \vec{r})$, i.e.,

$$b_{n,i}^{\Gamma_\alpha(\vec{k})}(\vec{k}, \vec{r}) = \sum_{m',j} C_{n,m'}^{i,j}(\vec{k}) \chi_{m',j}(\vec{k}, \vec{r}) \quad (3.7)$$

where $\vec{k} = (\vec{k}-\vec{k}_0)$. If Eq. (3.7) is substituted in Eq. (3.6) we obtain

$$H_0 b_{n,i}^{\Gamma_\alpha(\vec{k})}(\vec{k}, \vec{r}) = \sum_{m',j} C_{n,m'}^{i,j}(\vec{k}) e^{i\vec{k} \cdot \vec{r}} [E_m(\vec{k}_0) + \frac{\hbar^2 \vec{k}^2}{2m} - \frac{\hbar^4 \vec{k}^4}{8m^3 c^2} + \frac{\hbar \vec{k} \cdot \vec{\pi}}{m}] \times$$

$$b_{m',j}^{\Gamma_\beta(\vec{k}_0)}(\vec{k}_0, \vec{r}) = E_n(\vec{k}) \sum_{m',j} C_{n,m'}^{i,j}(\vec{k}) e^{i\vec{k} \cdot \vec{r}} b_{m',j}^{\Gamma_\beta(\vec{k}_0)}(\vec{k}_0, \vec{r}) \quad (3.8)$$

where

$$\vec{\pi} = \vec{p} + \frac{\hbar}{4mc^2} (\vec{\sigma} \times \nabla V) - \frac{1}{2m^2 c^2} \vec{p}^3 - \frac{\hbar^2}{2m^2 c^2} \vec{K}^2 \vec{p} - \frac{\hbar}{4m^2 c^2} \vec{K} \vec{p}^2 +$$

$$- \frac{\hbar}{2m^2 c^2} [\vec{K} \cdot \vec{p}] \vec{p} \quad (3.9.a)$$

If we multiply both sides of Eq. (3.8) by $\chi_{n,i}^*(\vec{K}, \vec{r})$ and integrate over the whole crystal we obtain

$$\sum_{m,j} \{ [E_m(\vec{k}_0) + \frac{\hbar^2 \vec{K}^2}{2m} - \frac{\hbar^4 \vec{K}^4}{8m^3 c^2} - E_n(\vec{k})] \delta_{m,n} \delta_{j,i} + \frac{\hbar}{m} \vec{K} \cdot \vec{\pi}_{n,m}^{i,j} \} C_{n,m}^{i,j}(\vec{K}) = 0 \quad (3.10)$$

which is true for all n . In Eq. (3.10) we have written

$$\vec{\pi}_{n,m}^{i,j} = \int_{\text{crystal}} d\vec{r} b_{n,i}^*(\vec{K}, \vec{r}) \vec{\pi} b_{m,j}(\vec{K}, \vec{r}) \quad (3.11)$$

In order for the system (3.10) to have a solution, it is necessary that

$$\det \left| [E_m(\vec{k}_0) + \frac{\hbar^2 \vec{K}^2}{2m} - \frac{\hbar^4 \vec{K}^4}{8m^3 c^2} - E_n(\vec{k})] \delta_{n,m} \delta_{i,j} + \frac{\hbar}{m} \vec{K} \cdot \vec{\pi}_{n,m}^{i,j} \right| = 0 \quad (3.12)$$

Because the off-diagonal terms are of the form $\vec{K} \cdot \vec{\pi}$, as we mentioned earlier, this method of extrapolation of the energy bands is referred to as the $\vec{K} \cdot \vec{\pi}$ scheme.

A confusion, without major consequences, has been made in reference 17 between the expression (3.9.a) for $\vec{\pi}$ and the expression for the operator $\vec{\pi}'$, analogous to $\vec{\pi}$ in the $\vec{K} \cdot \vec{\pi}$ perturbation theory. In the latter case we are mainly interested in the region near \vec{k}_0 , i.e., in the region where \vec{K} is small. The term $\frac{\hbar}{m} \vec{K} \cdot \vec{\pi}$ in Eq. (3.8)

is considered as a perturbation in the Brillouin-Wigner scheme and terms in \vec{K}^2 or higher are not considered in the expression for $\vec{\pi}$.

Then¹⁴

$$\vec{\pi}' = \vec{p} + \frac{\hbar}{4mc^2}(\vec{\sigma} \times \nabla V) - \frac{1}{2m^2 c^2} \vec{p}^3 - \frac{\hbar}{4m^2 c^2} \vec{K} \vec{p}^2 - \frac{\hbar}{2m^2 c^2} [\vec{K} \cdot \vec{p}] \vec{p} \quad (3.9.b)$$

A comparison between Eq. (3.9.a) and Eq. (3.9.b) shows that the term in \vec{K}^2 , namely $\frac{\hbar^2}{2m^2 c^2} \vec{K}^2 \vec{p}$ is missing. But this term is $\alpha^2 \vec{K}^2$

times smaller than the momentum term and can be completely neglected if K is small ($\alpha^2 = \frac{1}{2} = (137.08)^{-2}$ in atomic units).

No approximations have been made until this point. Solving Eq. (3.12) is completely equivalent to solving Eq. (3.6). As we mentioned earlier, however, the secular matrix (3.12) has infinite dimension and for practical purposes has to be truncated at some point. Because we are mainly interested in the valence and conduction bands, it is reasonable to expect that if a certain number of energy bands at \vec{k}_0 both above and below the conduction and valence bands is used in the expansion, good results will be obtained for these important bands. The dimensionality of the secular equation is chosen by considering the computational complexity versus the expected accuracy of the calculated energies and wavefunctions. Of course, the accuracy obtained with the $\vec{K} \cdot \vec{\pi}$ scheme depends not only on the number of bands used at \vec{k}_0 , but also on the accuracy of the calculated energies and momentum matrix elements.

Before we consider the practical application for PbTe, let us discuss more carefully the symmetry properties of Bloch functions and the $\vec{K} \cdot \vec{\pi}$ scheme.

3.3 - TRANSFORMATIONS PROPERTIES OF BLOCH FUNCTIONS AND THE $\vec{K} \cdot \vec{\pi}$ SCHEME

The effect of a general operation of the crystal space group on Bloch functions has been discussed by various authors²⁵, but we will summarize the important results here.

Let us denote an operation in the space group G of the crystal by $\{\alpha | \vec{t}_\alpha + \vec{R}_n\}$, where α is a rotation or reflection, \vec{t}_α is a non-primitive translation associated with α , and \vec{R}_n is a lattice translation. Associated with each one of these operations there is an operator that commutes with the one-electron Hamiltonian. No distinction will be made here between the operations and corresponding operators. Let \vec{r} be an arbitrary vector. If such an operator acts on \vec{r} , a new vector \vec{r}' is obtained such that

$$\vec{r}' = \{\alpha | \vec{t}_\alpha + \vec{R}_n\} \vec{r} = \alpha^{-1}(\vec{r} + \vec{t}_\alpha + \vec{R}_n) \quad (3.13)$$

We recall that the unit operator is given by $\{\epsilon | 0\}$, where ϵ is the identity rotation, and that the inverse operator $\{\alpha | \vec{t}_\alpha + \vec{R}_n\}^{-1}$ is defined as

$$\{\alpha | \vec{t}_\alpha + \vec{R}_n\}^{-1} = \{\alpha^{-1} | -\alpha^{-1}(\vec{t}_\alpha + \vec{R}_n)\} \quad (3.14)$$

The group multiplication is given by Eq. (3.15).

$$\{\alpha|\vec{t}_\alpha + \vec{R}_n\}\{\beta|\vec{t}_\beta + \vec{R}_m\} = \{\alpha\beta|\alpha(\vec{t}_\beta + \vec{R}_m) + \vec{t}_\alpha + \vec{R}_n\} \quad (3.15)$$

Generally speaking, we are interested in obtaining the irreducible representations of the space group G of the crystal, because the eigenfunctions of the one-electron Hamiltonian will transform like partners of these irreducible representations. It can be easily shown that every space group contains a group of pure lattice translations $\{\epsilon|\vec{R}_n\}$ as an invariant subgroup. The irreducible representations of this Abelian subgroup are one-dimensional and each one is characterized by a wave vector \vec{k} . We shall call this subgroup τ . Every one-electron wavefunction is thus characterized by a wave vector \vec{k} and must transform like Eq. (3.16) under an operation belonging to τ .

$$\{\epsilon|\vec{R}_m\} \Psi(\vec{k}, \vec{r}) = \Psi(\vec{k}, \vec{r} + \vec{R}_m) = e^{i\vec{k} \cdot \vec{R}_m} \Psi(\vec{k}, \vec{r}) \quad (3.16)$$

This condition is known as the "Bloch Theorem" and the basis functions are called Bloch functions.

Two other important groups are connected with the space group G : the point group ρ , and the group of the wave vector \vec{k}_1 , which we shall call κ . The first group is constituted by the rotational parts α of all operators $\{\alpha|\vec{t}_\alpha + \vec{R}_n\}$ in G , and the second is formed by all elements $\{\beta|\vec{b}\}$ of G , with $\vec{b} = \vec{t}_\beta + \vec{R}_p$, which has the property that $\exp(i\beta\vec{k}_1 \cdot \vec{R}_m) = \exp(i\vec{k}_1 \cdot \vec{R}_m)$ for all \vec{R}_m . This last condition can also be written as

$$\beta \vec{k}_i = \vec{k}_i + \vec{K}_q \quad (3.17)$$

where \vec{K}_q is a reciprocal lattice vector.

Of course, κ must be one of the possible space groups, and if G is symmorphic*, then ρ is a subgroup of G . It is also easy to observe that the rotational parts of the operators in κ must form a subgroup of ρ . We shall call this subgroup $\rho(\vec{k})$, indicating that it is the point group associated with the space group κ . Every operation of the space group G can be written as the product of a pure translation and an operation of the type $\{\alpha | \vec{t}_\alpha\}$, as can be seen by considering the law of multiplication (3.15):

$$\{\epsilon | \vec{R}_n\} \{\alpha | \vec{t}_\alpha\} = \{\epsilon \alpha | \epsilon(\vec{t}_\alpha) + \vec{R}_n\} = \{\alpha | \vec{t}_\alpha + \vec{R}_n\} \quad (3.18.a)$$

$$\{\alpha | \vec{t}_\alpha\} \{\epsilon | \alpha^{-1} \vec{R}_n\} = \{\alpha \epsilon | \alpha(\alpha^{-1} \vec{R}_n) + \vec{t}_\alpha\} = \{\alpha | \vec{t}_\alpha + \vec{R}_n\} \quad (3.18.b)$$

In Eq. (3.18.b) we have made use of the fact that $\alpha^{-1} \vec{R}_n$ is a lattice translation if \vec{R}_n is.

Assume that we know n orthonormal functions $b_{1,1}^{M(\vec{k})}(\vec{r}), \dots, b_{n,1}^{M(\vec{k})}(\vec{r})$, which satisfy Bloch condition with wave vector \vec{k} and transform like partners of the irreducible representation $M^{(\vec{k})}$ of the group of \vec{k} . Consider now the set of q operations $\{\alpha_i | \vec{a}_i\}$ with $\vec{a}_i = \vec{t}_{\alpha_i} + \vec{R}_n$, such that $\alpha_i \vec{k} = \vec{k}_i$, i.e., sends \vec{k} in one member of its star. Let us call κ_c this set of operations. It follows then that the set of (nq) functions

* The group is called symmorphic if \vec{t}_α is zero for all operations of G .

$$b_{j,i}^{M(\vec{k})}(\vec{r}) = \{\alpha_i | \vec{a}_i\} b_{j,1}^{M(\vec{k})}(\vec{r}) \quad (3.19)$$

form a basis for an irreducible representation of G^{26} , with $\{\alpha_i | \vec{a}_i\} = \{\epsilon | 0\}$. That $b_{j,i}^{M(\vec{k})}(\vec{r})$ satisfies the Bloch theorem with wave vector $\alpha_i \vec{k}$ can easily be verified by using Eq. (3.18). We have:

$$\{\epsilon | \vec{R}_m\} b_{j,i}^{M(\vec{k})}(\vec{r}) = \{\epsilon | R_m\} \{\alpha_i | \vec{a}_i\} b_{j,1}^{M(\vec{k})}(\vec{r}) \quad (3.20)$$

But

$$\begin{aligned} \{\epsilon | \vec{R}_m\} \{\alpha_i | \vec{a}_i\} &= \{\epsilon | \vec{R}_m\} \{\alpha_i | \vec{t}_{\alpha_i}\} \{\epsilon | \alpha_i^{-1} \vec{R}_n\} \\ &= \{\alpha_i | \vec{t}_{\alpha_i}\} \{\epsilon | \alpha_i^{-1} \vec{R}_m\} \{\epsilon | \alpha_i^{-1} \vec{R}_n\} \\ &= \{\alpha_i | \vec{a}_i\} \{\epsilon | \alpha_i^{-1} \vec{R}_m\} \end{aligned}$$

which allows us to write Eq. (3.20) as

$$\{\epsilon | \vec{R}_m\} b_{j,i}^{M(\vec{k})}(\vec{r}) = e^{i\vec{k} \cdot \alpha_i^{-1} \vec{R}_m} b_{j,i}^{M(\vec{k})}(\vec{r}) = e^{i\alpha_i \vec{k} \cdot \vec{R}_m} b_{j,i}^{M(\vec{k})}(\vec{r}) \quad (3.21)$$

because we have assumed at the beginning that $b_{j,1}^{M(\vec{k})}(\vec{r})$ satisfies the Bloch condition with wave-vector \vec{k} .

Now if \vec{k} is allowed to vary over the interior and surface of the Brillouin zone, all the irreducible representations of G can be obtained by finding irreducible representations of the space group κ associated with \vec{k} . Let us consider points in the interior of the Brillouin zone first. For these points the only value of \vec{K}_q for which $\beta \vec{k} = \vec{k} + \vec{K}_q$ is $\vec{K}_q = 0$. Let $\Gamma(\vec{k})$ be one irreducible represen-

tation of $\rho(\vec{k})$. It can be easily shown that we get an irreducible representation $M^{(\vec{k})}$ of κ by defining

$$M^{(\vec{k})}(\{\beta|\vec{b}\}) = e^{i\vec{k}\cdot\vec{b}} \Gamma^{(\vec{k})}(\beta) \quad (3.22)$$

Let us now consider a point on the surface of the zone. It is possible that, for some of these points, \vec{K}_q in Eq. (3.17) is a non-vanishing lattice vector in which case Eq. (3.22) does not hold in general. It does hold, however, if the space group is symmorphic, which means that the \vec{a} 's and \vec{b} 's are pure translations. In what follows we will deal with points in k-space where condition (3.22) holds.

We are now in a position to study the transformations properties of Bloch functions. Let us consider the function $b_{n,i}^{\Gamma_Y(\vec{k})}(\vec{k},\vec{r})$ which is characterized by wave vector \vec{k} and which transforms like the i-partner of the irreducible representation $\Gamma_Y^{(\vec{k})}$ of $\rho(\vec{k})$, i.e., if β belongs to $\rho(\vec{k})$ then

$$\beta b_{n,i}^{\Gamma_Y(\vec{k})}(\vec{k},\vec{r}) = \sum_j \Gamma_Y^{(\vec{k})}(\beta)_{j,i} b_{n,j}^{\Gamma_Y(\vec{k})}(\vec{k},\vec{r}) \quad (3.23)$$

Let us write $b_{n,i}^{\Gamma_Y(\vec{k})}(\vec{k},\vec{r})$ in the form $e^{i\vec{k}\cdot\vec{r}} u_{n,i}(\vec{k},\vec{r})$, where

$u_{n,i}(\vec{k},\vec{r})$ is a periodic function such that

$$u_{n,i}(\vec{k},\vec{r} + \alpha^{-1}\vec{a}) = u_{n,i}(\vec{k},\vec{r}) \quad (3.24)$$

where $\{\alpha|\vec{a}\}$ is an element of G . In this case, $b_{n,i}^{\Gamma_Y(\vec{k})}(\vec{k},\vec{r})$ also transforms like the i-partner of the irreducible representation

$M_Y^{\vec{k}}$ of the group of κ because

$$\begin{aligned} \{\beta|\vec{b}\} b_{n,i}^{\Gamma(\vec{k})}(\vec{k},\vec{r}) &= b_{n,i}^{\Gamma(\vec{k})}(\vec{k},\beta^{-1}(\vec{r}+\vec{b})) = e^{i\vec{k}\cdot\vec{b}} b_{n,i}^{\Gamma(\vec{k})}(\vec{k},\beta^{-1}\vec{r}) \\ &= e^{i\vec{k}\cdot\vec{b}} \sum_j \Gamma_Y^{\Gamma(\vec{k})}(\beta)_{j,i} b_{n,j}^{\Gamma(\vec{k})}(\vec{k},\vec{r}) \end{aligned} \quad (3.25)$$

In order to complete the study, let us analyze the functions

obtained from $b_{n,i}^{\Gamma(\vec{k})}(\vec{k},\vec{r})$ using Eq. (3.19), i.e.,

$$\{\alpha_j|\vec{a}_j\} b_{n,i}^{\Gamma(\vec{k})}(\vec{k},\vec{r}) \quad (3.26)$$

As discussed above, the function given by Eq. (3.25) is a partner of an irreducible representation of G . It can be shown²⁶ that for a given $\{\alpha|\vec{a}\}$ in G , there exist the elements $\{\alpha_m|\vec{a}_m\}$ and $\{\alpha_j|\vec{a}_j\}$ in κ_c , and an element $\{\beta|\vec{b}\}$ in κ , such that

$$\{\alpha|\vec{a}\} \{\alpha_j|\vec{a}_j\} = \{\alpha_m|\vec{a}_m\} \{\beta|\vec{b}\} \quad (3.27)$$

From Eq. (3.27) it can be seen that

$$\{\alpha|\vec{a}\} \{\alpha_j|\vec{a}_j\} b_{n,i}^{\Gamma(\vec{k})}(\vec{k},\vec{r}) = e^{i\vec{k}\cdot\vec{b}} \sum_j \Gamma_Y^{\Gamma(\vec{k})}(\beta)_{j,i} \{\alpha_m|\vec{a}_m\} b_{n,j}^{\Gamma(\vec{k})}(\vec{k},\vec{r}) \quad (3.28)$$

Now, because the operation $\{\alpha_j|\vec{a}_j\}$ is applied to a Bloch function and it can be written as the product of a pure translation by

$\{\alpha_j|\vec{t}_{\alpha_j}\}$ it is clear that we have to consider only the properties of $\{\alpha_j|\vec{t}_{\alpha_j}\} b_{n,i}^{\Gamma(\vec{k})}(\vec{k},\vec{r})$.

Eq. (3.21) shows that $\{\alpha_j | \vec{t}_{\alpha_j}\} b_{n,i}^{\Gamma}(\vec{k}, \vec{r})$ satisfies Bloch's theorem as if it had a wave vector $\alpha_j \vec{k}$. Thus

$$\{\alpha_j | \vec{t}_{\alpha_j}\} b_{n,i}^{\Gamma}(\vec{k}, \vec{r}) = e^{i \theta_{\alpha_j}(\vec{k})} B(\alpha_j \vec{k}, \vec{r}) \quad (3.29)$$

where $B(\alpha_j \vec{k}, \vec{r})$ is a Bloch function with wave vector $\alpha_j \vec{k}$ and $\theta_{\alpha_j}(\vec{k})$ is a real function of \vec{k} . But $\{\alpha_j | \vec{t}_{\alpha_j}\}$ being a space group operation leaves the crystal lattice and the electron charge density unchanged. Then, $\{\alpha_j | \vec{t}_{\alpha_j}\}$ will interchange members of the star of \vec{k} . The phase factor $\exp(i \theta_{\alpha_j}(\vec{k}))$ brought in by the symmetry operation $\{\alpha_j | \vec{t}_{\alpha_j}\}$ has to be specified and also one must express the function $B(\alpha_j \vec{k}, \vec{r})$ on the right-hand side of Eq. (3.29) in terms of the functions in the star of \vec{k} .

For a non-degenerate band, it is reasonable to define $b_n(\vec{k}, \alpha_j^{-1} \vec{r}) = b_n(\alpha_j \vec{k}, \vec{r})$ and in this case

$$\{\alpha_j | \vec{t}_{\alpha_j}\} b_n(\vec{k}, \vec{r}) = e^{i \alpha_j \vec{k} \cdot \vec{t}_{\alpha_j}} b_n(\alpha_j \vec{k}, \vec{r}) \quad (3.30)$$

Recently, however, Callaway and Hughes¹⁰, when studying bound states associated with localized defects in silicon, showed that if only non-degenerate bands are considered it is necessary to define

$$\{\alpha | \vec{t}_{\alpha}\} b_n(\vec{k}, \vec{r}) = \chi^{\Gamma}_{\beta}(\alpha) e^{i \alpha \vec{k} \cdot \vec{t}_{\alpha}} b_n(\alpha \vec{k}, \vec{r}) \quad (3.31)$$

in order that the periodic part of the Bloch function associated with band n vary smoothly in k-space. In Eq.(3.31) $\chi^{\Gamma}_{\beta}(\alpha)$ is the character of one

of the one-dimensional representation Γ_β of the point group and can only have the values ± 1 . This point is important in all problems where localized Wannier functions have to be defined, because the latter are localized at lattice sites only if the periodic parts of the Bloch functions vary smoothly in the Brillouin zone.

Later, Callaway²⁴ showed that Eq. (3.31) is a consequence of the $\vec{k} \cdot \vec{p}$ perturbation theory near $\vec{k}=0$ for a non-degenerate band. If Eq. (3.31) is satisfied at $\vec{k}=0$, it will be satisfied for all \vec{k} for which the perturbation series converges. In this case $\Gamma^\beta(\alpha)$ is the character of the irreducible representation of the band at $\vec{k}=0$.

Let us determine the properties of the Bloch functions obtained in the $\vec{k} \cdot \vec{\pi}$ scheme. We will limit ourselves to the case where the group of \vec{k}_0 is the point group of the crystal. In the $\vec{k} \cdot \vec{\pi}$ scheme, a Bloch function at \vec{k} is written, according to Eq.

$$(3.7) \text{ as } b_{n,i}^{\Gamma_Y(\vec{k})}(\vec{k}, \vec{r}) = \sum_{m,j} C_{n,m}^{i,j}(\vec{k}) e^{i\vec{k} \cdot \vec{r}} b_{m,j}^{\Gamma_\beta(\vec{k}_0)}(\vec{k}_0, \vec{r}) \quad (3.32)$$

Let $\{\alpha|\vec{a}\}$ be a general operation of the space group. In this case

$$\{\alpha|\vec{a}\} b_{n,i}^{\Gamma_Y(\vec{k})}(\vec{k}, \vec{r}) = \sum_{m,j} C_{n,m}^{i,j}(\vec{k}) e^{i\alpha\vec{k} \cdot (\vec{r}+\vec{a})} \sum_{\ell} \Gamma_\beta^{\Gamma(\vec{k}_0)}(\alpha)_{\ell,j} \times b_{m,\ell}^{\Gamma_\beta(\vec{k}_0)}(\vec{k}_0, \vec{r}) \quad (3.33)$$

At $\alpha\vec{k}$ the Bloch function for the same band n is given by Eq.

$$(3.34).$$

$$b_{n,i}^{\Gamma_Y(\alpha\vec{k})}(\alpha\vec{k},\vec{r}) = \sum_{m,j} C_{n,m}^{i,j}(\alpha\vec{k}) e^{i\alpha\vec{k}\cdot\vec{r}} b_{m,j}^{\Gamma_{\beta}(\vec{k}_0)}(\vec{k}_0,\vec{r}) \quad (3.34)$$

where we made use of the fact that $\alpha\vec{k}_0 = \vec{k}_0$. In order to relate Eq. (3.33) and Eq. (3.34) it is necessary to obtain the relation between $C_{n,m}^{i,j}(\vec{k})$ and $C_{n,m}^{i,j}(\alpha\vec{k})$.

The general term in the $\vec{k}\cdot\vec{\pi}$ secular matrix is given by Eq. (3.35.a) at \vec{k} , and by Eq. (3.36.a) at $\alpha\vec{k}$.

$$[E_m(\vec{k}_0) + \frac{\hbar^2 K^2}{2m} - \frac{\hbar^4 K^4}{8m^3 c^2} - E_n(\vec{k})] \delta_{n,m} \delta_{i,j} + \frac{\hbar^2 \vec{k}}{m} \cdot \langle b_{n,i}^{\Gamma_{\beta'}(\vec{k}_0)}(\vec{k}_0,\vec{r}) | \vec{\pi} | b_{m,j}^{\Gamma_{\beta}(\vec{k}_0)}(\vec{k}_0,\vec{r}) \rangle \quad (3.35.a)$$

$$[E_m(\vec{k}_0) + \frac{\hbar^2 K^2}{2m} - \frac{\hbar^4 K^4}{8m^3 c^2} - E_n(\alpha\vec{k})] \delta_{n,m} \delta_{i,j} + \frac{\hbar^2(\alpha\vec{k})}{m} \cdot \langle b_{n,i}^{\Gamma_{\beta'}(\vec{k}_0)}(\vec{k}_0,\vec{r}) | \vec{\pi} | b_{m,j}^{\Gamma_{\beta}(\vec{k}_0)}(\vec{k}_0,\vec{r}) \rangle \quad (3.36.a)$$

But because

$$\langle b_{n,i}^{\Gamma_{\beta'}(\vec{k}_0)}(\vec{k}_0,\vec{r}) | \vec{\pi} | b_{m,j}^{\Gamma_{\beta}(\vec{k}_0)}(\vec{k}_0,\vec{r}) \rangle = \langle \alpha b_{n,i}^{\Gamma_{\beta'}(\vec{k}_0)}(\vec{k}_0,\vec{r}) | (\alpha^{-1}\vec{\pi}) | \alpha b_{m,j}^{\Gamma_{\beta}(\vec{k}_0)}(\vec{k}_0,\vec{r}) \rangle \quad (3.37.a)$$

then

$$\begin{aligned} \alpha^{-1} \langle b_{n,i}^{\Gamma_{\beta'}(\vec{k}_0)}(\vec{k}_0,\vec{r}) | \vec{\pi} | b_{m,j}^{\Gamma_{\beta}(\vec{k}_0)}(\vec{k}_0,\vec{r}) \rangle &= \langle b_{n,i}^{\Gamma_{\beta'}(\vec{k}_0)}(\vec{k}_0,\vec{r}) | (\alpha^{-1}\vec{\pi}) | b_{m,j}^{\Gamma_{\beta}(\vec{k}_0)}(\vec{k}_0,\vec{r}) \rangle \\ &= \langle \alpha^{-1} b_{n,i}^{\Gamma_{\beta'}(\vec{k}_0)}(\vec{k}_0,\vec{r}) | \vec{\pi} | \alpha^{-1} b_{m,j}^{\Gamma_{\beta}(\vec{k}_0)}(\vec{k}_0,\vec{r}) \rangle \end{aligned} \quad (3.37.b)$$

In this case, Eq. (3.36.a) can be written as

$$[E_m(\vec{k}_0) + \frac{\hbar^2 K^2}{2m} - \frac{\hbar^4 K^4}{8m^3 c^2} - E_n(\alpha\vec{k})] \delta_{n,m} \delta_{i,j} + \frac{\hbar^2 \vec{k}}{m} \cdot \langle \alpha^{-1} b_{n,i}^{\Gamma_{\beta'}(\vec{k}_0)}(\vec{k}_0,\vec{r}) | \vec{\pi} | \alpha^{-1} b_{m,j}^{\Gamma_{\beta}(\vec{k}_0)}(\vec{k}_0,\vec{r}) \rangle \quad (3.36.b)$$

and the same coefficients are obtained using Eq. (3.36.a) or Eq. (3.36.b), the basis in the secular matrix being $e^{i\alpha\vec{k}\cdot\vec{r}} \Gamma_{\beta}^{(\vec{k}_0)} b_{n,i}(\vec{k}_0, \vec{r})$ in Eq. (3.36.a) and $e^{i\vec{k}\cdot\vec{r}} \alpha^{-1} \Gamma_{\beta}^{(\vec{k}_0)} b_{n,i}(\vec{k}_0, \vec{r})$ in Eq. (3.36.b).

Suppose we diagonalize Eq. (3.35.a) in a new basis, namely $e^{i\vec{k}\cdot\vec{r}} \alpha^{-1} \Gamma_{\beta}^{(\vec{k}_0)} b_{n,i}(\vec{k}_0, \vec{r})$. The general term in the secular matrix is now

$$[E_m(\vec{k}_0) + \frac{\hbar^2 \vec{k}^2}{2m} - \frac{\hbar^4 \vec{k}^4}{8m^3 c^2} - E_n(\vec{k})] \delta_{n,m} \delta_{i,j} + \frac{\hbar \vec{k} \cdot \alpha^{-1} \Gamma_{\beta}^{(\vec{k}_0)} b_{n,i}(\vec{k}_0, \vec{r}) | \vec{r} | \alpha^{-1} \Gamma_{\beta}^{(\vec{k}_0)} b_{m,j}(\vec{k}_0, \vec{r})}{m} \quad (3.35.b)$$

the Bloch function (3.32) being given by

$$\begin{aligned} \Gamma_{\beta}^{(\vec{k})} b_{n,i}(\vec{k}, \vec{r}) &= \sum_{m,l} C_{n,m}^{i,l(\text{new})}(\vec{k}) e^{i\vec{k}\cdot\vec{r}} \alpha^{-1} \Gamma_{\beta}^{(\vec{k}_0)} b_{m,l}(\vec{k}_0, \vec{r}) \\ &= \sum_{m,l} C_{n,m}^{i,l(\text{new})}(\vec{k}) \sum_j \Gamma_{\beta}^{(\vec{k}_0)}(\alpha^{-1})_{j,l} e^{i\vec{k}\cdot\vec{r}} \Gamma_{\beta}^{(\vec{k}_0)} b_{m,j}(\vec{k}_0, \vec{r}) \end{aligned} \quad (3.38.a)$$

From Eq. (3.32) and Eq. (3.38.a) we obtain

$$C_{n,m}^{i,j}(\vec{k}) = \sum_l C_{n,m}^{i,l(\text{new})}(\vec{k}) \Gamma_{\beta}^{(\vec{k}_0)}(\alpha^{-1})_{j,l} \quad (3.39.a)$$

But Eq. (3.36.b) and Eq. (3.35.b) are identical. Then

$$C_{n,m}^{i,l(\text{new})}(\vec{k}) = C_{n,m}^{i,l}(\alpha\vec{k}) \quad (3.39.b)$$

and taking into account the unitary nature of $\Gamma_{\beta}^{(\vec{k}_0)}(\alpha^{-1})$ we conclude that

$$C_{n,m}^{i,j}(\alpha\vec{k}) = \sum_l C_{n,m}^{i,l}(\vec{k}) \Gamma_{\beta}^{(\vec{k}_0)}(\alpha)_{j,l} \quad (3.40)$$

Comparison between Eq. (3.39) and Eq. (3.33) gives

$$\{\alpha|\vec{a}\} b_{n,i}^{\Gamma(\vec{k})}(\vec{k},\vec{r}) = e^{i\alpha\vec{k}\cdot\vec{a}} b_{n,i}^{\Gamma(\vec{k})}(\alpha\vec{k},\vec{r}) \quad (3.41)$$

which shows us that the application of one operation of the space group to a Bloch function at \vec{k} will produce a Bloch function in the star, corresponding to the same band and partner as the original Bloch function at \vec{k} . The $\vec{K}\cdot\vec{\pi}$ method, however, does not produce Bloch functions that vary smoothly in the Brillouin zone. We can easily verify this by considering, for example, the region near \vec{k}_0 . Consider a point \vec{k} and a band n and assume that at \vec{k}_0 , the i -partner of this band corresponds to the i' -partner of band n' , i.e.,

$$C_{n,m}^{i,j}(0) = \delta_{m,n'} \delta_{j,i'} \quad (3.42)$$

If we are seeking for a smooth function, then Eq. (3.42) must hold approximately near \vec{k}_0 , which means that if $K \approx 0$

$$\begin{aligned} C_{n,n'}^{i,i'}(\vec{K}) &\approx 1 \\ C_{n,m}^{i,j}(\vec{K}) &\approx 0 \quad , \text{ for } j \neq i' \text{ or } m \neq n' \end{aligned} \quad (3.43)$$

Consider now the Bloch function at $\alpha\vec{k}$. According to Eq. (3.40)

$$\begin{aligned} C_{n,m}^{i,j}(\alpha\vec{k}) &= \sum_{\ell} C_{n,m}^{i,\ell}(\vec{K}) \Gamma_{\beta}^{(\vec{k}_0)}(\alpha)_{j,\ell} \\ &\approx C_{n,m}^{i,i'}(\vec{K}) \Gamma_{\beta}^{(\vec{k}_0)}(\alpha)_{j,i'} \delta_{m,n'} \end{aligned} \quad (3.44)$$

where we have made use of Eq. (3.43). Thus

$$C_{n,n}^{i,j}(\alpha\vec{k}) \approx \Gamma_{\beta}^{(\vec{k}_0)}(\alpha)_{j,i}, \quad \text{for all } j$$

$$C_{n,m}^{i,j}(\alpha\vec{k}) \approx 0, \quad \text{for } m \neq n'$$
(3.45)

From Eq. (3.43) and Eq. (3.45) we can conclude that the periodic part of the Bloch function will not vary smoothly near \vec{k}_0 .

For the purposes of obtaining localized Wannier functions we are interested in generating Bloch functions that exhibit reasonable continuity near \vec{k}_0 . One way of doing this is to consider, for every α , a new set of values for the coefficients, which we will call $C_{n,n'}^{i,j(\text{mod})}(\alpha\vec{k})$, such that they vary smoothly near \vec{k}_0 . Define

$$C_{n,n'}^{i,j(\text{mod})}(\alpha\vec{k}) = \sum_q \{ \Gamma_{\beta}^{(\vec{k}_0)}(\alpha)^{-1} \}_{j,q} C_{n,n'}^{i,q}(\alpha\vec{k})$$
(3.46)

In this case

$$C_{n,n'}^{i,j(\text{mod})}(\alpha\vec{k}) = \sum_q [\Gamma_{\beta}^{(\vec{k}_0)}(\alpha)^{-1}]_{j,q} \sum_{\ell} \Gamma_{\beta}^{(\vec{k}_0)}(\alpha)_{q,\ell} C_{n,n'}^{i,\ell}(\vec{k})$$

$$= \sum_{\ell} \delta_{j,\ell} C_{n,n'}^{i,\ell}(\vec{k}) = C_{n,n'}^{i,j}(\vec{k})$$
(3.47)

The transformation we have performed is unitary, because the matrices for the representation at \vec{k}_0 are unitary. If bands n and n' are one-dimensional, then

$$C_{n,n'}^{1,1(\text{mod})}(\alpha\vec{k}) = \chi_{\beta}^{\Gamma_{\beta}^{(\vec{k}_0)}(\alpha)} C_{n,n'}^{1,1}(\alpha\vec{k})$$
(3.48)

which is similar to the result obtained by Callaway²⁴.

When $|\vec{k}-\vec{k}_0|$ is large, probably other bands besides n' contribute

significantly to band n at \vec{k} . In this case the coefficients corresponding to these bands will not be continuous with the above transformation. Further considerations about the proper choice of the phases of Bloch functions will be made in section (4.3) in connection with the study of Wannier functions in PbTe.

Now, if \vec{k} is a symmetry point, i.e., there exist operations α other than identity such that

$$\alpha \vec{k} = \vec{k} \quad (3.49)$$

Bloch functions at this point have to transform under α like partners of the irreducible representations of the group of \vec{k}

$$\alpha b_{n,i}^{\Gamma_{\beta}(\vec{k})}(\vec{k}, \vec{r}) = \sum_{\ell} \Gamma_{\beta}(\alpha)_{\ell,i} b_{n,\ell}^{\Gamma_{\beta}(\vec{k})}(\vec{k}, \vec{r}) \quad (3.50)$$

In this case by means of suitable rotations of the basis functions the $\vec{k} \cdot \vec{r}$ matrix can be factored, each block corresponding to a certain irreducible representation of the group of \vec{k} . Only partners of the irreducible representations of the group of \vec{k}_0 compatible with partners of a certain irreducible representation of the group \vec{k} will enter the block corresponding to the latter representation. Examples of this and also of the special points on the zone faces where $\alpha \vec{k} = \vec{k} + \vec{K}_1$, will be discussed in section (3.4).

3.4 $\vec{k} \cdot \vec{\pi}$ - APW RESULTS FOR PBTE

Let us now apply the theory of section 3.2 to PbTe. Point \vec{k}_0 is chosen to be the point Γ in k-space and in this case the group of \vec{k}_0 is the point group of the crystal.

As mentioned in Chapter 2, the first step in the APW calculation consists of obtaining the non-relativistic bands, i.e., the eigenfunctions and eigenvalues of $H_0 = \vec{p}^2/2m + V(\vec{r})$, where $V(\vec{r})$ is the periodic potential. The Darwin and mass-velocity corrections are introduced next and because they have the full crystal symmetry only a mixing between eigenfunctions of H_0 with the same symmetry occurs. Although there is a considerable change in the energy eigenvalues, the eigenfunctions are almost the same, i.e., the mixing between them is small. The change in energy is essentially due to the diagonal matrix elements of the Darwin and mass-velocity corrections, rather than to matrix elements between different bands. Spin-orbit interaction is finally taken into account and the double group irreducible representations have to be considered.

Fig. 3.1 shows schematically the non-relativistic and full relativistic bands obtained by Conklin¹² at Γ . In this figure and in the subsequent considerations we will represent the energy bands by the corresponding irreducible representations. Because this labelling is not unique, an extra index m is introduced. Thus ${}^m\Gamma_{n,i}$ will represent the i -partner of the m^{th} band which transforms like the irreducible representation Γ_n . Fig. 3.1 also shows the

unnormalized energies* in atomic units.

$2\Gamma_1$	0.90630	$2\Gamma_8^+$	0.84236
Γ_{12}	0.86858	$2\Gamma_6^+$	0.76205
Γ_2^-	0.71545	Γ_7^-	0.71544
Γ_{25}^-	0.67443	Γ_7^+, Γ_8^+	0.65688
$2\Gamma_{15}$	0.60947	$2\Gamma_6^-$	0.53923
	GAP	$2\Gamma_6^-$	0.41076
$1\Gamma_{15}$	0.17921		GAP
$1\Gamma_1$	0.10285	$1\Gamma_8^-$	0.14172
		$1\Gamma_6^-$	0.06586
		$1\Gamma_6^+$	0.20857
$3\Gamma_1$	-0.53758	$3\Gamma_6^+$	0.67639

a) non-relativistic

a) relativistic

Fig. 3.1 - Schematic representation of the energy levels at Γ for PbTe (after Conklin)

Due to the fact that Γ is a point of high symmetry, only a few SAPW's are necessary in order to obtain a reasonable energy convergence. In fact, Conklin used 9 SAPW's for Γ_1 -levels, 11 for Γ_{15} -levels, 7 for Γ_{25}' -levels, and 4 for Γ_2^- and Γ_{12} -levels. The transformation properties of the partners of the single-group

* In order to obtain the correct or normalized energies the value of the constant potential (-0.80138 a.u.) must be added.

irreducible representations are shown in Table 3.1, where a system of coordinates with axes in the (100), (010) and (001) directions is considered.

TABLE 3.1 - Transformation properties of the single-group irreducible representations at Γ .

Representation		Transformation properties
	Partner	
Γ_1		s
Γ_{15}	1 st	x
	2 nd	y
	3 rd	z
Γ_{12}	1 st	$\sqrt{3} (x^2 - y^2)$
	2 nd	$3z^2 - r^2$
Γ'_2		xyz
Γ'_{25}	1 st	yz
	2 nd	xz
	3 rd	xy

Table 3.2 shows how to write the partners of the double-group irreducible representations in terms of the single-group irreducible representations. In that table, $\Gamma_{n,i}(\Gamma_m)$ represents the i-partner of the Γ_n -double-group irreducible representation

TABLE 3.2 - Relations between partners of the double-group and single-group irreducible representations at Γ .

$\Gamma_{6,1}^+(\Gamma_1) = \Gamma_1 S_\alpha$ $\Gamma_{6,2}^+(\Gamma_1) = \Gamma_1 S_\beta$
$\Gamma_{7,1}^+(\Gamma'_{25}) = \frac{1}{\sqrt{3}} [(-i\Gamma'_{25,1} + \Gamma'_{25,2})S_\beta - i\Gamma'_{25,3}S_\alpha]$ $\Gamma_{7,2}^+(\Gamma'_{25}) = \frac{1}{\sqrt{3}} [(-i\Gamma'_{25,1} - \Gamma'_{25,2})S_\alpha + i\Gamma'_{25,3}S_\beta]$
$\Gamma_{8,1}^+(\Gamma'_{25}) = \frac{1}{\sqrt{6}} [(i\Gamma'_{25,1} + \Gamma'_{25,2})S_\alpha + 2i\Gamma'_{25,3}S_\beta]$ $\Gamma_{8,4}^+(\Gamma'_{25}) = \frac{1}{\sqrt{6}} [(-i\Gamma'_{25,1} + \Gamma'_{25,2})S_\beta + 2i\Gamma'_{25,3}S_\alpha]$ $\Gamma_{8,3}^+(\Gamma'_{25}) = \frac{1}{\sqrt{2}} (i\Gamma'_{25,1} - \Gamma'_{25,2})S_\alpha$ $\Gamma_{8,2}^+(\Gamma'_{25}) = \frac{1}{\sqrt{2}} (-i\Gamma'_{25,1} - \Gamma'_{25,2})S_\beta$
$\Gamma_{6,1}^-(\Gamma_{15}) = \frac{1}{\sqrt{3}} [(-i\Gamma_{15,1} + \Gamma_{15,2})S_\beta - i\Gamma_{15,3}S_\alpha]$ $\Gamma_{6,2}^-(\Gamma_{15}) = \frac{1}{\sqrt{3}} [(-i\Gamma_{15,1} - \Gamma_{15,2})S_\alpha + i\Gamma_{15,3}S_\beta]$
$\Gamma_{7,1}^-(\Gamma'_2) = \Gamma'_2 S_\alpha$ $\Gamma_{7,2}^-(\Gamma'_2) = \Gamma'_2 S_\beta$
$\Gamma_{8,1}^-(\Gamma_{15}) = \frac{1}{\sqrt{2}} (-i\Gamma_{15,1} + \Gamma_{15,2})S_\alpha$ $\Gamma_{8,4}^-(\Gamma_{15}) = \frac{1}{\sqrt{2}} (i\Gamma_{15,1} + \Gamma_{15,2})S_\beta$ $\Gamma_{8,3}^-(\Gamma_{15}) = \frac{1}{\sqrt{6}} [(\Gamma_{15,1} + \Gamma_{15,2})S_\alpha + 2i\Gamma_{15,3}S_\beta]$ $\Gamma_{8,2}^-(\Gamma_{15}) = \frac{1}{\sqrt{6}} [(-i\Gamma_{15,1} + \Gamma_{15,2})S_\beta + 2i\Gamma_{15,3}S_\alpha]$

coming from the Γ_m -single-group irreducible representation at Γ , and S_α and S_β are the common "spin-up" and "spin-down" functions. It can be observed that the partners of the double-group representations form Kramers pairs. For two-dimensional representations $\Gamma_{n,2} = K\Gamma_{n,1}$, where here K is the time-reversal operator and for four-dimensional representations, $\Gamma_{n,4} = K\Gamma_{n,1}$ and $\Gamma_{n,2} = K\Gamma_{n,3}$.

The coefficients of the mixing between the non-relativistic bands due to the relativistic corrections at Γ are shown in Table 3.3. For the bands not shown in that table the coefficient is 1.0.

TABLE 3.3 - Mixing between the non-relativistic bands due to the relativistic corrections, in Conklin's calculation.

	$\Gamma_6^+(^1\Gamma_1)$	$\Gamma_6^+(^2\Gamma_1)$	$\Gamma_6^+(^3\Gamma_1)$	$\Gamma_6^-(^1\Gamma_{15})$	$\Gamma_6^-(^2\Gamma_{15})$	$\Gamma_8^-(^1\Gamma_{15})$	$\Gamma_8^-(^2\Gamma_{15})$
$1\Gamma_6^+$	0.9833	0.1622	+0.0821	0.0	0.0	0.0	0.0
$2\Gamma_6^+$	-0.1686	+0.9826	0.0776	0.0	0.0	0.0	0.0
$3\Gamma_6^+$	0.0681	0.0902	-0.9936	0.0	0.0	0.0	0.0
$1\Gamma_6^-$	0.0	0.0	0.0	+0.9963	0.0861	0.0	0.0
$2\Gamma_6^-$	0.0	0.0	0.0	0.0861	-0.9963	0.0	0.0
$1\Gamma_8^-$	0.0	0.0	0.0	0.0	0.0	+0.9996	0.0287
$2\Gamma_8^-$	0.0	0.0	0.0	0.0	0.0	0.0287	-0.9996

As we have seen in section 3.2, in order to obtain the $\vec{k} \cdot \vec{\pi}$ secular matrix elements it is necessary to calculate the matrix

elements of $\vec{\pi}$ between Bloch functions at Γ , $\vec{\pi}$ being given by (3.9.a). Because the relativistic bands are written in terms of the non-relativistic bands (multiplied by appropriate spin functions) we have to determine, first, the matrix elements of $\vec{\pi}$ between the non-relativistic bands.

The calculation of the matrix elements of the first three terms in (3.9.a), which are \vec{K} -independent, can be performed by a computer program originally written by Dr. L. G. Ferreira and modified by us in order to make it applicable to the Γ point. As it happens at the L point¹⁴, the second and third terms give matrix elements which are 10^{-3} to 10^{-6} smaller than the corresponding momentum matrix elements and can be disregarded. The three other terms in (3.9.a), which are \vec{K} -dependent, and do not enter in the effective-mass calculations, where \vec{K} is assumed small, were studied by us. A computer program was written in order to calculate the matrix elements of these terms between the non-relativistic bands. Results at Γ showed that they are also of the order of 10^{-3} to 10^{-6} compared with any other term, if \vec{K} is limited to the first Brillouin zone. These considerations show us that only the momentum matrix elements themselves are important in the calculations. This does not mean that we are disregarding the relativistic corrections. What have been disregarded are the contributions of these terms to the $\vec{\pi}$ operator. Observe that H_0 in (3.5) contains all relativistic corrections.

Let us determine the expressions for the momentum matrix elements between single-group representations at Γ . This can be easily done by noting that \vec{p} transforms like Γ_{15} and using the transformation properties of table 3.1. Because the group of Γ (point group) contains inversion, then the only non-zero matrix elements are those relating bands with different parities. The results are shown in table 3.4, where the three expressions for each matrix element correspond to the matrix elements of p_x , p_y and p_z , respectively.

The momentum matrix elements between double-group representations can be obtained through tables 3.2 and 3.4. They are shown in table 3.5 for one member of each Kramers pairs.

The matrix elements between different partners are not all independent but are related by

$$\langle \Gamma_{n,2} | \vec{p} | \Gamma_{m,1} \rangle = \langle \Gamma_{n,1} | \vec{p} | \Gamma_{m,1} \rangle^* \quad (3.51.a)$$

$$\langle \Gamma_{n,2} | \vec{p} | \Gamma_{m,1} \rangle = -\langle \Gamma_{n,1} | \vec{p} | \Gamma_{m,2} \rangle^* \quad (3.51.b)$$

We recall that for four-dimensional double-group representations there are two Kramers pairs and the results are valid for each pair separately.

TABLE 3.4 - Momentum matrix elements between single-group irreducible representations at Γ .

	Γ'_2	$\Gamma_{15,1}$	$\Gamma_{15,2}$	$\Gamma_{15,3}$
Γ_1	0 0 0	$M_{1;15}$ 0 0	0 $M_{1;15}$ 0	0 0 $M_{1;15}$
$\Gamma_{12,1}$	0 0 0	$M_{12;15}$ 0 0	0 $-M_{12;15}$ 0	0 0 0
$\Gamma_{25,2}$	0 0 0	$\frac{-1}{\sqrt{3}}M_{12;15}$ 0 0	0 $\frac{-1}{\sqrt{3}}M_{12;15}$ 0	0 0 $\frac{2}{\sqrt{3}}M_{12;15}$
$\Gamma'_{25,1}$	$M_{25;2}$ 0 0	0 0 0	0 0 $M_{25;15}$	0 $M_{25;15}$ 0
$\Gamma'_{25,2}$	0 $M_{25;2}$ 0	0 0 $M_{25;15}$	0 0 0	$M_{25;15}$ 0 0
$\Gamma'_{25,3}$	0 0 $M_{25;2}$	0 $M_{25;15}$ 0	$M_{25;15}$ 0 0	0 0 0

TABLE 3.5 - Momentum matrix elements between double-group representations at Γ .
 (a = $1/\sqrt{3}$; b = $1/\sqrt{2}$; c = $1/\sqrt{6}$; d = $1/3$)

	$\Gamma_{6,1}^-(\Gamma_{15})$	$\Gamma_{6,2}^-(\Gamma_{15})$	$\Gamma_{7,1}^-(\Gamma_2')$	$\Gamma_{7,2}^-(\Gamma_2')$	$\Gamma_{8,1}^-(\Gamma_{15})$	$\Gamma_{8,2}^-(\Gamma_{15})$	$\Gamma_{8,3}^-(\Gamma_{15})$	$\Gamma_{8,4}^-(\Gamma_{15})$
$\Gamma_{6,1}^+(\Gamma_1)$	0 0 -iaM _{1,15}	-iaM _{1,15} - aM _{1,15} 0	0 0 0	0 0 0	-ibM _{1,15} bM _{1,15} 0	0 0 2icM _{1,15}	icM _{1,15} cM _{1,15} 0	0 0 0
$\Gamma_{7,1}^+(\Gamma_{25}')$	0 0 0	0 0 0	0 0 iaM _{25,2}	iaM _{25,2} aM _{25,2} 0	icM _{25,15} cM _{25,15} 0	0 0 0	ibM _{25,15} -bM _{25,15} 0	0 0 2icM _{25,15}
$\Gamma_{8,1}^+(\Gamma_{25}')$	-ibM _{25,15} - bM _{25,15} 0	0 0 0	-icM _{25,2} cM _{25,2} 0	0 0 -2icM _{25,2}	0 0 -iaM _{25,15}	0 0 0	0 0 0	-iaM _{25,15} aM _{25,15} 0
$\Gamma_{8,3}^+(\Gamma_{25}')$	icM _{25,15} -cM _{25,15} 0	0 0 2icM _{25,15}	-ibM _{25,2} - bM _{25,2} 0	0 0 0	0 0 0	-iaM _{25,15} aM _{25,15} 0	0 0 -iaM _{25,15}	0 0 0
$\Gamma_{8,1}^+(\Gamma_{12})$	iaM _{12,15} aM _{12,15} 0	0 0 0	0 0 0	0 0 0	0 0 0	icM _{12,15} cM _{12,15} 0	0 0 0	-ibM _{12,15} bM _{12,15} 0
$\Gamma_{8,3}^+(\Gamma_{12})$	-idM _{12,15} dM _{12,15} 0	0 0 -2idM _{12,15}	0 0 0	0 0 0	0 0 0	-idbM _{12,15} dbM _{12,15} 0	0 0 -4idbM _{12,15}	icM _{12,15} cM _{12,15} 0

The eleven independent momentum matrix elements were calculated using Conklin's non-relativistic bands at Γ . Although a good energy convergence was obtained, the same was not true for all momentum matrix elements, as it can be observed in figure 3.2, where the dependence of the matrix elements on the number of SAPW's is shown. In that figure the SAPW's are included in the order of decreasing magnitude of their K_q -vector. It can be easily seen that some of the momentum matrix elements present a good convergence, but others do not. For all of them a tentative extrapolation based on the behavior of the curves was performed* and the extrapolated values used in the solution of the $\vec{K} \cdot \vec{\pi}$ secular equation for the symmetry axes. The values of the matrix elements calculated with the maximum number of SAPW's available and the extrapolated values are shown in table 3.6.

As we mentioned at the end of section 3.3, the compatibility relations between the irreducible representations of the various groups of k-vector and the transformation properties of their basis functions can be used to factor the $\vec{K} \cdot \vec{\pi}$ secular matrix along the symmetry axes. Table 3.7 shows the compatibility relations between the important irreducible representations of the group of Γ and the groups of Δ , Λ and Σ , respectively.

Suppose we wish to obtain the energy bands on the Δ -axis.

* In this extrapolation we did not take into consideration the dashed-line part of the curves.

TABLE 3.6 - Matrix elements of $\frac{\hbar}{m} \vec{p}$ between basis functions at Γ . In this table we represent $\langle {}^n\Gamma_i | \frac{\hbar}{m} \vec{p} | {}^m\Gamma_j \rangle$ by $\frac{\hbar}{m} M_{i;j}^{n;m}$. The calculated values refer to the values calculated with the maximum number of SAPW's available.

Matrix elements (a.u)	Ref. No. on Figs. 3.2 & 3.	Conklin's bands		New calculation	
		calcu- lated	extrapo- lated	calcu- lated	extrap- lated
$\frac{\hbar}{m} M_{1;15}^{1;1}$	9	1.029	1.045	0.969	0.969
$\frac{\hbar}{m} M_{1;15}^{1;2}$	4	0.261	0.250	0.250	0.250
$\frac{\hbar}{m} M_{1;15}^{2;1}$	- 3	-0.269	-0.270	-0.155	-0.155
$\frac{\hbar}{m} M_{1;15}^{2;2}$	8	0.830	0.790	1.180	1.180
$\frac{\hbar}{m} M_{1;15}^{3;1}$	2	0.421	0.418	0.437	0.437
$\frac{\hbar}{m} M_{1;15}^{3;2}$	- 1	-0.213	-0.212	-0.225	-0.225
$\frac{\hbar}{m} M_{12;15}^{1;1} \frac{\sqrt{6}}{2}$	6	0.516	0.496	0.534	0.534
$\frac{\hbar}{m} M_{12;15}^{1;2} \frac{\sqrt{6}}{2}$	7	-1.381	-1.350	-1.456	-1.456
$\frac{\hbar}{m} M_{25;2}$	10	0.929	0.926	0.949	0.949
$\frac{\hbar}{m} M_{25;15}^{1;1} \frac{\sqrt{3}}{2}$	11	1.038	1.021	1.068	1.068
$\frac{\hbar}{m} M_{25;15}^{1;2} \frac{\sqrt{3}}{2}$	5	0.442	0.448	0.460	0.460

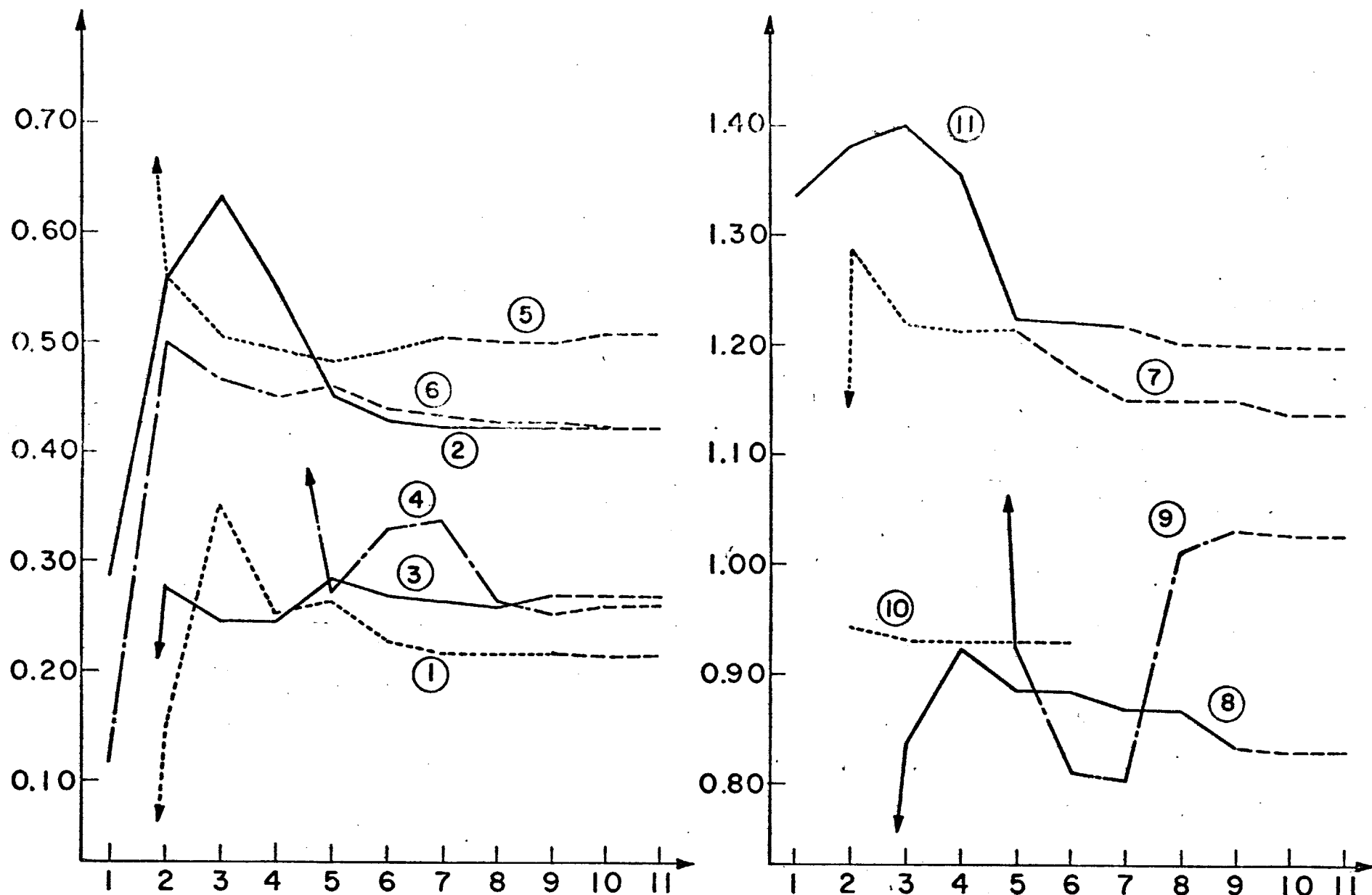


FIGURE 3.2 - Momentum matrix elements at Γ obtained with the non-relativistic bands of Conklin's APW calculation plotted against the number of SAPW's constituting the wave-functions. The dashed-line parts of the curves correspond to the matrix elements calculated considering the variation of the number of SAPW's of only one wave-function (the wave-functions have been calculated with different number of SAPW's)

TABLE 3.7 - Compatibility relations between the interesting irreducible representations of the group of Γ and the groups of Δ , Σ and Λ respectively.

Γ -point	Γ_1	Γ_{12}	Γ'_{25}	Γ'_2	Γ_{15}	Γ_6^\pm	Γ_7^\pm	Γ_8^\pm
Δ -axis	Δ_1	$\Delta_1+\Delta_2$	$\Delta'_2+\Delta_5$	Δ'_2	$\Delta_1+\Delta_5$	Δ_6	Δ_7	$\Delta_6+\Delta_7$
Σ -axis	Σ_1	$\Sigma_1+\Sigma_4$	$\Sigma_1+\Sigma_2+\Sigma_3$	Σ_3	$\Sigma_1+\Sigma_3+\Sigma_4$	Σ_5	Σ_5	$\Sigma_5+\Sigma_5$
Λ -axis	Λ_1	Λ_3	$\Lambda_1+\Lambda_3$	Λ_1	$\Lambda_1+\Lambda_3$	Λ_6	Λ_6	$\Lambda_6+\Lambda_4, \Lambda_5$

The Δ_6 levels are obtained by diagonalizing the $\vec{k} \cdot \vec{\pi}$ secular matrix that contains only the Γ_6^\pm and Γ_8^\pm bands, because only they are compatible with Δ_6 . This conclusion could be also obtained from table 3.5 remembering that on the $\langle 100 \rangle$ axis only the x component of \vec{p} is non-zero. Further simplifications can be achieved by using the fact that due to time reversal symmetry the two partners of the Δ_6 levels must form a Kramers pair. The diagonalization is then performed for each partner separately, thereby reducing the dimension of the secular matrix by half. From table 3.5 and relations (3.51) we obtain that the first partner of Δ_6 , for example, is given by

$$\Gamma_{6,1}^+; (c\Gamma_{8,2}^+ - b\Gamma_{8,4}^+) / (c^2 + b^2)^{1/2}; \Gamma_{6,2}^-; (b\Gamma_{8,1}^- - c\Gamma_{8,3}^-) / (c^2 + b^2)^{1/2}$$

while the second partner is obtained from

$$\Gamma_{6,2}^+; (b\Gamma_{8,1}^+ - c\Gamma_{8,3}^+) / (c^2 + b^2)^{1/2}; \Gamma_{6,1}^-; (c\Gamma_{8,2}^- - b\Gamma_{8,4}^-) / (c^2 + b^2)^{1/2}$$

On the other hand, the first partner of Δ_7 will have contributions coming from

$$\Gamma_{7,1}^+; (b\Gamma_{8,2}^+ + c\Gamma_{8,4}^+) / (c^2 + b^2)^{1/2}; \Gamma_{7,2}^-; (c\Gamma_{8,1}^- + b\Gamma_{8,3}^-) / (c^2 + b^2)^{1/2}$$

The second partner of Δ_7 is obtained from

$$\Gamma_{7,2}^+; (c\Gamma_{8,1}^+ + b\Gamma_{8,3}^+) / (c^2 + b^2)^{1/2}; \Gamma_{7,1}^-; (b\Gamma_{8,2}^- + c\Gamma_{8,4}^-) / (c^2 + b^2)^{1/2}$$

The same kind of reduction can easily be performed along the (110) and (111) axis.

When reaching the zone faces a special care has to be taken with respect to the wave-functions, because there are some special points such as L, X, etc., for which $\alpha\vec{k} = \vec{k} + \vec{K}_1$, where \vec{K}_1 is a reciprocal lattice vector and α is an operation of the crystal point group. Let us consider the L-point, for example. Although the energies at this point can be obtained by diagonalizing the $\vec{K} \cdot \vec{\pi}$ secular matrix on the Λ -axis for $\vec{k}_L = \frac{\pi}{a} (1,1,1)$, the wave-functions will not have the proper symmetry. Because the L-point [$\vec{k}_{-L} = \frac{\pi}{a} (-1,-1,-1)$] is equivalent to L [$\vec{k}_L = \frac{\pi}{a} (1,1,1)$] we must find linear combinations of the functions obtained by the above diagonalizations at L and -L, that transform like the irreducible representations of the group of L. This can be accomplished by using projection operators or by arguments similar to the following. Suppose that when performing the diagonalization in the Λ -axis for $\vec{k} = \vec{k}_L$ the following linear combination is obtained for a Λ_6 -level

$$b_{n,i}^{\Lambda_6}(\vec{k}_L, \vec{r}) = e^{i\vec{k}_L \cdot \vec{r}} \sum_{m,j} C_{n,m}^{i,j}(\vec{k}_L) b_{m,j}^{\Gamma_\beta}(0, \vec{r}) \quad (3.52)$$

At $-L$ the same band will be given by

$$b_{n,i}^{\Lambda_6}(-\vec{k}_L, \vec{r}) = e^{-i\vec{k}_L \cdot \vec{r}} \sum_{m,j} C_{n,m}^{i,j}(-\vec{k}_L) b_{m,j}^{\Gamma_\beta}(0, \vec{r}) \quad (3.53)$$

Observe that in both expressions the only Bloch functions at Γ that enter are those which transform like irreducible representations compatible with Λ_6 .

As both L_6^+ and L_6^- are compatible with Λ_6 , we have to find out which linear combinations of (3.52) and (3.53) will transform as L_6^+ or L_6^- . The group of L contains, besides the operations α of the group of Λ , also the operations $J\alpha$, where J is the inversion operation. No distinction can be made between the L_6^+ and L_6^- representations as far as the operations of the group of Λ are concerned.

Under the operations of the group of Λ the functions (3.51) and (3.52), or any combination of them, transform in the same way, i.e., as the i -partner of the Λ_6 irreducible representation (also as the i -partner of the L_6^+ or L_6^- representations). Consider now an operation $J\alpha$ of the group of L . This operation sends \vec{k}_L to $-\vec{k}_L$ and when applied to (3.51) or (3.52) gives $e^{-i\vec{k}_L \cdot \vec{r}}$ or $e^{i\vec{k}_L \cdot \vec{r}}$ multiplied by the same linear combination which is obtained when α is applied to (3.51) or (3.52), with the exception that the terms corresponding to odd parity bands are multiplied by -1 . The operation that transforms \vec{k}_L into $-\vec{k}_L$ is J and according to (3.40)

$$C_{n,m}^{i,j}(-\vec{k}_L) = \sum_{\ell} C_{n,m}^{i,\ell}(\vec{k}_L) \Gamma_{\beta} (J)_{j,\ell} = C_{n,m}^{i,j}(\vec{k}_L) \Gamma_{\beta} (J)_{j,j} \quad (3.54)$$

If the representation Γ_{β} has even parity $\Gamma_{\beta}(J)_{j,j}=1$ and $C_{n,m}^{i,j}(-\vec{k}_L) = C_{n,m}^{i,j}(\vec{k}_L)$. On the other hand if Γ_{β} has odd parity $\Gamma_{\beta}(J) = -1$ and $C_{n,m}^{i,j}(-\vec{k}_L) = -C_{n,m}^{i,j}(\vec{k}_L)$. Thus

$$\begin{aligned} b_{n,i}^{\Lambda_6}(\vec{k}_L, \vec{r}) &= e^{i\vec{k}_L \cdot \vec{r}} \left[\sum_{m,j} (+) C_{n,m}^{i,j}(\vec{k}_L) (+) b_{m,j}^{\Gamma_{\beta}^+}(0, \vec{r}) \right. \\ &+ \left. \sum_{m,j} (-) C_{n,m}^{i,j}(\vec{k}_L) (-) b_{m,j}^{\Gamma_{\beta}^-}(0, \vec{r}) \right] \end{aligned} \quad (3.55.a)$$

$$\begin{aligned} b_{n,i}^{\Lambda_6}(-\vec{k}_L, \vec{r}) &= e^{-i\vec{k}_L \cdot \vec{r}} \left[\sum_{m,j} (+) C_{n,m}^{i,\ell}(\vec{k}_L) (+) b_{m,j}^{\Gamma_{\beta}^+}(0, \vec{r}) + \right. \\ &- \left. \sum_{m,j} (-) C_{n,m}^{i,j}(\vec{k}_L) (-) b_{m,j}^{\Gamma_{\beta}^-}(0, \vec{r}) \right] \end{aligned} \quad (3.55.b)$$

where in expressions (3.55) we have separated the contributions coming from the even and odd-parity representations. We can easily observe that

$$J\alpha b_{n,i}^{\Lambda_6}(\pm \vec{k}_L, \vec{r}) = \alpha b_{n,i}^{\Lambda_6}(\pm \vec{k}_L, \vec{r}) \quad (3.56)$$

But since

$$J\alpha b_{n,i}^{L_6^+}(\vec{k}_L, \vec{r}) = \alpha b_{n,i}^{L_6^+}(\vec{k}_L, \vec{r}) \quad (3.57.a)$$

$$J\alpha b_{n,i}^{L_6^-}(\vec{k}_L, \vec{r}) = -\alpha b_{n,i}^{L_6^-}(\vec{k}_L, \vec{r}) \quad (3.57.b)$$

we conclude that

$$b_{n,i}^{L+}(\vec{k}_L, \vec{r}) = \frac{b_{n,i}^{\Lambda_6}(\vec{k}_L, \vec{r}) + b_{n,i}^{\Lambda_6}(-\vec{k}_L, \vec{r})}{\sqrt{2}} \quad (3.58.a)$$

$$b_{n,i}^{L-}(\vec{k}_L, \vec{r}) = \frac{b_{n,i}^{\Lambda_6}(\vec{k}_L, \vec{r}) - b_{n,i}^{\Lambda_6}(-\vec{k}_L, \vec{r})}{\sqrt{2}} \quad (3.58.b)$$

Although the calculated bands along the symmetry axes did not agree very well with Conklin's results and the calculated gap was much bigger than the experimental gap, the qualitative behavior of Conklin's bands was obtained. This suggested to us that if an APW band calculation was to be performed at Γ with more SAPW for each level, certainly better results could be achieved. Based on this idea, a new APW calculation was performed at Γ using 15 SAPW's for each level. Although the energy levels and mixing changed very little compared with Conklin's results, as can be deduced from figures 3.3 and 3.1 and tables 3.8 and 3.3, an excellent convergence was now obtained for all momentum matrix elements as seen in table 3.6 or figure 3.4. The new values for the momentum matrix elements were then used in the $\vec{K} \cdot \vec{\pi}$ secular matrix, which was diagonalized for values of \vec{k} along the symmetry axes.

With these new matrix elements the energy gap at L was found to be equal to 0.0256Ry (0.340ev), which is bigger than the experimental gap of 0.023Ry (0.31ev).³

A quantitative study of the influence of the various momentum matrix elements in the $\vec{K} \cdot \vec{\pi}$ bands, along the symmetry axes, was then

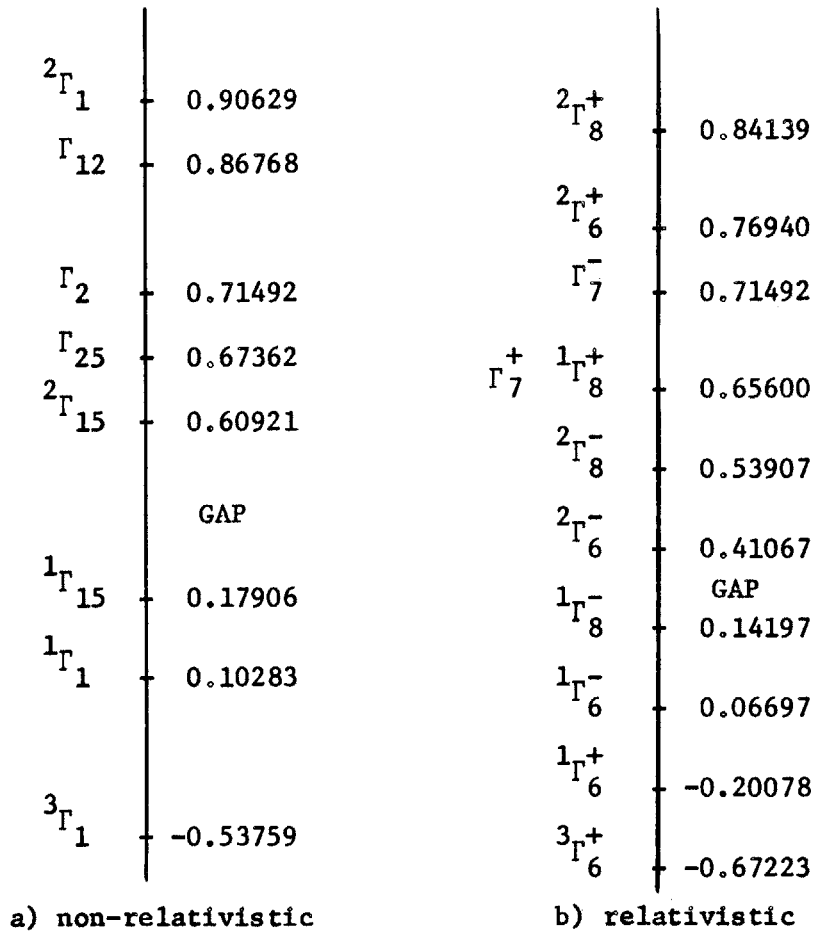


Fig. 3.3 - Schematic representation of the energy levels at Γ for PbTe (new calculation).

TABLE 3.8 - Mixing between the non-relativistic bands due to the relativistic corrections in the new calculation.

	$\Gamma_6^+(1\Gamma_1)$	$\Gamma_6^+(2\Gamma_1)$	$\Gamma_6^+(3\Gamma_1)$	$\Gamma_6^-(1\Gamma_{15})$	$\Gamma_6^-(2\Gamma_{15})$	$\Gamma_8^-(1\Gamma_{15})$	$\Gamma_8^-(2\Gamma_{15})$
$1\Gamma_6^+$	0.9881	0.1443	0.0528	0.0	0.0	0.0	0.0
$2\Gamma_6^+$	-0.1481	0.9860	0.0768	0.0	0.0	0.0	0.0
$3\Gamma_6^+$	0.0410	0.0837	-0.9957	0.0	0.0	0.0	0.0
$1\Gamma_6^-$	0.0	0.0	0.0	0.9965	0.0839	0.0	0.0
$2\Gamma_6^-$	0.0	0.0	0.0	0.0839	-0.9965	0.0	0.0
$1\Gamma_8^-$	0.0	0.0	0.0	0.0	0.0	0.9996	0.0280
$2\Gamma_8^-$	0.0	0.0	0.0	0.0	0.0	0.0280	-0.9996

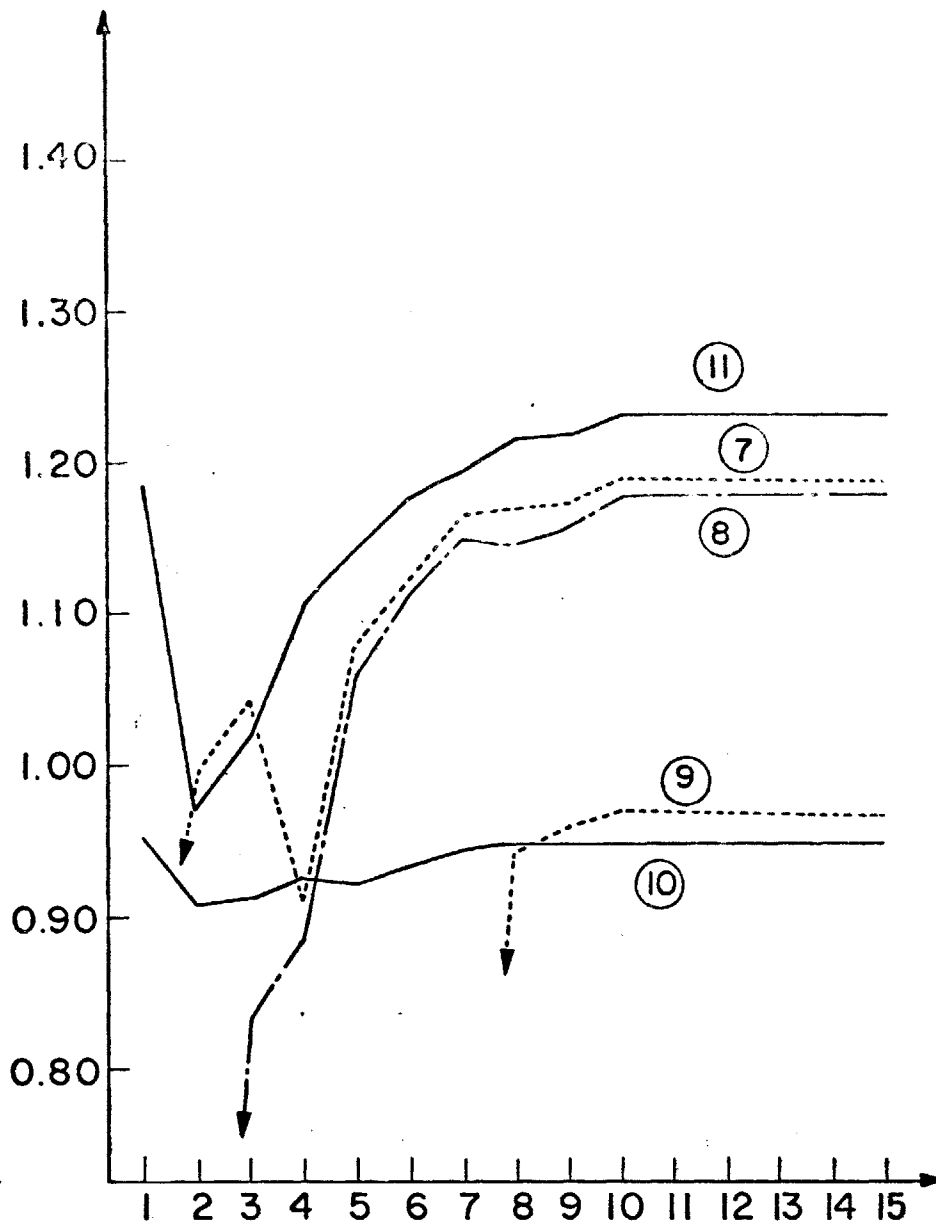
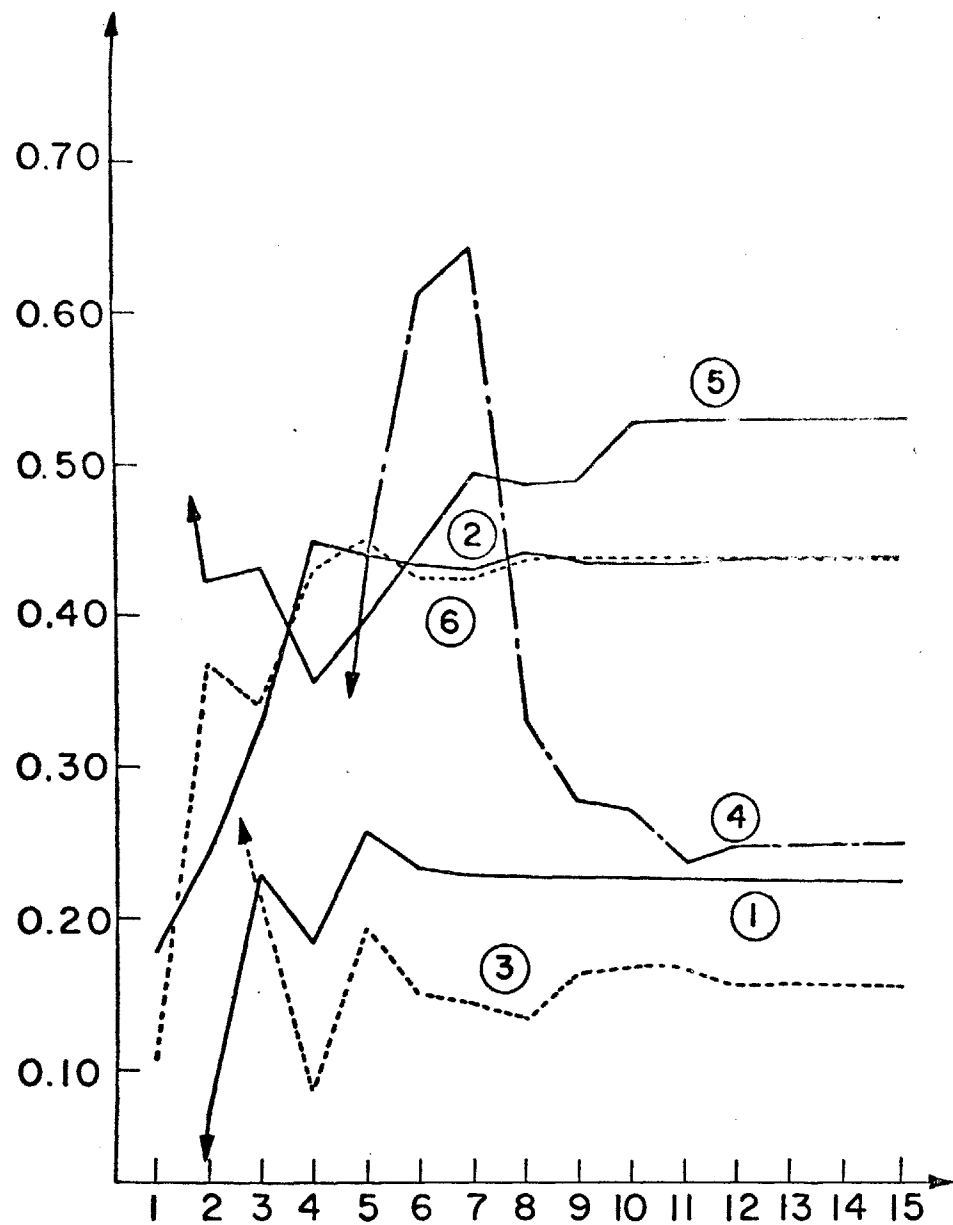


FIGURE 3.4 - Momentum matrix elements at Γ obtained with the non-relativistic bands of the new APW calculation (15 SAPW's) plotted against the number of SAPW's

performed. There are several matrix elements whose variation changes the gap at L. However, there is one momentum matrix element, namely $M_{1;15}^{2;2}$, which besides changing strongly the gap, also changes the bands at other symmetry points in such a way that the $\vec{K} \cdot \vec{\pi}$ bands move towards Conklin's bands. The variation of the gap with $M_{1;15}^{2;2}$ is shown in figure 3.5. It can be observed that this variation is almost linear and that the experimental gap at L is obtained if a value of 1.210 a.u. instead of 1.180 a.u. is used for the matrix element. This corresponds to a change of 2.5% in $M_{1;15}^{2;2}$.

Due to the symmetries in a f.c.c. unit cell, energies and wave-functions need to be calculated only for points in a region corresponding to 1/48 of the first Brillouin zone. A possible choice is¹⁹

$$\left\{ \begin{array}{l} k_x \geq k_y \geq k_z \\ k_x \leq (2\pi)/a \\ (k_x + k_y + k_z) \leq (3\pi)/a \end{array} \right. \quad (3.59)$$

which corresponds to the region A limited by the points Γ -L-K-W-P-X in figure 3.6.

The energy levels and corresponding wave-functions were obtained on a regular mesh of 152 points in A, the distance between two adjacent points in the mesh being $\Delta k_1 = 0.20 (\pi/a)$. This mesh has 4288 points in the first Brillouin zone, and is very suitable for interpolations of both the energy levels and the $\vec{K} \cdot \vec{\pi}$ coefficients of the wave-functions.

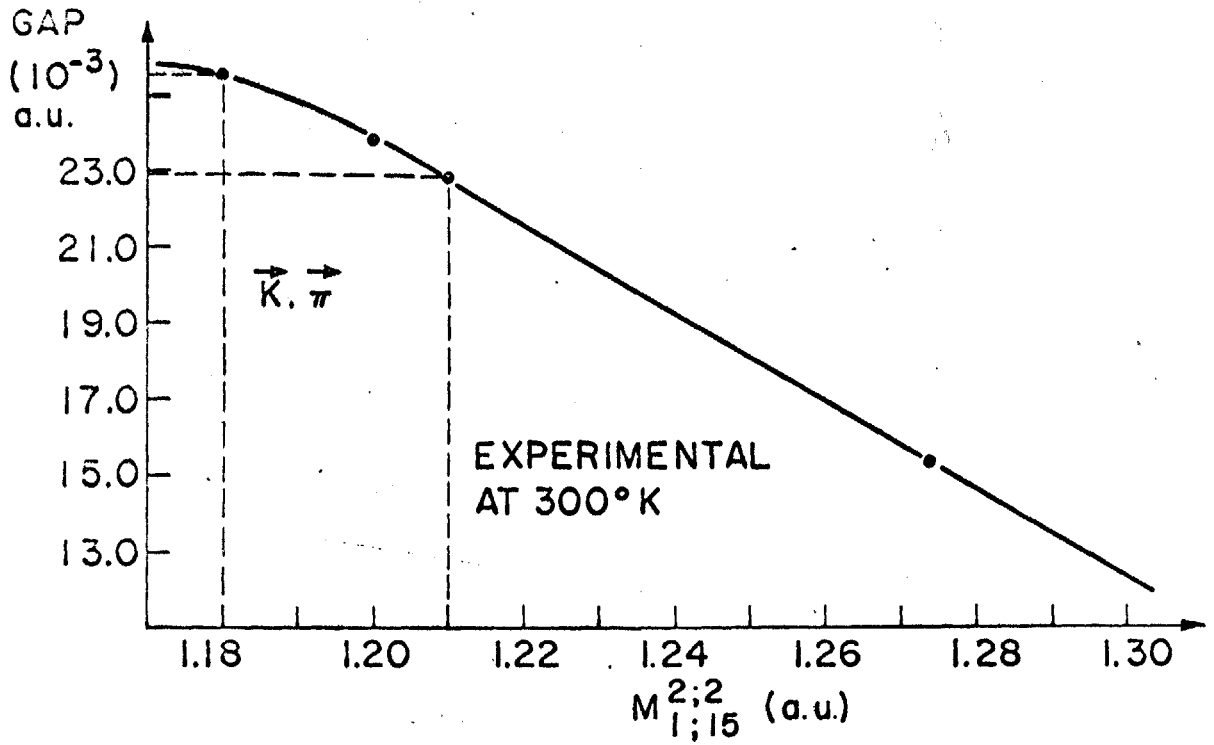


FIGURE 3.5 - Variation of the energy gap at L as a function of $M_{1;15}^{2;2}$.

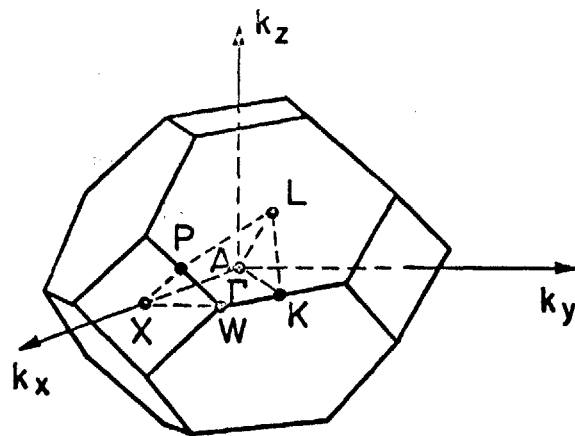


FIGURE 3.6 - First Brillouin zone for a f.c.c. lattice.

Figures 3.7, 3.8 and 3.9 show the $\vec{K} \cdot \vec{\pi}$ bands obtained in the $\langle 100 \rangle$, $\langle 110 \rangle$ and $\langle 111 \rangle$ directions, respectively. The circles in these figures represent the values obtained by Conklin. In figure 3.10 we present the \vec{K} -dependence of the important $\vec{K} \cdot \vec{\pi}$ coefficients of the first partners of the conduction and valence bands along the symmetry axes. The coefficients not shown in these figures are smaller than 0.05 a.u. We can observe the rapid change in the coefficients due to interaction between bands with the same parity.

On the Δ -axis (figure 3.10.a) the coefficients for the Luttinger-Kohn functions corresponding to odd-parity bands at Γ are real, while the coefficients for the even parity bands are pure imaginary, and for the Γ_8^+ -bands the coefficients correspond to $(c\Gamma_{8,3}^+ - b\Gamma_{8,1}^+) / (c^2 + b^2)^{1/2}$, where $c = 1/\sqrt{6}$ and $b = 1/\sqrt{2}$. For the Γ_8^- -bands they correspond to $(b\Gamma_{8,4}^- - c\Gamma_{8,2}^-) / (c^2 + b^2)^{1/2}$. We could have chosen the bands at Γ in such a way that all the coefficients along this axis are real, but this is not essential. Figure 3.10.b shows the coefficients along the $\langle 110 \rangle$ axis and figure 3.10.c presents them in the $\langle 111 \rangle$ direction. On the $\langle 110 \rangle$ axis the coefficients of $\Gamma_{6,1}^-$ and $\Gamma_{8,2}^-$ are real, but the coefficients of $\Gamma_{8,4}^-$ are pure imaginary. For $\Gamma_{6,2}^+$ and $\Gamma_{8,3}^+$ we have to multiply the coefficients by $(1-i)/\sqrt{2}$ for the conduction band and multiply by $(1-i)$ for the valence band, and for $\Gamma_{7,2}^+$ and $\Gamma_{8,1}^+$ by $(1+i)/\sqrt{2}$ for the conduction and by $(1+i)$ for the valence band. On the $\langle 111 \rangle$ axis all partners at Γ contribute to the Bloch functions.

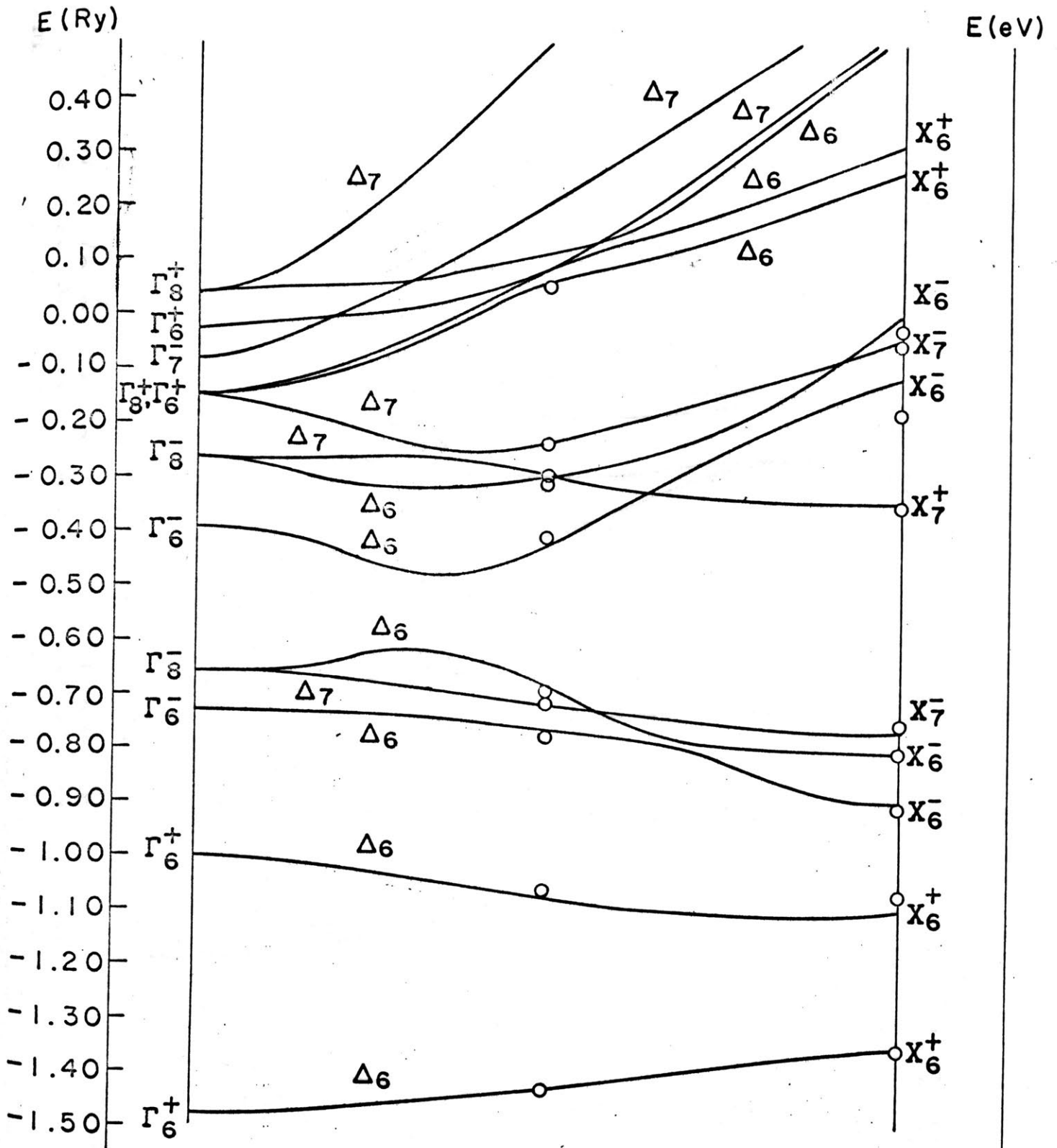


FIGURE 3.7 - $\vec{k} \cdot \vec{\pi}$ Energy Bands for the $\langle 100 \rangle$ direction.

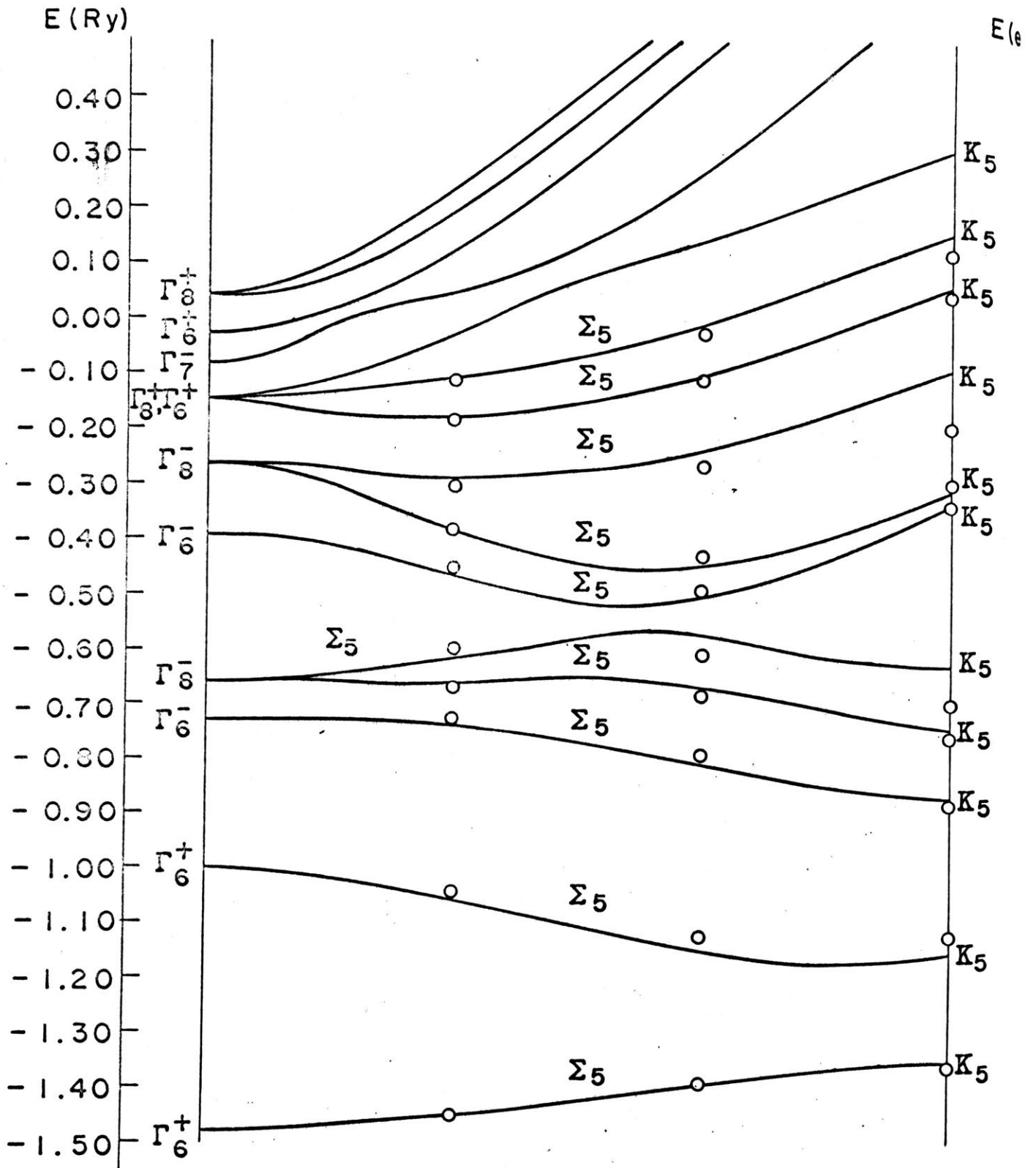


FIGURE 3.8 - $\vec{k} \cdot \vec{\pi}$ Energy Bands for the <110> direction.

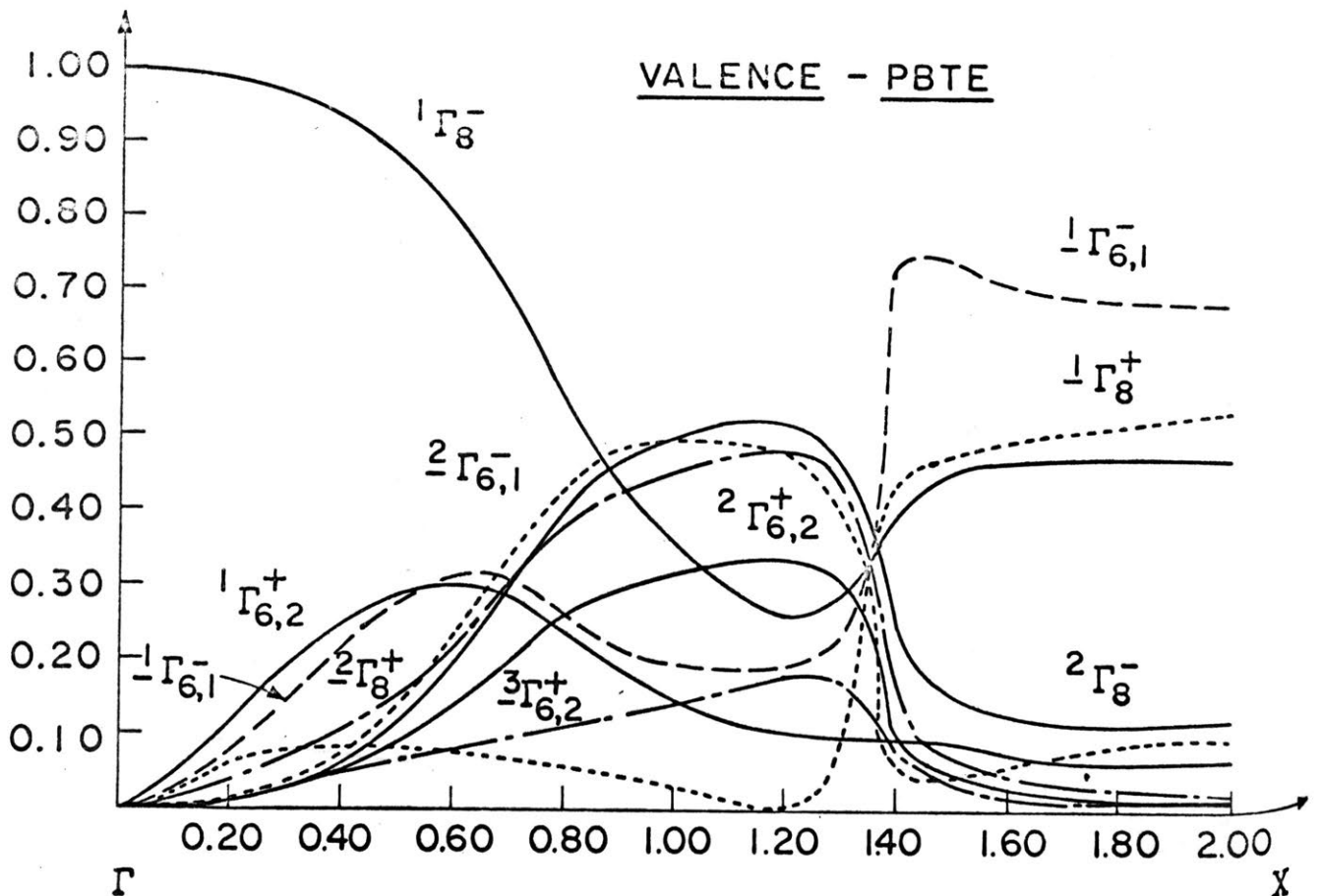
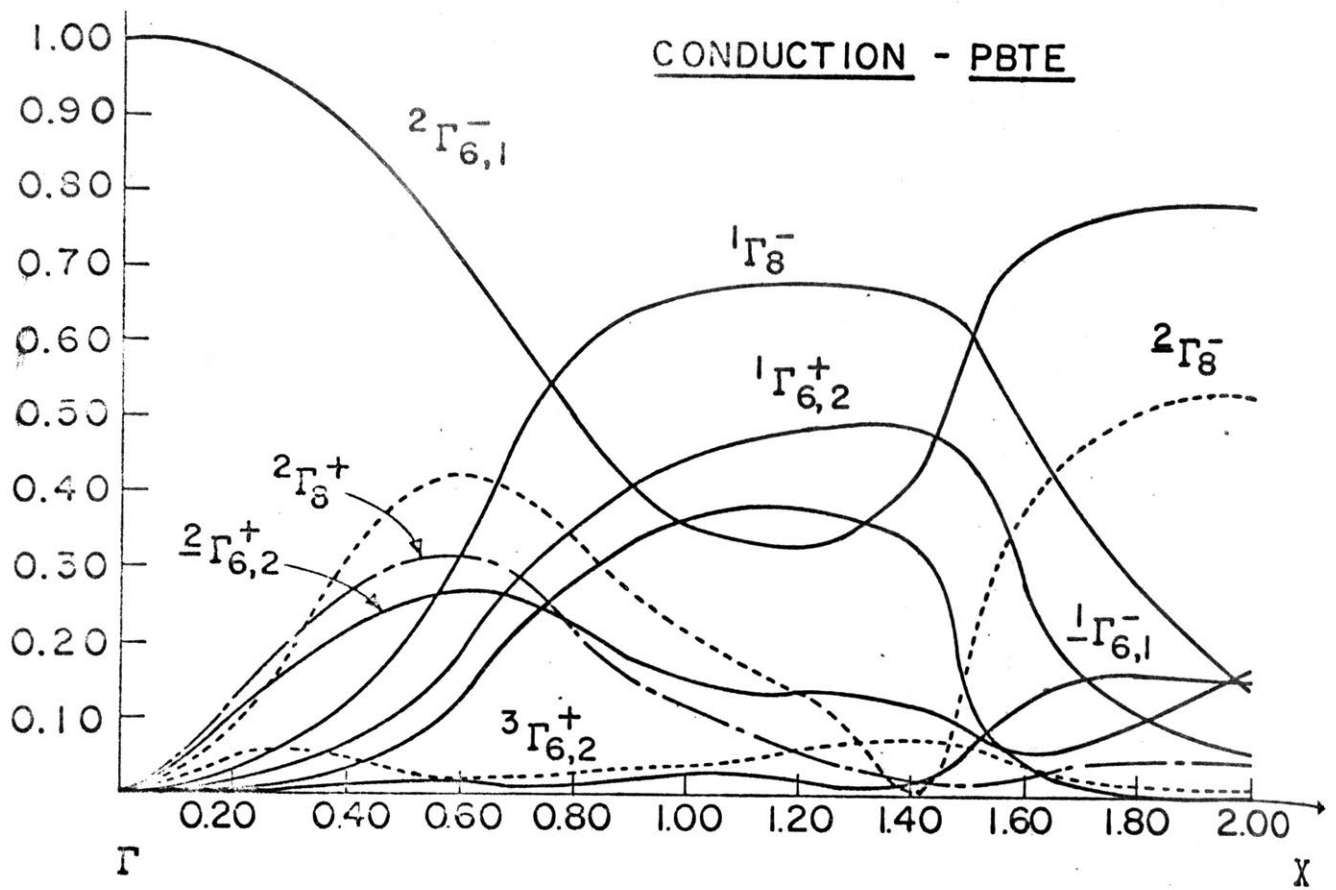
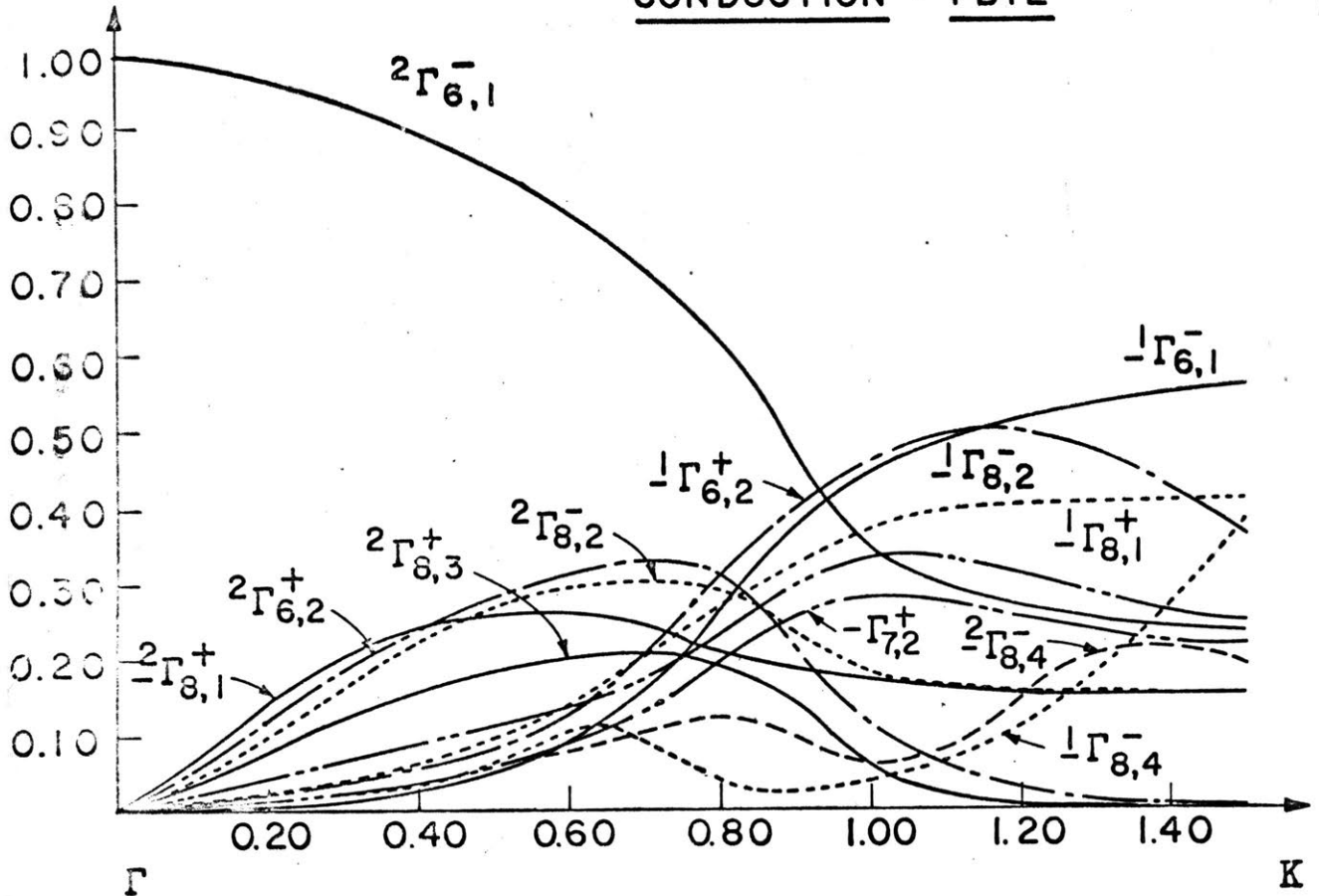


FIGURE 3.10.a - $\vec{k} \cdot \vec{\pi}$ coefficients for the lowest conduction and the highest valence bands along the $\langle 100 \rangle$ direction. The curves are labeled by the corresponding bands at Γ .

CONDUCTION - PBTE

71



VALENCE - PBTE

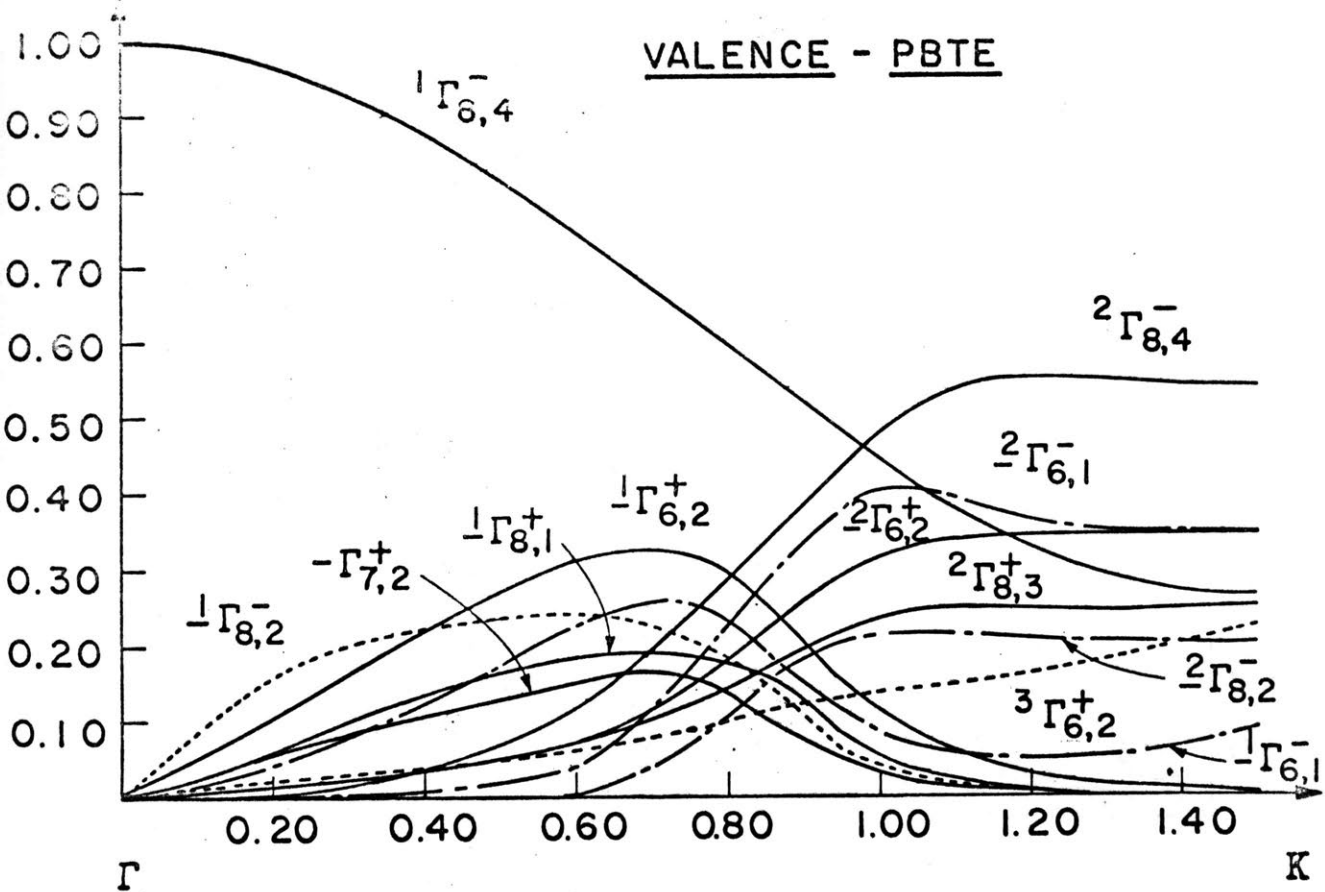


FIGURE 3.10.b - $\vec{k} \cdot \vec{\pi}$ coefficients for the lowest conduction and highest valence bands along the $\langle 110 \rangle$ direction. The curves are labeled by the corresponding bands at Γ .

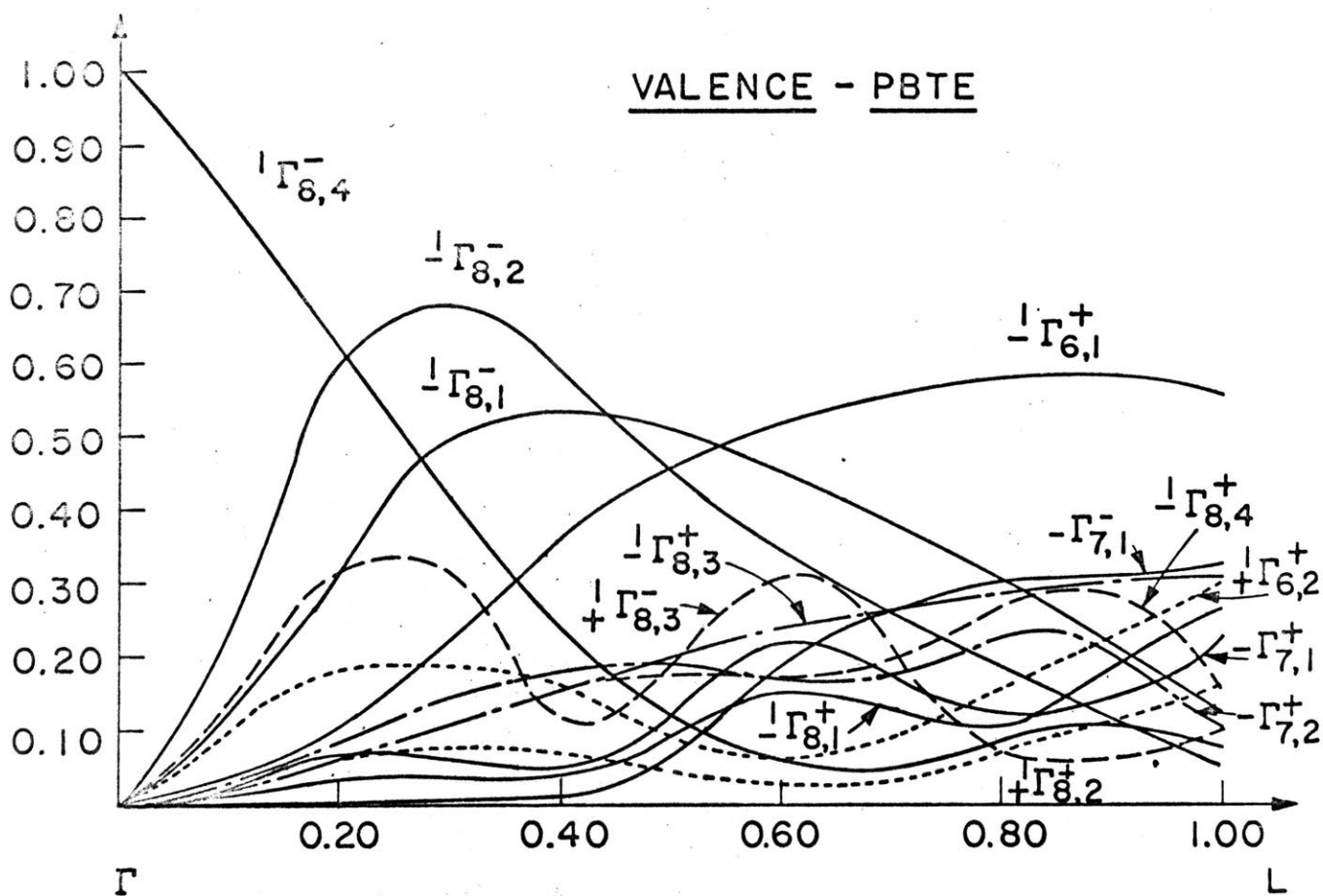
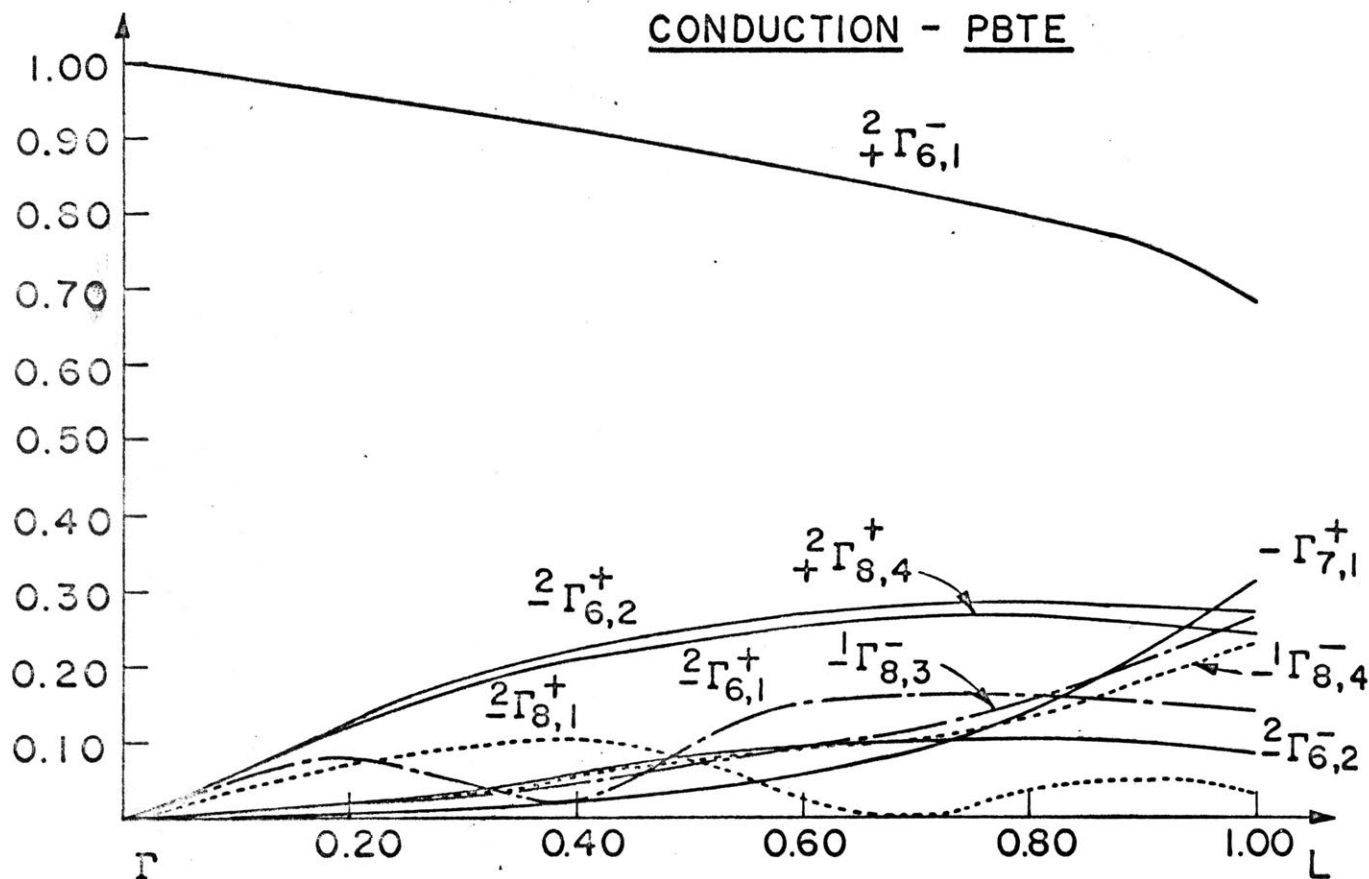


FIGURE 3.10.c - $\vec{k} \cdot \vec{\pi}$ coefficients for the lowest conduction and highest valence bands along the $\langle 111 \rangle$ direction. The curves are labeled by the corresponding bands at Γ .

For the conduction band, the coefficients of $\Gamma_{7,2}^+$, $\Gamma_{8,1}^+$, $\Gamma_{6,2}^-$, $\Gamma_{8,3}^-$ are real; the coefficients of $\Gamma_{6,2}^+$, $\Gamma_{8,3}^+$, $\Gamma_{7,2}^-$, $\Gamma_{8,1}^-$ are pure imaginary; the coefficients of $\Gamma_{6,1}^+$, $\Gamma_{8,2}^+$, $\Gamma_{7,1}^-$, $\Gamma_{8,4}^-$ have to be multiplied by $(1+i)/2$ and the coefficients of $\Gamma_{7,1}^+$, $\Gamma_{8,4}^+$, $\Gamma_{6,1}^-$, $\Gamma_{8,2}^-$ by $(1-i)/2$. For the valence band, however, the coefficients of $\Gamma_{6,1}^+$, $\Gamma_{8,2}^+$, $\Gamma_{7,1}^-$, $\Gamma_{8,4}^-$ are real; the coefficients of $\Gamma_{7,1}^+$, $\Gamma_{8,4}^+$, $\Gamma_{6,1}^-$, $\Gamma_{8,2}^-$ are pure imaginary; the coefficients of $\Gamma_{6,2}^+$, $\Gamma_{8,3}^+$, $\Gamma_{7,2}^-$, $\Gamma_{8,1}^-$ have to be multiplied by $(1+i)/2$ and the coefficients of $\Gamma_{7,2}^+$, $\Gamma_{8,1}^+$, $\Gamma_{6,2}^-$, $\Gamma_{8,3}^-$ by $(1-i)/2$.

The general behavior of the bands in any other direction in k-space is similar to that shown in the above figures, with the exception that the band-crossings occurring in the $\langle 100 \rangle$ axis are not allowed at general points. When going away from the $\langle 100 \rangle$ axis the crossing-bands start to repel each other and as a consequence the $\vec{k} \cdot \vec{\pi}$ coefficients vary rapidly in this region. This behavior is shown in figure 3.11, where we present the bands on the line $k = \frac{\pi}{a}(x, 0.2, 0.2)$ where x varies from 0.0 to 2.0.

Knowledge of the wave functions allows us to obtain the matrix elements of the linear momentum between the relativistic bands over the entire Brillouin zone. They were calculated by us on the 152 point regular mesh and the results were used by Buss²⁷ to calculate the optical dielectric constant $\epsilon(q=0, \omega)$ of PbTe. The comparison with the measured value of Cardona and Greenaway²⁸ for the real part of the dielectric constant showed that the calculated value agrees with the experiment to within 50%²⁷ (figure 3.12).

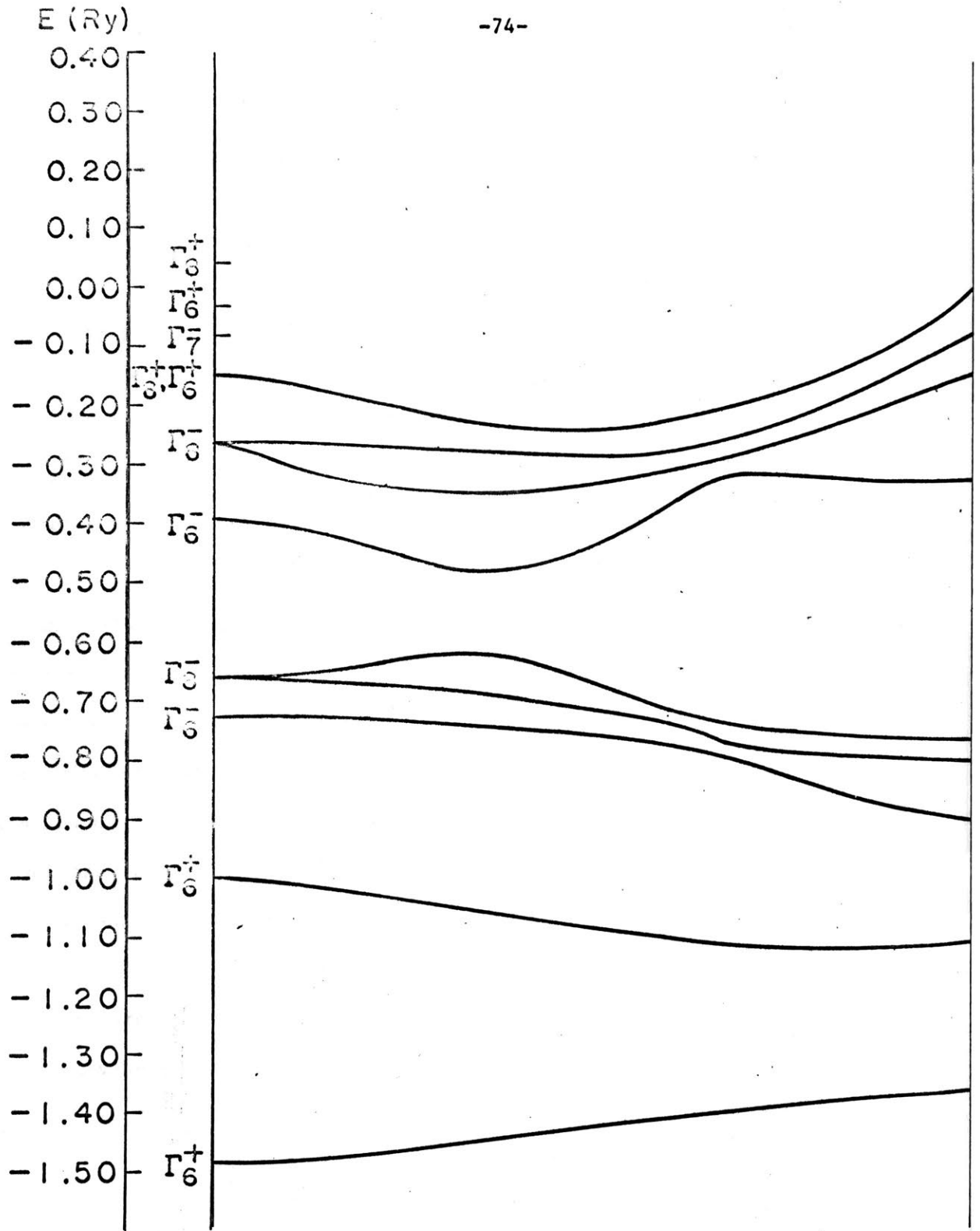
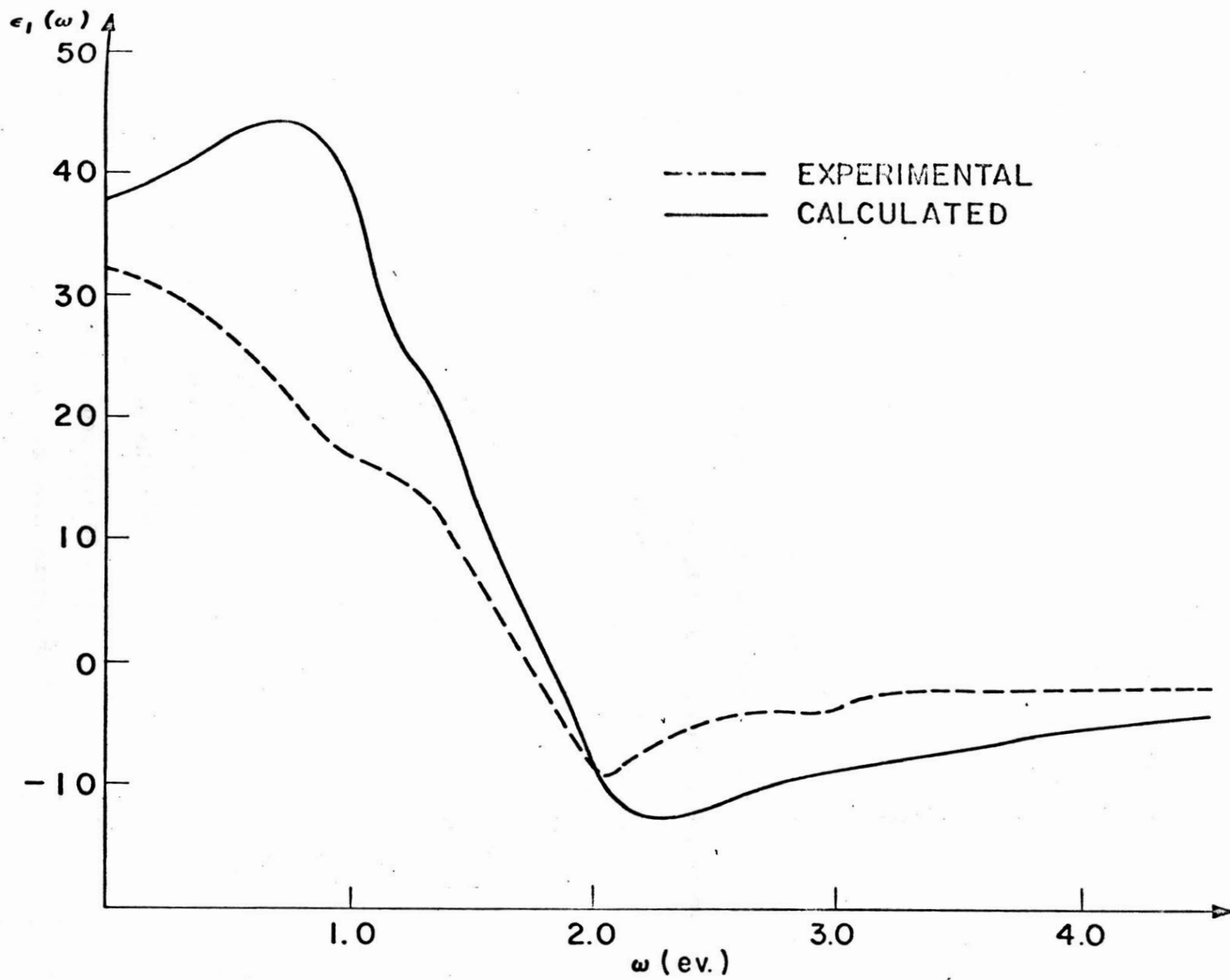


FIGURE 3.11 - $\vec{k} \cdot \vec{\pi}$ Energy Bands for the line $\vec{k} = \frac{\pi}{a}(x, 0.2, 0.2)$ where x varies from 0.0 to 2.0.



-75-

FIGURE 3.12 - Real part of the optical dielectric constant
 $\epsilon_1(q=0, \omega)$ (after Buss).

Figure 3.13 presents the matrix element of p_x between the valence and conduction bands on the $\langle 100 \rangle$ axis, where we are using a system of coordinates with x, y and z-axis corresponding to the $\langle 100 \rangle$, $\langle 010 \rangle$ and $\langle 001 \rangle$ directions respectively. The peak of the curve occurs at the minimum gap between the conduction and valence bands and the rapid change in the momentum matrix element in the region between $|\vec{k}| = \frac{\pi}{a} 1.2$ and $|\vec{k}| = \frac{\pi}{a} 1.4$ is due to the interaction between the two Δ_6 -valence bands and also to the interaction between the two Δ_6 -conduction bands. The matrix elements of p_y and p_z between the valence and conduction bands, which are zero by symmetry, were calculated to be smaller than 0.01 a.u.* Although the gap is bounded by the Δ_7 valence and conduction bands for k greater than $\frac{\pi}{a} 1.40$, the matrix element between these bands is very small and can be neglected.

Figure 3.14.a shows the real and imaginary parts of the matrix element of p_x between the valence and conduction bands on the Σ -axis. The matrix element of p_y can be obtained by

$$\langle \Sigma_{5,1}^{\text{val}} | p_y | \Sigma_{5,1}^{\text{cond}} \rangle = -\langle \Sigma_{5,1}^{\text{val}} | p_x | \Sigma_{5,1}^{\text{cond}} \rangle \quad (3.61)$$

and the matrix element of p_z is zero** by symmetry. The matrix elements of the momentum parallel to the Σ -axis is purely imaginary and equal to $\sqrt{2} \text{Im} [\langle \Sigma_{5,1}^{\text{val}} | p_x | \Sigma_{5,1}^{\text{cond}} \rangle]$, while the matrix element of the momentum perpendicular to that axis is real and equal to $\sqrt{2} \text{Re} [\langle \Sigma_{5,1}^{\text{val}} | p_x | \Sigma_{5,1}^{\text{cond}} \rangle]$. Both matrix elements are shown in figure 3.14.b. We can observe that the Σ -axis is also important in studying optical phenomena, because although the momentum matrix

* This value can be considered as a measure of the accuracy of the calculation.

** As along the Δ -axis, the calculated value is smaller than 0.01 a.u.

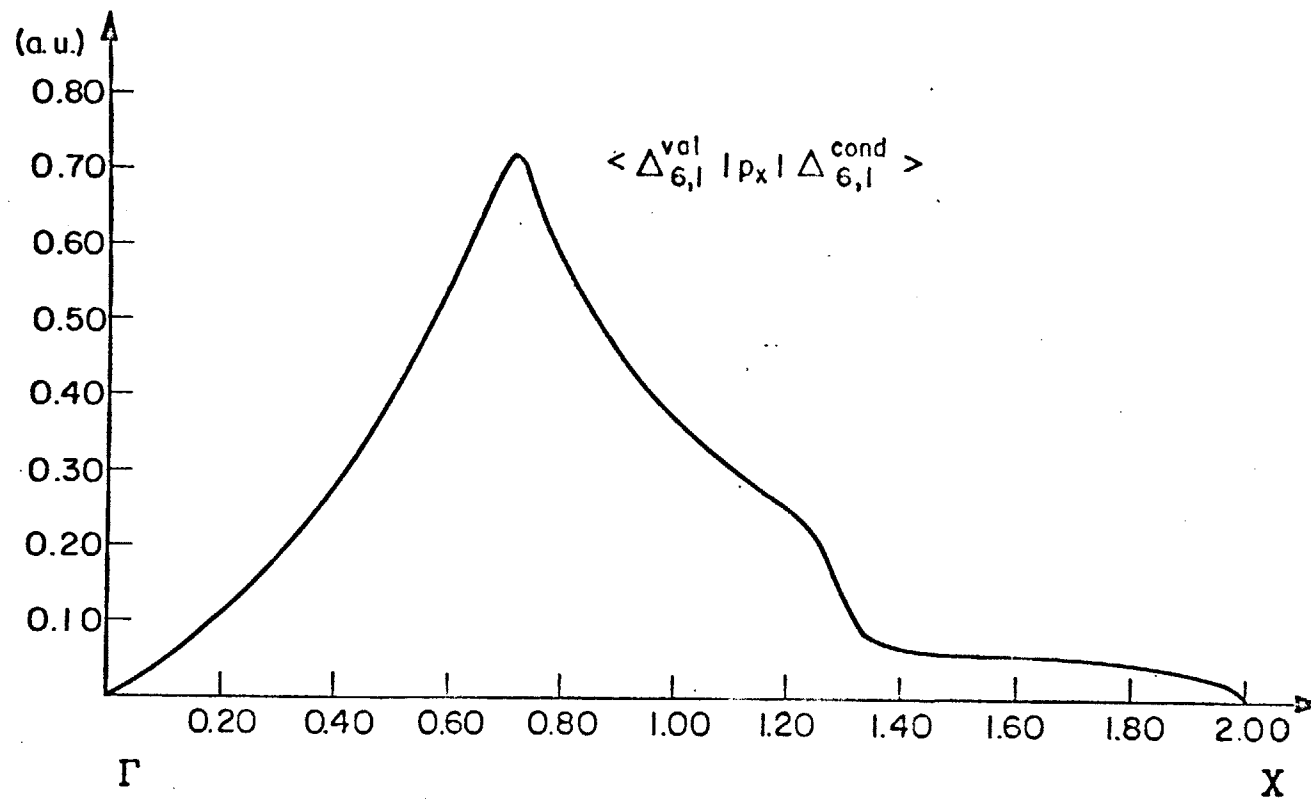


FIGURE 3.13 - Matrix element of p_x between the lowest conduction and the highest valence bands along the $\langle 100 \rangle$ direction.

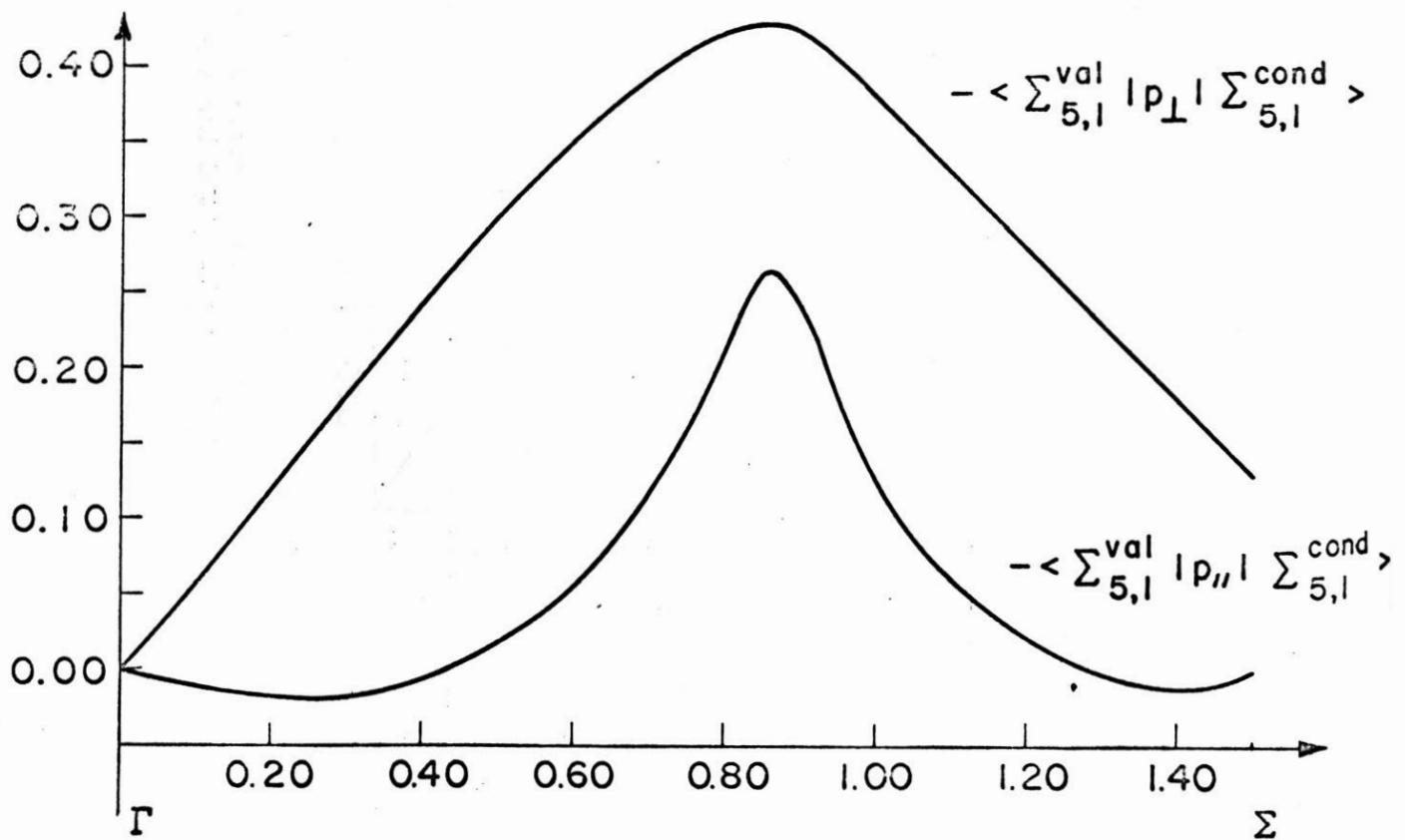
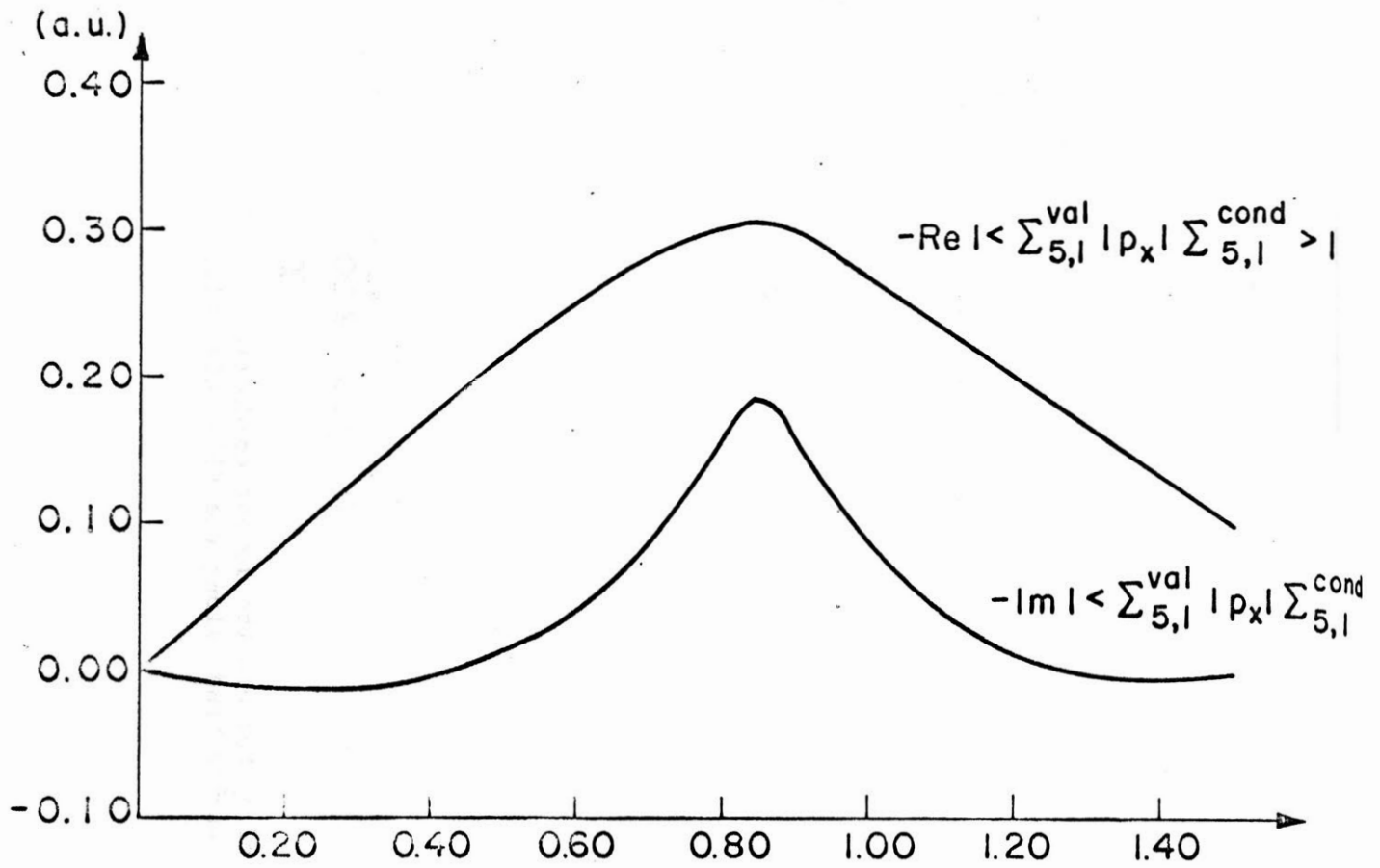


FIGURE 3.14 - Matrix elements of momentum between the lowest conduction and highest valence bands along the $\langle 110 \rangle$ axis. In the figures // and \perp denote parallel and perpendicular to the axis, respectively.

elements are smaller than on the Δ -axis, the minimum gap on the Σ -axis is smaller than on the Δ -axis.

Finally the momentum matrix elements parallel and perpendicular to the Λ -axis are presented in Figure 3.15. The matrix elements of p_x , p_y and p_z can easily be obtained if we remember that

$$p_{//} = \frac{p_x + p_y + p_z}{\sqrt{3}} \quad (3.62)$$

$$p_{\perp} = p_{x'} = \frac{p_x - p_y}{\sqrt{2}} \quad (3.63)$$

The matrix element of p_y is related to the matrix elements of p_x by

$$\langle \Lambda_{6,1}^{\text{val}} | p_y | \Lambda_{6,1}^{\text{cond}} \rangle = - \langle \Lambda_{6,1}^{\text{val}} | p_x | \Lambda_{6,1}^{\text{cond}} \rangle^* \quad (3.62)$$

$$\langle \Lambda_{6,1}^{\text{val}} | p_y | \Lambda_{6,2}^{\text{cond}} \rangle = i \langle \Lambda_{6,1}^{\text{val}} | p_x | \Lambda_{6,2}^{\text{cond}} \rangle \quad (3.63)$$

The momentum matrix elements between the remaining partners can be obtained through Eq. (3.51).

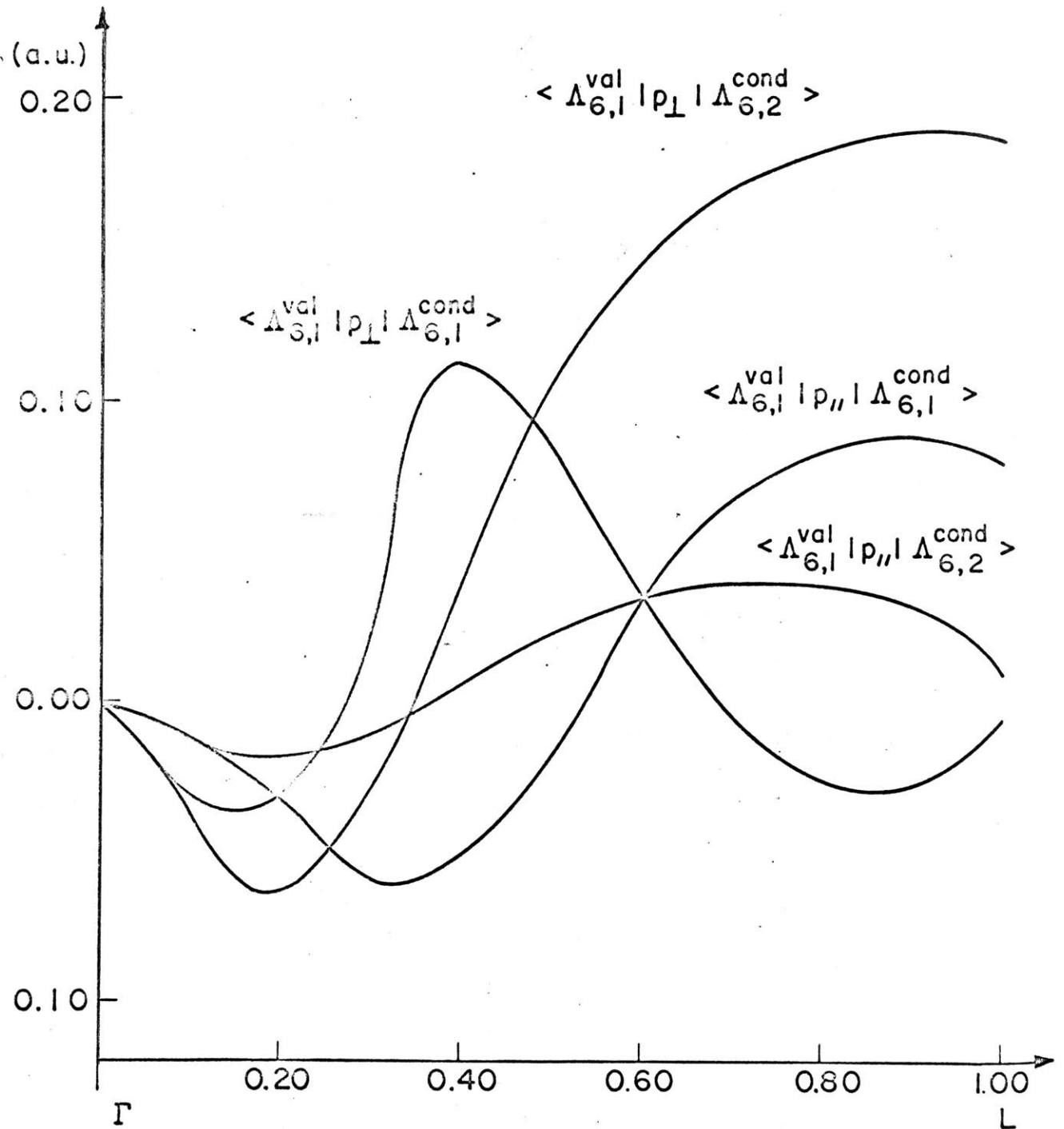


FIGURE 3.15 - Matrix elements of momentum between the lowest conduction and the highest valence bands along the $\langle 111 \rangle$ axis.

CHAPTER IV

→ →
LOCALIZED DEFECTS IN THE $K \cdot \pi$ - APW SCHEME

4.1 INTRODUCTION

Crystal imperfections such as impurities and vacancies produce electronic states different from those of a perfect crystal.

The effect of these imperfections is to modify the periodic potential of the host crystal. Let us assume that the perturbed crystal potential can be written as the sum of the unperturbed potential plus a time-independent term called the impurity potential that represents the effect of the imperfections. Normal perturbation theory can be applied. The perturbed wave functions are expanded in a convenient basis, normally a complete set of wave functions for the unperturbed case, and one seeks for the solutions of the stationary Schrodinger equation

$$[H_0 + U(\vec{r})]\psi(\vec{r}) = E\psi(\vec{r}) \quad (4.1)$$

where H_0 is the unperturbed one-electron Hamiltonian and $U(\vec{r})$ is the time-independent perturbing potential.

The eigenfunctions of H_0 are Bloch functions $b_{n,i}^{\Gamma(\vec{k})\alpha}(\vec{k}, \vec{r})$ i.e.,

$$H_0 b_{n,i}^{\Gamma(\vec{k})\alpha}(\vec{k}, \vec{r}) = E_n(\vec{k}) b_{n,i}^{\Gamma(\vec{k})\alpha}(\vec{k}, \vec{r}) \quad (4.2)$$

which transform like the i -partner of the irreducible representation $\Gamma_{\alpha}(\vec{k})$ of the group of the wave vector \vec{k} .

Different complete sets have been used for expanding $\psi(\vec{r})$. Bloch functions are the most natural choice: they are eigenfunctions of H_0 and form a complete set of orthonormal functions for every wave vector \vec{k} , band index n and partner i of the irreducible representation associated with n . If $\psi(\vec{r})$ is expanded in terms of Bloch functions,

$$\psi(\vec{r}) = \sum_{n,i,k} A_{n,i}(\vec{k}) b_{n,i}^{\Gamma_{\alpha}(\vec{k})}(\vec{k}, \vec{r}) \quad (4.3)$$

the equation satisfied by the expansion coefficients $A_{n,i}(\vec{k})$ is given Eq. (4.4).

$$\sum_{n,i,k} \{ [E_n(\vec{k}) - E] \delta_{n,n'} \delta_{i,i'} \delta_{\vec{k}, \vec{k}'} + U_{n',n}^{i',i}(\vec{k}', \vec{k}) \} A_{n,i}(\vec{k}) = 0 \quad (4.4)$$

where

$$U_{n',n}^{i',i}(\vec{k}', \vec{k}) = \langle b_{n',i'}^{\Gamma_{\beta'}(\vec{k}')}(\vec{k}', \vec{r}) | U(\vec{r}) | b_{n,i}^{\Gamma_{\beta}(\vec{k})}(\vec{k}, \vec{r}) \rangle \quad (4.5)$$

The representation obtained in this way has been called the "crystal momentum representation" (CMR) by Adams,²⁹ because Bloch functions are eigenfunctions of the crystal momentum operator. In order to obtain the coefficients $A_{n,i}(\vec{k})$ it is necessary to solve the secular equation (4.4). The dimension of the secular matrix is $n_p \times n_p$, where n_p is the

number of unperturbed energy bands used in the expansion (with the proper degeneracy taken into account) and m is the number of allowed \vec{k} vectors. Even if the one band approximation is made, the number of allowed \vec{k} 's still make this diagonalization prohibitive in practice.

Another very important set of functions is the Wannier set which is expressed in terms of the Bloch set. For non-degenerate bands, the Wannier functions $a_n(\vec{r}-\vec{R}_q)$, which are localized around lattice sites \vec{R}_q with an average radius approximately equal to a lattice parameter, are defined as a linear combination of Bloch functions belonging to a single band, i.e.,

$$a_n(\vec{r}-\vec{R}_q) = \frac{\Omega^{1/2}}{(2\pi)^{3/2}} \int d\vec{k} e^{-i\vec{k}\cdot\vec{R}_q} b_n(\vec{k},\vec{r}) \quad (4.6)$$

where Ω is the volume of the unit cell and the integration is performed in the interior and surface of the first Brillouin zone. These functions form a complete set of orthonormal functions for every lattice site \vec{R}_q and band index n . The perturbed wave function $\psi(\vec{r})$ can be expanded in terms of this set. If this is done, i.e.,

$$\psi(\vec{r}) = \sum_{n,q} A_n(\vec{R}_q) a_n(\vec{r}-\vec{R}_q) \quad (4.7)$$

the equation analogous to Eq. (4.4) for the coefficients of the expansion is

$$\sum_{n,q} \{ [E_n(\vec{R}_q, -\vec{R}_q) - E \delta_{q',q}] \delta_{n',n} + U_{n',n}(\vec{R}_q, \vec{R}_q) \} A_n(\vec{R}_q) = 0 \quad (4.8)$$

where $E_n(\vec{R}_q)$ is the Fourier component of the energy*, i.e.,

$$E_n(\vec{k}) = \sum_q E_n(\vec{R}_q) e^{-ik \cdot \vec{R}_q} \quad (4.9)$$

and

$$U_{n',n}(\vec{R}_{q'}, \vec{R}_q) = \langle a_{n'}(\vec{r}-\vec{R}_{q'}) | U(\vec{r}) | a_n(\vec{r}-\vec{R}_q) \rangle \quad (4.10)$$

Eq. (4.8) can also be written as the difference equation

$$[E_{n'}(\frac{1}{i} \nabla_{\vec{R}_{q'}}) - E] A_{n'}(\vec{R}_{q'}) + \sum_{n,q} U_{n',n}(\vec{R}_{q'}, \vec{R}_q) A_n(\vec{R}_q) = 0 \quad (4.11)$$

where the coefficients $A_n(\vec{R}_q)$ are considered as a continuous function of the variable \vec{R}_q . The expression $E_{n'}(\frac{1}{i} \nabla_{\vec{R}_{q'}})$ means that we are to substitute $\frac{1}{i} \frac{\partial}{\partial \vec{R}_{q'}}$ for \vec{k} wherever \vec{k} appears in the expression for the energy of the unperturbed band n' as a function of \vec{k} . This is analogous to say that A_n is a function of r and $E_n(\frac{1}{i} \frac{\partial}{\partial \vec{r}})$ means that we are to substitute $\frac{1}{i} \frac{\partial}{\partial \vec{r}}$ for \vec{k} wherever \vec{k} appears in^q the expression for the energy of the unperturbed band n' and the whole expression is evaluated at $\vec{r} = \vec{R}_{q'}$. The representation obtained in this way is called "crystal coordinate representation" (CCR), because Wannier functions are eigenfunctions of the crystal coordinate operator.³⁰ The coefficients $A_n(\vec{R}_q)$

* $E_n(\vec{k})$ is a periodic function in the reciprocal lattice.

are then obtained by diagonalizing a secular equation with dimension $n \times p$, where n is the number of energy bands and p is the number of lattice sites which are taken into account. As in the case of the CMR, even if the one band approximation is assumed, in the general case, the number of lattice sites makes the diagonalization prohibitive.

There is, however, a limiting case that can be solved in both the CMR and CCR, namely, the point impurity. By a point impurity is meant a strongly localized perturbation such that its matrix element between two Wannier functions satisfies

$$\langle a_n(\vec{r}-\vec{R}_q) | U(\vec{r}) | a_n(\vec{r}-\vec{R}_q) \rangle = U_n \delta_{n',n} \delta_{q',q} \delta_{q,0} \quad (4.12)$$

In Eq. (4.12) the perturbation is assumed to be localized at the origin. From Eq. (4.12) it is evident that a one band approximation is assumed. The corresponding matrix element between Bloch functions is given by

$$\langle b_n(\vec{k}', \vec{r}) | U(\vec{r}) | b_n(\vec{k}, \vec{r}) \rangle = \frac{\Omega}{(2\pi)^3} U_n \delta_{n',n} \quad (4.13)$$

i.e., they are independent of \vec{k} and \vec{k}' and diagonal in the band parameter. In this case, the secular equation factors into n decoupled secular equations, one for each band.

This problem was first analysed by Koster and Slater¹ in the CCR. They considered the case of a one-dimensional crystal of equally spaced atoms where the impurity potential does not mix Wannier functions separated by distances larger than the nearest neighbor distance, nor does it mix bands. Due to the symmetry of the problem, the solutions

for the coefficients of the Wannier functions have to be symmetric or antisymmetric with respect to the lattice vectors R_q . If periodic boundary conditions are assumed, i.e., $A(R_{p+2N}) = A(R_p)$, then $2n$ states are to be obtained. Koster and Slater showed in this case the appearance of $(N-1)$ antisymmetric states in the band, which are not affected by the perturbation, N symmetric states in the band and a bound state, with energy given by

$$E = E(R_0=0) + 2E(R_1) \left\{ 1 + \left[\frac{U(0)}{2E(R_1)} \right]^{1/2} \right\} \quad (4.14)$$

if the perturbation $U(0)$ has the same sign as the nearest neighbor interactions. In Eq. (4.14), $U(0)$ is the matrix element of the potential between Wannier functions centered at the origin. In this case the bound state pushes out of the band at the point where $E = E(R_0=0) + 2E(R_1)$. If the signs are different, then the bound state will push out of the band at the point where $E = E(R_0=0) - 2E(R_1)$. By (4.14) it can easily be seen that for small perturbations the bound state leaves the band quadratically in $U(0)$, and as $U(0)$ increases the energy becomes linear with the perturbation. Further complications were, then, introduced by the authors, namely, next nearest neighbor interactions between Wannier functions and again they were able to show the existence of antisymmetric states not perturbed by the impurities, symmetric states and a bound state, whose energy behaves in a manner similar to the simpler case.

In a subsequent paper, Koster and Slater¹ considered the problem of a point impurity in the center of a three-dimensional cubic crystal

in which there is only one band of energies and the Wannier functions only have interactions between each other when they are centered at nearest neighbors or closer. Because the perturbation potential was assumed to have full cubic symmetry, the solution for the problem transforms like a basis partner for one of the irreducible representations of the cubic group. But since the potential is strongly localized at the origin, it is evident that one has to look for a function that transforms like the identity (Γ_1) representation (s-like symmetry), because any other irreducible representation would have a vanishing contribution from the Wannier functions at the origin and would not be perturbed by the potential. Koster and Slater showed that there is no bound state unless the potential is greater than a critical value ($U(0) > \frac{2E(R_1)}{0.499}$), and $U(0)$ and $E(R_1)$ have the same sign. For perturbations slightly above the critical value the energy depends quadratically on $U(0)$ and, for larger perturbations, the dependence becomes linear. The wave function for the bound state was also obtained.

Finally, a more extended perturbation was assumed, namely the case where the matrix elements of the perturbation potential between Wannier functions centered at the atoms near the origin also are different from zero, i.e.,

$$\langle a_{\vec{n}}(\vec{r}-\vec{R}_q) | U(\vec{r}) | a_{\vec{n}}(\vec{r}-\vec{R}_q) \rangle = U_{n,q} \delta_{n',n} \delta_{q',q} \delta^{0,1} \quad (4.15)$$

where $\delta^{0,1}$ means that the matrix element (4.15) is different from zero

only if $\vec{R}_q = 0$ or $\vec{R}_q = \vec{R}_1$. In this case,* assuming that the wave function vanishes at infinity, seven bound states were found: two s-like states, three p-type states and two d-like states, which exist for certain values of the perturbation. The effect of the size of the crystal and of the perturbation on the wave functions were also discussed.

Recently Kilby³¹ proposed a variational method for the treatment of localized perturbations in solids. He worked in the single band approximation but was able to treat the cubic and the diamond structures. In the case of the cubic crystal his results are in fair agreement with that of Koster and Slater.

In the Koster-Slater scheme we do not use Eq. (4.8) or Eq. (4.9) for the coefficients of the expansion of the perturbed wave function in terms of Wannier functions. Instead an equation is used where the energy $E_n(\vec{k})$ appears explicitly. This equation is deduced in reference 3 and the principal steps are the following. First, the perturbed wave function is expanded in terms of the unperturbed Bloch functions obtaining Eq. (4.4) for the coefficients of the expansion. Then, the relation between the matrix elements of the perturbing potential in the CMR and CCR as expressed by

* For a cubic lattice we have seven non-zero matrix elements for each band. Observe that the potential can not be considered as a point impurity any more as far as Eq. (4.12) is concerned.

$$U_{n',n}^{i',i}(\vec{k}',\vec{k}) = \frac{1}{N} \sum_{R_q, R_{q'}} e^{i\vec{k}\cdot\vec{R}_q} e^{-i\vec{k}'\cdot\vec{R}_{q'}} U_{n',n}^{i',i}(R_{q'}, R_q) \quad (4.16)$$

is used and Eq. (4.4) is written as

$$\begin{aligned} [E_n(\vec{k}') - E] A_{n',i}(\vec{k}') + \frac{1}{N} \sum_{n,k,i} \sum_{R_{q'}, R_q} e^{-i\vec{k}'\cdot\vec{R}_{q'}} e^{i\vec{k}\cdot\vec{R}_q} U_{n',n}^{i',i}(R_{q'}, R_q) A_{n,i}(\vec{k}) \\ = 0 \end{aligned} \quad (4.17)$$

In Eq. (4.16), N is the number of primitive translations in the crystal over which periodic boundary conditions are defined or equivalently the number of allowed k -vectors in the Brillouin zone. For every band n and partner i a Wannier function has been defined by*

$$a_{n,i}(\vec{r}-\vec{R}_q) = \frac{1}{\Omega_k^{1/2}} \int_{BZ} d\vec{k} e^{-i\vec{k}\cdot\vec{R}_q} \Gamma_{n,i}^{\beta}(\vec{k}) e^{i\Theta_n(\vec{k})} \quad (4.18)$$

where $\Omega_k = (2\pi)^3/\Omega$ is the volume of the first Brillouin zone, and $\Theta_n(\vec{k})$ is a phase factor. These phase factors are necessary because if they are chosen properly, localized Wannier functions are obtained.

As we are looking for bound states, we can divide Eq. (4.17) by $[E_n(\vec{k}') - E]$, multiply by $(1/N^{1/2}) e^{i\vec{k}'\cdot\vec{R}_p}$ and sum on \vec{k}' . Using the

* At symmetry points, problems may arise because of this definition. This point will be discussed later, in Section 4.2.

relation

$$A_{n,i}(\vec{R}_p) = \frac{1}{N^{1/2}} \sum_{\vec{k}} e^{i\vec{k} \cdot \vec{R}_p} A_{n,i}(\vec{k}) \quad (4.19)$$

we finally obtain

$$\sum_{n,i,R_q} \left\{ \delta_{n',n} \delta_{i',i} \delta_{\vec{R}_p, \vec{R}_q} + \sum_{R_q'} \left[\frac{1}{N} \sum_{\vec{k}'} \frac{e^{i\vec{k}' \cdot (\vec{R}_p - \vec{R}_{q'})}}{E_{n'}(\vec{k}') - E} \right] U_{n',n}^{i',i}(\vec{R}_{q'}, \vec{R}_q) \right\} A_{n,i}(\vec{R}_q) = 0 \quad (4.20)$$

This equation is valid for all n' , i' and \vec{R}_p . For the system to have a non-trivial solution, it is necessary that

$$\det \left| \delta_{n',n} \delta_{i',i} \delta_{\vec{R}_p, \vec{R}_q} - \sum_{R_q'} \left[\frac{1}{N} \sum_{\vec{k}'} \frac{e^{i\vec{k}' \cdot (\vec{R}_p - \vec{R}_{q'})}}{E - E_{n'}(\vec{k}')} \right] U_{n',n}^{i',i}(\vec{R}_{q'}, \vec{R}_q) \right| = 0 \quad (4.21)$$

In the above secular matrix the general row or column is characterized by the band index n , the partner index i and the lattice site \vec{R}_q . If the term

$$G_{n',n}^{i',i}(\vec{R}_p - \vec{R}_{q'}, E) = \frac{1}{N} \sum_{\vec{k}} \frac{e^{i\vec{k} \cdot (\vec{R}_p - \vec{R}_{q'})}}{E - E_n(\vec{k})} \delta_{n',n} \delta_{i',i} \quad (4.22)$$

is considered as the general element of a matrix G , Eq. (4.21) can be written as

$$\det|I-GU| = 0 \quad (4.23)$$

In Eq. (4.23) I is the identity matrix and the matrix U has $U_{n',n}^{i',i}(\vec{R}_q, \vec{R}_q)$ as a general element.

If the perturbation $U(\vec{r})$ is well localized, the matrix U can be well approximated as having only a finite number of non-zero elements. Let us rearrange rows and columns of the U-matrix such that those non-zero elements appear in the upper-left corner of the matrix. If we decide to consider a perturbation which has non-zero elements between n_n bands* and n_R sites, the non-zero part of U is of dimension $N \times N$, where $N = n_n n_R$. Let us denote this part by U_{NN} . Matrix U can, then, be written in block form

$$U = \begin{pmatrix} U_{NN} & 0 \\ 0 & 0 \end{pmatrix} \quad (4.24)$$

Correspondingly, matrices G and I can be written as

$$G = \begin{pmatrix} G_{NN} & G_{NZ} \\ G_{ZN} & G_{ZZ} \end{pmatrix}; \quad I = \begin{pmatrix} I_{NN} & 0 \\ 0 & I_{ZZ} \end{pmatrix} \quad (4.25)$$

*In n_n we include also the different partners of the bands.

Then, we obtain

$$I-GU = \begin{pmatrix} I_{NN} - G_{NN} U_{NN} & 0 \\ -G_{ZN} U_{NN} & I_{ZZ} \end{pmatrix} \quad (4.26)$$

and Eq. (4.23) becomes

$$\det | I_{NN} - G_{NN} U_{NN} | = 0 \quad (4.27)$$

which shows that it is necessary to consider only the G_{NN} part of G when calculating the energy levels of bound states. Eq. (4.27) can be rewritten as

$$\det | G_{NN}^{-1} - U_{NN} | = 0 \quad (4.28)$$

where G_{NN}^{-1} is the inverse matrix of G_{NN} . Eq. (4.28) is preferred over Eq. (4.27) because $I_{NN} - G_{NN} U_{NN}$ is not Hermitian, even though G_{NN} and U_{NN} are Hermitian.

The Koster-Slater method is sometimes called the Green's function in the CCR because Eq. (4.21) can also be obtained if the perturbed wave-functions are expanded in terms of the Green's functions $G(\vec{r}, \vec{r}')$ for the unperturbed Hamiltonian H_0 , that is, in terms of the solutions of the differential equation

$$(H_0 - E)G(\vec{r}, \vec{r}') = \delta(\vec{r} - \vec{r}') \quad (4.29)$$

which are expressed in terms of the eigenstates of the unperturbed Hamiltonian (Bloch functions) by

$$G(\vec{r}, \vec{r}') = \sum_{n, k} \frac{b_n(\vec{k}, \vec{r}')^* b_n(\vec{k}, \vec{r})}{E_n(\vec{k}) - E} \quad (4.30)$$

The perturbed wave-function $\psi(\vec{r})$ is expressed in the form of an integral equation

$$\psi(\vec{r}') = \int \psi(\vec{r}) U(\vec{r}) G(\vec{r}, \vec{r}') d\vec{r} \quad (4.31)$$

If now the perturbed and unperturbed wave-functions in Eq. (4.31) are written in terms of Wannier functions, Eq. (4.21) is obtained. The proof is presented in the Appendix of reference 1.

Energy E in Eq. (4.21) or Eq. (4.30) is a real number if we are limited to states lying in the energy gap of the host material (bound states). In the case where we are dealing with states whose energies coincide with energies in the spectrum of H_0 , as in the scattering problem, E must be allowed to have an infinitesimal imaginary part.

The problem connected with the scattering of excitations in solids by localized imperfections in the Koster-Slater model was first considered by Koster,³² in the case of electrons, and a general theory, which is applicable to phonons and spin waves as well as electrons is presented by Callaway.³³

As can be observed, the Koster-Slater scheme is extraordinarily useful when the perturbing potential $U(\vec{r})$ is well localized. In this case, only matrix elements of U between Wannier functions centered at the site where U is localized or neighboring sites have to be considered.

This scheme has been successfully used in the problem of impurities in metals, where localized states are closely confined about the impurity center, and in the case of localized defects in semiconductors, such as vacancies for example.

The basic ideas about the electronic structure of impurities in metals before 1961 are presented in reference 57 and of particular interest is the work of Friedel,³⁴ where the scattering of electrons in a free-electron conduction band by an impurity potential is considered and virtual states bound to the impurity ion center are shown to exist. In 1961, Anderson³⁵ and Wolff³⁶ developed and applied the Green's function method of Koster and Slater to the interesting problem of magnetized local states in transition metals. A single band approximation was assumed and the impurity potential was considered closely confined to the site of the foreign atom. Wolff,³⁶ for example, treated the problem by considering the scattering of conduction electrons in the host metal from the potential due to a (single) ion impurity. This potential was assumed to have a spin-dependent part; the wave-functions were obtained and used to determine the self-consistent Hartree-Fock potential for the impurity. Virtual states* were proven to exist and if they are sharp and close enough to the Fermi level, the impurity ion develops an exchange potential that polarizes the electrons in its vicinity.

* The connection between the Koster-Slater method and the phase-shift analysis of Friedel was established by Clogston,³⁷ who showed that no real distinction exists between Friedel's virtual states and bound states.

The theory of Anderson and Wolff was used by Clogston et al.³⁸ in order to explain the localized magnetic moments experimentally observed by them in various transition-metal alloys with iron as impurity. The theory was later improved by Clogston,³⁹ by taking partial account of correlations and the many-band structure of the transition metals, and by Sokoloff,⁴⁰ who determine the electronic structure of dilute substitutional alloys of iron series impurities in copper, taking into consideration the actual band structure of copper.

Localized states due to impurities in semiconductors can fall into two categories: (1) shallow states, characterized by binding energies of the order of 0.01 eV to 0.1 eV and in general much smaller than the energy gap, and (2) deep states, characterized by larger binding energies, as in the case of Cu and Au in silicon and germanium (~ 0.5 eV).

In the description of the shallow impurity state, the most common approximation is the effective-mass theory (EMA)⁴¹. In this approximation, the impurity electron (hole) is considered as revolving round the impurity ion in orbits with large diameters (e.g. 50 \AA) and with an effective-mass m_{ef} , under the influence of a long-range screened potential $-1/\kappa r$ (κ being the dielectric constant), due to the extra charge in the impurity ion, considered at the origin of the system of coordinates. Thus, a hydrogenic-like equation⁴¹ is obtained for the envelope function and a Rydberg series of energy levels is expected to be obtained below (above) the band extremum.

Using the many-electron Hamiltonian including full electron-electron interaction and the static periodic potential Kohn⁴² was able to justify the EMA in the case of large orbits and weak bonding. The method was extended by Dresselhaus⁴³ for excitons and Kohn and Luttinger⁴⁴ for impurity states to include degenerate extrema.

Improvements have been made in the past years to the EMA. The first one,^{44,45} was to solve the Schrodinger equation for the electron near the impurity using the true potential and true electron mass and to match the solution to the EMA solution, which is valid far away from the impurity. Later, using the Green's function method which includes the full electron-electron interaction Sham⁴⁶ showed that corrections that are inversely proportional to the square of r exist at large distances from the impurity. They shift the impurity levels relative to one another and are not the commonly termed central cell corrections. While the former depend only on the properties of the host material and on the valency of the impurity atom, the latter corrections depend on the properties of the impurity atom.

On the other hand, deep states were for many years treated by a model originally conceived by Frenkel⁴⁷ for excitons and which has been improved by many authors.⁴⁸ According to Frenkel, the excitonic states can be interpreted in terms of a Heitler-London model, in which the excited electron is in an atomic-like state confined to the neighborhood of the lattice site from which it was excited. But, the optical experiments of Baldini⁴⁹ have shown that deep excitons in Kr and Xe have

energies not far from the EMA predictions which are obtained by extrapolating the Rydberg series of the shallow excitons. Moved by this surprising result, Hermanson and Phillips⁵⁰ investigated the validity of the EMA from a microscopic viewpoint, taking into account in their analysis the central cell corrections due to short-wavelength variations of the periodic and impurity potentials. The impurity equation obtained by them is not easily solved due to the interband matrix elements of the impurity potential. But they were able to apply a single band approximation by transforming to a pseudo-potential representation, where the effective potential is substantially cancelled within the impurity atom, thereby reducing tremendously the interband matrix elements. The theory was then used by one of the authors⁵¹ to calculate excitonic and impurity states in rare-gas solids.

The first application of the Koster-Slater method to vacancies in semiconductors was recently made by Callaway and Hughes¹⁰ for neutral single and divacancies in silicon. They used the pseudopotential method to determine the energy bands of the perfect crystal and represented the effect of the vacancy by the negative of an atomic pseudopotential. For the perfect crystal the empirical pseudopotentials of Brust¹⁹ were used and a fourth order polynomial in \vec{k} was used to interpolate between the values calculated at reciprocal lattice vectors. The origin was taken midway between the two atoms in a silicon unit cell and, in the case of a single vacancy, one of these atoms was removed. The group of the defect potential is therefore C_{3v} and only localized states

that belong to the totally symmetric Λ_1 representation were analysed. With six bands and ten sites the potential U had to be multiplied by a factor of about 1.6 in order for a bound state to be localized within the energy gap. More details about their calculation will be given in the next sections.

Recently, Johnson⁵² has derived a powerful method for treating bound states as well as scattering states due to imperfections. This method is based on the method he derived to calculate bound one-electron eigenstates for polyatomic molecules⁵³ and molecular ions,⁵⁴ the latter method being the complement of the KKR method for calculating the electronic energy bands of infinite crystals.

In the following sections we apply the Koster-Slater scheme to the study of vacancies in PbTe.

According to Eq. (4.28), the determinant of $(I_{NN} - G_{NN} U_{NN})$ has to be calculated for different values of the energy E lying outside the energy bands of the host crystal. The energy of a bound state is the one for which the determinant is zero. Matrix G_{NN} can be easily obtained if the unperturbed bands are known on a mesh of points in the Brillouin zone. For values of E near the bottom or top of the band, the general element of G_{NN} depends strongly on the details of the energy bands near these maxima and therefore on the number of points in the energy mesh. On the other hand, to obtain the elements of U_{NN} knowledge of the Wannier functions and the localized perturbing potential is needed.

In Section 4.2 we derive the expression for the general element of the U-matrix where the Bloch functions are calculated in the $\vec{K} \cdot \vec{\pi}$ - APW scheme. The choice of the phase factors that multiply Bloch functions in the definition of the Wannier functions is also discussed.

Section 4.3 is devoted to the solution of the vacancy problem in PbTe. There we show how to obtain the vacancy potential and how to define completely the Wannier functions for the valence and conduction bands. After the matrices G_{NN} and U_{NN} are calculated, Eq. (4.28) is solved first for the five valence bands in a single-band approximation, and, then the results are presented in the case where the five valence bands and four conduction bands are considered all together. In all these calculations 13 sites were considered.

4.2 The U Matrix in the $\vec{K} \cdot \vec{P}$ - APW Scheme

The purpose of this section is to determine the expressions for the matrix U in the $\vec{K} \cdot \vec{\pi}$ -APW scheme.

As we have seen in Chapter 3, in the $\vec{K} \cdot \vec{\pi}$ -APW scheme, a Bloch function for a point \vec{k} in the first Brillouin zone which transforms like the i-partner of the irreducible representation $\Gamma_{\alpha}^{(\vec{k})}$ of the group of \vec{k} is expressed in terms of the Bloch functions at a particular point \vec{k}_0 , which transform like partners of the irreducible representation $\Gamma_{\alpha}^{(\vec{k}_0)}$ of the group of \vec{k}_0 . The relation is

$$b_{n,i}^{\Gamma}(\vec{k}) = \sum_{n',i'} C_{n,n'}^{i,i'}(\vec{K}) e^{i\vec{K}\cdot\vec{r}} b_{n',i'}^{\Gamma}(\vec{k}_0) \quad (4.32)$$

First of all we will discuss how to construct Wannier functions from the complete set of Bloch functions, in the general case where spin is present and the band structure of the material presents both degeneracies required by symmetry, accidental degeneracies, and quasi-degeneracies which occur when energy bands approach each other at some points of the Brillouin zone.

Let us first consider the region A of the Brillouin zone which contains general points, i.e., points of no symmetry.* If the operation α of the crystal point group are applied to the wave-vector \vec{k} in A, a set of vectors $\alpha\vec{k}$, also in A, is obtained. This set is known as the star of \vec{k} and for a general point it contains G elements, where G is the number of operations in the crystal point group.

It is well known that at a general point, band crossing is unlikely to occur. All energy bands are doubly degenerate, and Bloch functions for one band are partners of the identity double-group irreducible representation Γ_6 of the group of \vec{k} . For every band n and every lattice vector \vec{R}_q , we could consider two Wannier functions, one for each partner of the band, the contribution from the Bloch functions being

* The only symmetry operation of the group of \vec{k} is the identity operation.

$$e^{-i\vec{k}\cdot\vec{R}_{n,i}} \Gamma_6(\vec{k}) e^{i\theta_n(\vec{k})}$$
 , for the Wannier function corresponding to the i -partner. But for some materials, as PbTe for example, quasi-degeneracies are found to be rather numerous in A. Near a quasi-degeneracy the energy bands almost cross. In fact, they do not but the wave-functions change drastically. Two different points of view can be taken when defining the Wannier functions near quasi-degeneracies.

According to the first point of view, the bands are not allowed to cross and are defined in their order of increasing energy. In this case a continuous energy band will be produced and the G-matrix will have the proper asymptotic behavior for large values of E. The wave-functions, however, may vary wildly in the zone, making the definition of localized Wannier functions more difficult, but not impossible. In this case, under the operations of the crystal point group, the localized Wannier functions will not exhibit simple transformation properties and larger matrices will have to be diagonalized in solving the defect problem.

The second point of view consists of departing from the above band ordering according to increasing energy by defining bands with smooth Bloch function in k -space.* In this case the points where the quasi-degeneracies occur have to be excluded from the definition of the

* By a smooth Bloch function we mean a Bloch function whose periodic part varies slowly in k -space.

Wannier functions and consequently the G-matrix does not have the proper behavior for larger values of E. But localized Wannier functions with simple transformation properties can be obtained, and smaller matrices will have to be solved. In both cases, however, orthonormal Wannier functions are obtained, if each Bloch function contributes to only one Wannier function.

In the present work we will adopt the first point of view because for PbTe, which is a small gap semiconductor, quasi-degeneracies occur in a large region of \vec{k} -space, both for the valence and conduction bands. The upper valence band and the lowest conduction band also come close together in a region of k-space and in this region the corresponding Bloch functions do not behave as smooth functions.

Now let us consider the contributions coming from symmetry points, where the bands can have degeneracy greater than two, and band crossing is allowed between bands that transform like different irreducible representations. Let us call \vec{k}_S the wave-vector of a certain symmetry point S inside or on the boundary of the first Brillouin zone. As far as degeneracy is concerned, two cases are possible: a single band in A corresponds to a single band at S, or two or more bands in A will join at S, giving rise to a band with degeneracy greater than two. In the first case, point S can be treated as a general point, but the second case can present difficulties. If, however, a certain partner j of a band m at S corresponds to the partner i of a particular band n at all points in A near S, then the contribution from S to the Wannier

function corresponding to the i-partner of band n in A is $e^{-i\vec{k}_s \cdot \vec{R}_q} e^{i\theta_n(\vec{k}_s)}$ multiplied by the j-partner of band m in S. In order to clarify this point let us consider one example. Suppose that we have a four-fold degenerate band n with symmetry $\Gamma_\alpha^{(\vec{k}_s)}$ at S. This band will split into two two-fold degenerate $\Gamma_\beta^{(\vec{k}_T)}$ bands when going from S to a general point T in A. Now, if for example the second and third partners of $\Gamma_\alpha^{(\vec{k}_s)}$ correspond to the first and second partners of the first of the $\Gamma_\beta^{(\vec{k}_T)}$ bands, then the contribution to the Wannier functions corresponding to these partners will be $e^{-i\vec{k}_s \cdot \vec{R}_q} \Gamma_\alpha^{(\vec{k}_s)} e^{i\theta_n(\vec{k}_s)}$ and $e^{-i\vec{k}_s \cdot \vec{R}_q} \Gamma_\alpha^{(\vec{k}_s)} e^{i\theta_n(\vec{k}_s)}$ respectively. But the above behavior does not always happen as, for example, for the Γ_8^- -bands. While along the Δ -axis the first partner of a Δ_6 -band corresponds to $(b\Gamma_{8,4}^-, -c\Gamma_{8,2}^-)$, where $b=1/\sqrt{2}$ and $c=1/\sqrt{6}$, along the Σ -axis the same has to have a Σ_5 -symmetry and the first partner of a Σ_5 -band corresponds to $\Gamma_{8,4}^-$. We could however, exclude the symmetry axes from the definition of the Wannier functions, but we should not forget that for points near these axes the behavior of the Bloch functions is similar.

Points like Γ can be excluded in the definition of the Wannier functions, because we are interested in matrix elements of these functions, and in integrations a finite number of points can be disregarded without altering the results.

On the surface of the Brillouin zone problems also arise at points \vec{k} where there exist operations α in the point group such that $\alpha\vec{k}=\vec{k}+\vec{K}_1$, \vec{K}_1 being a reciprocal lattice vector. One example is the

L-point in the f.c.c. lattice. Due to the special transformation properties of the wave-functions, discontinuities may occur in the $\vec{K} \cdot \vec{\pi}$ coefficients. However, points like that can also always be excluded.

Let us assume now that on a symmetry axis Q two bands with different symmetries, Q_a and Q_b , cross at a point P (figure 4.1.a). Along a general line parallel and adjacent to Q (figure 4.1.b) the bands do not cross but strong quasi-degeneracies occur and the $\vec{K} \cdot \vec{\pi}$ coefficients change drastically near P^+ . At the Q-axis the contribution to the Wannier function corresponding to band 1 (2) can be considered as given by the Bloch functions of Q_a , (Q_b) on the left of P, and by the Bloch functions of Q_b , (Q_a) on the right of P. Consequently, at P it will make no difference which Bloch function is chosen, but once the Bloch function of Q_a is chosen for band 1, for example, then the Bloch function of Q_b has to be used for band 2. This particular definition along a symmetry axis is not essential because we may always define Wannier functions excluding the points on this axis when calculating matrix elements; however, it is desirable, when a reasonable interpolation in the wave-functions is needed for the region near the axis.

It is easy to see that the Wannier functions defined in this way form a complete orthonormal set, because the Bloch function corresponding to one band contributes to one and only one Wannier function. The choice of the phase factors $\theta_n(k)$ is made in order to obtain localized Wannier functions. This point, together with

the transformations properties of Wannier functions, will be discussed later.

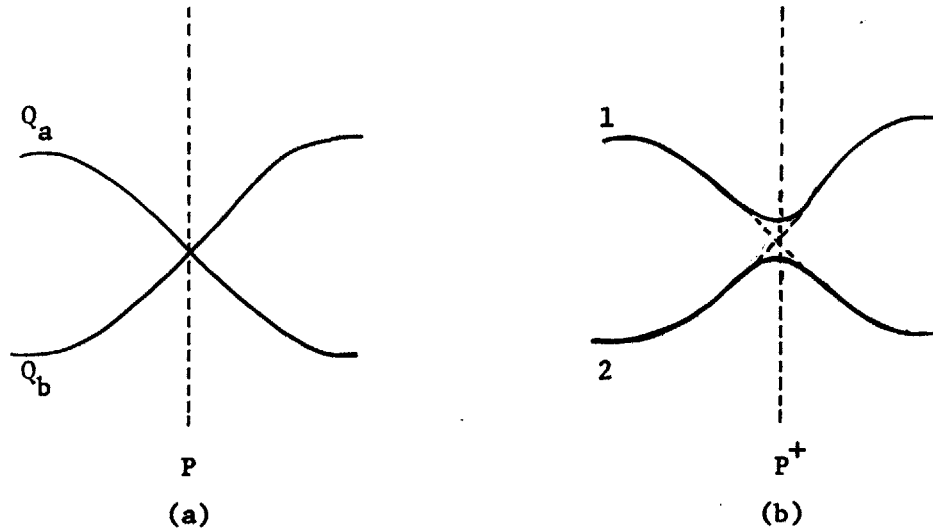


Fig. 4.1 - Example of band-crossing in a symmetry axis (a) and how the bands are in a general axis adjacent to it (b).

Let us now determine the expressions for the elements of the U matrix. The general term in this matrix is given by

$$\begin{aligned}
 U_{n',n}^{i',i}(\vec{R}'_q, \vec{R}_q) &= \int d\vec{r} a_{n',i'}^*(\vec{r}-\vec{R}'_q) U(\vec{r}) a_{n,i}(\vec{r}-\vec{R}_q) \\
 &= \frac{1}{N} \sum_{\vec{k}, \vec{k}'} e^{i\vec{k}' \cdot \vec{R}'_q} e^{-i\vec{k} \cdot \vec{R}_q} U_{n',n}^{i',i}(\vec{k}', \vec{k})
 \end{aligned} \tag{4.33}$$

where the sums on \vec{k} and \vec{k}' include only the points in the first Brillouin zone that make contributions to the Wannier functions*, and

$$U_{n',n}^{i',i}(\vec{k}', \vec{k}) = \int d\vec{r} b_{n',i'}(\vec{k}', \vec{r}) U(\vec{r}) b_{n,i}(\vec{k}, \vec{r}) e^{-i\theta_{n'}(\vec{k}')} e^{i\theta_n(\vec{k})} \tag{4.34}$$

* We are allowing here the case where points in the symmetry axes are not considered when calculating matrix elements.

If Eq. (4.32) is used for obtaining the Bloch functions at \vec{k} in terms of Bloch functions at \vec{k}_0 , as a result of the $\vec{K} \cdot \vec{\pi}$ scheme, then Eq.

(4.34) can be written as

$$U_{n,n}^{i,j;i,j}(\vec{k}',\vec{k}) = \sum_{m',j'} \sum_{m,j} C_{n,m'}^{i,j'}(\vec{k}')^* C_{n,m}^{i,j}(\vec{k}) e^{i\theta_{n'}(\vec{k}')} e^{i\theta_n(\vec{k})} \times \int d\vec{r} [b_{m',j'}^{\Gamma(\vec{k}_0)}(\vec{k}_0,\vec{r})]^* e^{-i(\vec{k}'-\vec{k}) \cdot \vec{r}} U(\vec{r}) b_{m,j}^{\Gamma(\vec{k}_0)}(\vec{k}_0,\vec{r}) \quad (4.35)$$

Because at \vec{k}_0 the relativistic bands are expressed in terms of the non-relativistic bands, in the APW scheme, the integral part of Eq. (4.35) will be written as a linear combination of integrals involving the non-relativistic bands. In the Appendix we derive the expression for the last integral, i.e., the matrix element of $e^{-i(\vec{k}'-\vec{k}) \cdot \vec{r}} U(\vec{r})$ between non-relativistic bands at \vec{k}_0 . As is observed from Eq. (A.13) this matrix element can be written as the product of three functions: one independent of \vec{k} and \vec{k}' , the second depending only on $|\vec{k}-\vec{k}'|$ and the third depending only on the direction of $(\vec{k}'-\vec{k})$ or, more precisely, on the group of $(\vec{k},-\vec{k})$ when $U(\vec{r})$ has the same symmetry as the group of \vec{k}_0 . But in Eq. (4.35), \vec{k}' and \vec{k} can take general values in k-space and even if a reasonable mesh of points is used, the number of matrix elements to be calculated would be enormous and the computational time involved probably prohibitive. However, if $U(\vec{r})$ is a localized perturbation we expect that simplifications can be made. In fact, if $U(\vec{r})$ is very localized near the origin,

* We are allowing here the case where points in the symmetry axes are not considered when calculating matrix elements.

then the exponential $e^{-i(\vec{k}'-\vec{k})\cdot\vec{r}}$ can be expanded in Taylor's series near the origin and the integral part in Eq. (4.35) be written as

$$\begin{aligned} & \int d\vec{r} [b_{m,j}^{\Gamma\beta'}(\vec{k}_0)]^* e^{-i(\vec{k}'-\vec{k})\cdot\vec{r}} U(\vec{r}) b_{m,j}^{\Gamma\beta}(\vec{k}_0) \\ &= \int d\vec{r} [b_{m,j}^{\Gamma\beta'}(\vec{k}_0)]^* U(\vec{r}) b_{m,j}^{\Gamma\beta}(\vec{k}_0) \\ &+ i(\vec{k}-\vec{k}') \cdot \int d\vec{r} [b_{m,j}^{\Gamma\beta'}(\vec{k}_0)]^* \vec{r} U(\vec{r}) b_{m,j}^{\Gamma\beta}(\vec{k}_0) + \dots (4.36) \end{aligned}$$

If $U(\vec{r})$ is well localized then only a few terms in this expansion need be considered. In the case of vacancies in PbTe, as we will see later, only the first two terms in Eq. (4.36) need to be considered if \vec{k} and \vec{k}' are restricted to the first Brillouin zone.

Define

$$C_{n,m}^{i,j}(\vec{R}_q) = \frac{1}{N} \sum_{\vec{k}} C_{n,m}^{i,j}(\vec{k}) e^{-i\vec{k}\cdot\vec{R}_q} e^{i\theta_n(\vec{k})} \quad (4.37)$$

$$\begin{aligned} D_{n,m}^{i,j}(\vec{R}_q) &= \frac{1}{N} \sum_{\vec{k}} C_{n,m}^{i,j}(\vec{k}) e^{-i\vec{k}\cdot\vec{R}_q} \vec{k} e^{i\theta_n(\vec{k})} \\ &= [i \frac{\partial}{\partial \vec{r}} C_{n,m}^{i,j}(\vec{r})]_{\vec{r}=\vec{R}_q} \quad (4.38) \end{aligned}$$

where in the last part of Eq. (4.38) we take $C_{n,m}^{i,j}(\vec{R}_q)$ to be a continuous function in the lattice sites \vec{R}_q , although it is a discrete function. The general element (4.33) of the matrix U will then be written as

* We are allowing here the case where points in the symmetry axes are not considered when calculating matrix elements.

$$\begin{aligned}
 U_{n,n}^{i,i}(\vec{R}', \vec{R}_q) &= \sum_{m',j'} \sum_{m,j} C_{n,m'}^{i,j'}(\vec{R}_q) * C_{n,m}^{i,j}(\vec{R}_q) T_{m',m}^{j',j} \\
 &+ \sum_{m',j'} \sum_{m,j} [C_{n,m'}^{i,j'}(\vec{R}_q) * D_{n,m}^{i,j}(\vec{R}_q) - C_{n,m}^{i,j}(\vec{R}_q) D_{n,m'}^{i,j'}(\vec{R}_q) *] N_{m',m}^{j',j} \quad (4.39)
 \end{aligned}$$

where

$$T_{m',m}^{j',j} = \frac{N}{B_{\text{norm}}} \int d\vec{r} [b_{m',j'}^{\Gamma_{\beta'}}(\vec{k}_o, \vec{r})]^* U(\vec{r}) b_{m,j}^{\Gamma_{\beta}}(\vec{k}_o, \vec{r}) \quad (4.40)$$

$$N_{m',m}^{j',j} = \frac{N}{B_{\text{norm}}} \int d\vec{r} [b_{m',j'}^{\Gamma_{\beta'}}(\vec{k}_o, \vec{r})]^* \vec{r} U(\vec{r}) b_{m,j}^{\Gamma_{\beta}}(\vec{k}_o, \vec{r}) \quad (4.41)$$

with

$$B_{\text{norm}} = [\int d\vec{r} |b_{m',j'}^{\Gamma_{\beta'}}(\vec{k}_o, \vec{r})|^2]^{1/2} [\int d\vec{r} |b_{m,j}^{\Gamma_{\beta}}(\vec{k}_o, \vec{r})|^2]^{1/2} \quad (4.42)$$

If the group of \vec{k}_o contains inversion and $U(\vec{r})$ has at least the same symmetry as \vec{k}_o , then the element (4.40) of the T matrix is different from zero only if the representations $\Gamma_{\beta'}(\vec{k}_o)$ and $\Gamma_{\beta}(\vec{k}_o)$, and the partners j' and j are the same. However, in order for the element (4.41) of matrix N to be different from zero, it is necessary that the above representations have different parity.

If \vec{k}' and \vec{k} are general points in k-space, then, because $U(\vec{r})$ is invariant under time-reversal,

$$\int d\vec{r} [b_{n,i}^{\Gamma_{\beta'}}(\vec{k}', \vec{r})]^* U(\vec{r}) b_{n,i}^{\Gamma_{\beta}}(\vec{k}, \vec{r}) = U_{n,n}(\vec{k}', \vec{k}) \delta_{i',i} \quad (4.43)$$

i.e., the partners have to be the same and the result is independent of the partner. Then,

$$U_{n;n}^{i,i}(\vec{R}'_q, \vec{R}_q) = U_{n;n}(\vec{R}'_q, \vec{R}_q) \delta_{i,i} \quad (4.44)$$

Let us now determine the expressions (4.37) and (4.38) in the case where we have a f.c.c. lattice and the group of \vec{k}_0 contains inversion. The integration on k-space need be performed only over 1/48 of the Brillouin zone if the relations between the coefficients $C_{n,m}^{i,j}(\vec{k})$ and $C_{n,m}^{i,j'}(\alpha\vec{k})$, where α is an operation of the point group, and the phases $\theta_n(\vec{k})$ are known. If the $\vec{K} \cdot \vec{\pi}$ relation (3.40) is assumed, then

$$C_{n,m}^{i,j}(\vec{R}_q) = \frac{1}{N} \sum'_{\vec{k}} \frac{1}{t(\vec{k})} \sum_{\alpha} \sum_{\ell} C_{n,m}^{i,\ell}(\vec{k}) \Gamma_{\beta}^{(\vec{k}_0)}(\alpha)_{j,\ell} e^{-i\alpha\vec{k} \cdot \vec{R}_q} e^{i\theta_n(\alpha\vec{k})} \quad (4.45)$$

$$D_{n,m}^{i,j}(\vec{R}_q) = \frac{1}{N} \sum'_{\vec{k}} \frac{1}{t(\vec{k})} \sum_{\alpha} \sum_{\ell} C_{n,m}^{i,\ell}(\vec{k}) \Gamma_{\beta}^{(\vec{k}_0)}(\alpha)_{j,\ell} e^{-i\alpha\vec{k} \cdot \vec{R}_q} e^{i\theta_n(\alpha\vec{k})} \quad (4.46)$$

where \vec{k} is now restricted to 1/48 of the zone. We indicate this fact by the primed sum on \vec{k} . If \vec{k} is a general point, then $\alpha\vec{k}$ is different from \vec{k} if $\alpha \neq \epsilon$, and the application of the 48 operations of the point group will give 48 different points in the sum on \vec{k} . However, if \vec{k} is for example the Γ -point, the application of the 48 operations will give 48 equal contributions to Eq. (4.45) and Eq. (4.46), but as we should have only one contribution because there is only one Γ -point, the total contribution coming from this point has to be divided by 48. This multiple counting is corrected by the weighting factor $t(\vec{k})$. For reference on the weighting factor for all points in the 1/48 of the zone, see, for example, Brust.¹⁹

As we mentioned before, the phases $e^{i\theta_n(\alpha\vec{k})}$ have to be chosen

in order to produce reasonably localized Wannier functions. This is a very difficult problem if the material under consideration presents a complicate energy band structure.

The case of non-degenerate bands and well behaved Bloch functions was studied by Callaway and Hughes¹⁰ and Callaway²⁴, as discussed in Chapter 3. For PbTe, for example, because the relativistic corrections are important, the bands at a general point are doubly-degenerate and at the Γ -point some of the important bands have degeneracy greater than two. The conduction and valence bands come close together in certain regions of k-space and due to the mutual interaction, the $\vec{K} \cdot \vec{\pi}$ coefficients change drastically, which causes the Bloch functions to vary rapidly in these regions. This fact by itself is enough to cause the non-localization of the Wannier functions.

Suppose we have a mesh of p general points ($t(\vec{k}) = 1$) in 1/48 of the Brillouin zone. Because for every point \vec{k}' in this region there are 47 other points in the star of \vec{k}' , the total number of points is 48p. The most reasonable procedure for obtaining the optimal Wannier function for a particular band is to assign a phase factor for each one of the 48p Bloch functions, to calculate the matrix element of the impurity potential between Wannier functions centered at the origin and vary each one of these phase factors until a maximal value for the matrix element is obtained. This method, however, is exhaustive and time consuming. In the case

of localized perturbations it is possible to make reasonable choices just by examining the expressions for the matrix elements. In this case, the Wannier functions can be considered well localized if the matrix element of the perturbation $U(\vec{r})$ between the Wannier functions centered at the site where the perturbation is concentrated is much larger than any other matrix elements relating Wannier functions.

For a particular band, the phases in $1/48$ of the zone are chosen to produce the best Bloch functions. This is achieved by making the important $\vec{k} \cdot \vec{\pi}$ coefficients vary in the smoothest possible way in this region of k -space. This is a tedious work but can be easily done if a reasonable mesh of points is considered. Besides being the best choice for Wannier functions, it is important when interpolation is needed in order to obtain the wave-functions at points other than the points in the mesh.

In order to decrease the number of possible choices we will assume that the phase associated with a point in the star of \vec{k} , where \vec{k} is in $1/48$ of the zone, is obtained by adding a \vec{k} -independent constant to the phase associated with \vec{k} . It can be easily shown that this is a good assumption if the important $\vec{k} \cdot \vec{\pi}$ coefficients do not change drastically in $1/48$ of the zone. So, given a Bloch function with k -vector in this region, the Bloch functions in the star of \vec{k} will enter into the construction of the Wannier function multiplied by a phase factor which is only function of α , where α is an operation of the crystal point group. For every

possible set $\{\theta_n(\alpha_i); i=1,48\}$ and every band we should calculate the matrix elements of $U(\vec{r})$ between the Wannier functions and pick out the set that maximizes the localization of these functions, i.e., $\int d\vec{r} a_{n,i}^*(\vec{r}-\vec{R}_p) U(\vec{r}) a_{n,i}(\vec{r}-\vec{R}_q)$ is maximal for $\vec{R}_p = \vec{R}_q = 0$, that is, it is much bigger than the matrix elements with others \vec{R}_p and \vec{R}_q and where we assume that the perturbation $U(\vec{r})$ is localized at the origin. Because the leading term in the expression (4.33) for $U_{n,n}^{i,i}(\vec{R}_q, \vec{R}_q)$ is the first we can write approximately:

$$U_{n,n}^{i,i}(0,0) \sim \sum_{m,m',j} C_{n,m}^{i,j}(\vec{R}_p=0)^* C_{n,m}^{i,j}(\vec{R}_p=0) T_{m',m} \quad (4.47)$$

In obtaining Eq. (4.47) we made use of the fact that $T_{m',m}^{j,j} = T_{m',m} \delta_{j',j}$ and we recall that the representation corresponding to bands m' and m have to be the same. According to Eq. (4.45)

$$C_{n,m}^{i,j}(\vec{R}_p=0) = \frac{1}{N} \sum_{\vec{k}} \frac{1}{t(\vec{k})} \sum_{\alpha} \sum_{\ell} C_{n,m}^{i,\ell}(\vec{k}) \Gamma_{\beta}^{(k_0)}(\alpha)_{j,\ell} e^{i\theta_n(\alpha)} \quad (4.48)$$

If partner i of band n corresponds to partner r of band m_s at \vec{k}_0 it is possible that for a large portion of the 1/48 region of \vec{k} -space the leading $\vec{k} \cdot \vec{\pi}$ coefficient of the former band is the one corresponding to the later band. Let us emphasize this point when calculating $U_{n,n}^{i,i}(0,0)$. Assume that for every \vec{k} in the 1/48 region $C_{n,m_s}^{i,r}(\vec{k})$ is the leading coefficient.* If band m_s transforms like the irreducible representation $\Gamma_{\gamma}^{(k_0)}$ we can write

$$U_{n,n}^{i,i}(0,0) \sim A_{n,m_s}^{i,r} \sum_j Q_{j,r}^* Q_{j,r} \quad (4.49)$$

* In PbTe this is not true for all bands.

where

$$A_{n,m_s}^{i,r} = \left[\frac{1}{N^2} \sum_{k,k'} \frac{1}{t(\vec{k}) t(\vec{k}')} C_{n,m_s}^{i,r}(\vec{k}')^* C_{n,m_s}^{i,r}(\vec{k}) \right] T_{m_s,m_s} \quad (4.50)$$

$$Q_{j,r} = \sum_{\alpha} \Gamma_{\gamma}^{(\vec{k}_o)}(\alpha)_{j,r} e^{i\theta_n(\alpha)} \quad (4.51)$$

But $Q_{j,r}^* Q_{j,r} = |Q_{j,r}|^2$ and $U_{n,n}^{i,i}(0,0)$ will be maximum if $\sum_j |Q_{j,r}|^2$ is maximum. Let $a_{j,r}$ and $b_{j,r}$ be the real and imaginary parts of $Q_{j,r}$, respectively. Then

$$U_{n,n}^{i,i}(0,0) \sim A_{n,m_s}^{i,r} \sum_j [a_{j,r}^2 + b_{j,r}^2] \quad (4.52)$$

and the larger the numbers $|a_{j,r}|$ and $|b_{j,r}|$, the larger $U_{n,n}^{i,i}(0,0)$ will be. For simplicity we will assume that $e^{i\theta_n(\alpha)} = \pm 1$.

One way of obtaining a maximum value for Eq. (4.52) is to choose

$\theta_n(\alpha)$ such that one element, $a_{r,r}$ say, is the largest possible.

But there will be some α 's that do not contribute to $a_{r,r}$. Then,

we choose part of the remaining $\theta_n(\alpha)$ such that another element

is the largest possible and continue in this way until all $\theta_n(\alpha)$

have been chosen. We can now quickly choose the phase factor of

an improper rotation in terms of the corresponding proper rotation,

in the case where the group of \vec{k}_o contains inversion. If $\Gamma_{\beta}^{(\vec{k}_o)}$ has

even parity, then $\Gamma_{\beta}^{(\vec{k}_o)}(J\alpha) = \Gamma_{\beta}^{(\vec{k}_o)}(\alpha)$, where J is the inversion opera-

tor and in this case we have to have $e^{i\theta(J\alpha)} = e^{i\theta(\alpha)}$. However, if

$\Gamma_{\beta}^{(\vec{k}_o)}$ has odd parity, $\Gamma_{\beta}^{(\vec{k}_o)}(J\alpha) = -\Gamma_{\beta}^{(\vec{k}_o)}(\alpha)$ and we should choose $e^{i\theta(J\alpha)}$

$= -e^{i\theta(\alpha)}$. In the next section, we will apply the above results to PbTe.

4.3 - VACANCIES IN PBTE

Let us apply the formalism developed in the previous sections to the case where the perturbing potential $U(\vec{r})$ is due to a neutral Pb-or Te-vacancy.

In the APW method one starts with the non-relativistic self-consistent Hartree-Fock atomic potential and radial wave-functions for the atoms under consideration (neutral Pb and Te in our case), as obtained from the program of Herman and Skillman.⁵⁵ The charge densities are then calculated, together with the Coulomb potential, which arises from the fixed charges and the charge density of all electrons. The crystal potential within each sphere is constructed by adding to the Coulomb potential and charge density the spherical average of the Coulomb potentials and charge densities of the neighboring spheres. The total spherically averaged charge density is then used to obtain the total exchange potential. The crystal potential is the sum of the total Coulomb potential and total exchange. In the region outside the spheres the crystal potential is the sum of the Coulomb potential obtained by averaging the Coulomb potentials from all the atoms in that region, and the exchange potential evaluated by finding the total charge in the region and assuming it to be uniform over the region.

Assume that one atom, Pb say, is missing and that no lattice deformation or screening occur. The crystal potential at the sphere corresponding to this atom is only due to the contribution coming from the neighboring spheres and the perturbing

potential is given by the negative of the crystal potential decreased by this contribution. In the neighboring Te-spheres the spherically averaged contribution of the Pb-atom is missing and it represents the perturbing potential in these spheres. The same can be said about the perturbing potential in the neighboring Pb-spheres. In the constant potential region, the contribution of the Pb-sphere is missing both in the Coulomb potential and in the charge density and the perturbing potential can easily be obtained.

Table 4.1 presents some values for the perturbing potential at Pb and Te spheres due to a Pb- and Te-vacancies, together with the crystal potentials. The perturbing potential is important only at the sphere in which the vacancy occurs and its value in the other spheres is disregarded in the calculations. The perturbing and crystal potentials multiplied by the radius r are shown in figure 4.2 (Pb-vacancy) and 4.3 (Te-vacancy).

The perturbing potential can be calculated in the plane-wave region by performing the same averaging used in obtaining the constant crystal potential. Near the vacancy a value of 0.070 a.u. for a Te-vacancy and 0.118 a.u. for a Pb-vacancy were obtained and the values in other regions are completely negligible.

It is evident that the potential constructed in such a way has the point group symmetry and is important only in the cell where the vacancy is located.

Let us now calculate the matrix elements of the operator

r (a.u.)	Crystal potential V(r) Pb-sphere (a.u.)	Pb-vacancy			Crystal potential V(r) Te-sphere (a.u.)	Te-vacancy		
		Pb-sphere (a.u.)	Te-sphere (neighbor) (10 ⁻² a.u.)	Pb-sphere (neighbor) (10 ⁻³ a.u.)		Te-sphere (a.u.)	Pb-sphere (neighbor) (10 ⁻² a.u.)	Te-sphere (neighbor) (10 ⁻³ a.u.)
0.0006	-271607.531	271607.527	0.832	0.47	-172385.926	172385.229	0.185	0.04
0.0024	-29335.669	29335.396	0.426	0.32	-18719.808	18719.366	0.115	0.16
0.0102	-15100.241	15099.972	0.440	0.32	-9682.410	9682.050	0.110	0.05
0.0204	-7112.004	7111.731	0.425	0.32	-4612.999	4612.659	0.111	0.06
0.0300	-4601.703	4601.434	0.429	0.31	-2995.684	2995.340	0.109	0.06
0.0408	-3209.595	3209.335	0.425	0.31	-2103.063	2102.720	0.108	0.06
0.0504	-2483.934	2483.675	0.423	0.31	-1637.268	1636.926	0.107	0.06
0.0816	-1332.464	1332.199	0.425	0.31	-894.974	894.630	0.108	0.06
0.1032	-965.904	965.621	0.423	0.31	-655.947	655.604	0.112	0.06
0.2088	-327.587	327.324	0.426	0.31	-233.469	233.127	0.109	0.06
0.3528	-126.081	125.815	0.431	0.31	-97.549	97.207	0.113	0.06
0.6024	-42.097	41.826	0.456	0.32	-35.366	35.017	0.122	0.06
0.8328	-20.270	19.988	0.494	0.33	-17.502	17.142	0.139	0.06
1.2168	-8.168	7.865	0.590	0.37	-7.276	6.897	0.181	0.07
1.4856	-4.873	4.544	0.714	0.42	-4.500	4.099	0.243	0.09
1.8312	-2.910	2.547	0.933	0.52	-2.782	2.347	0.371	0.11
2.2152	-1.873	1.460	1.287	0.69	-1.842	1.362	0.633	0.16
2.5992	-1.325	0.832	1.874	1.01	-1.332	0.792	1.195	0.24
3.0216	-1.045	0.463	3.157	1.46	-1.033	0.390	2.160	0.44
3.1752	-0.990	0.367	3.677	1.66	-0.981	0.304	2.659	0.54

TABLE 4.1 - Crystal potential and vacancy potentials due to a Pb- and a Te-vacancy. Radius r refers to the center of the spheres.

($R_{Te} = 2.9958$ a.u.; $R_{Pb} = 3.1005$ a.u.)

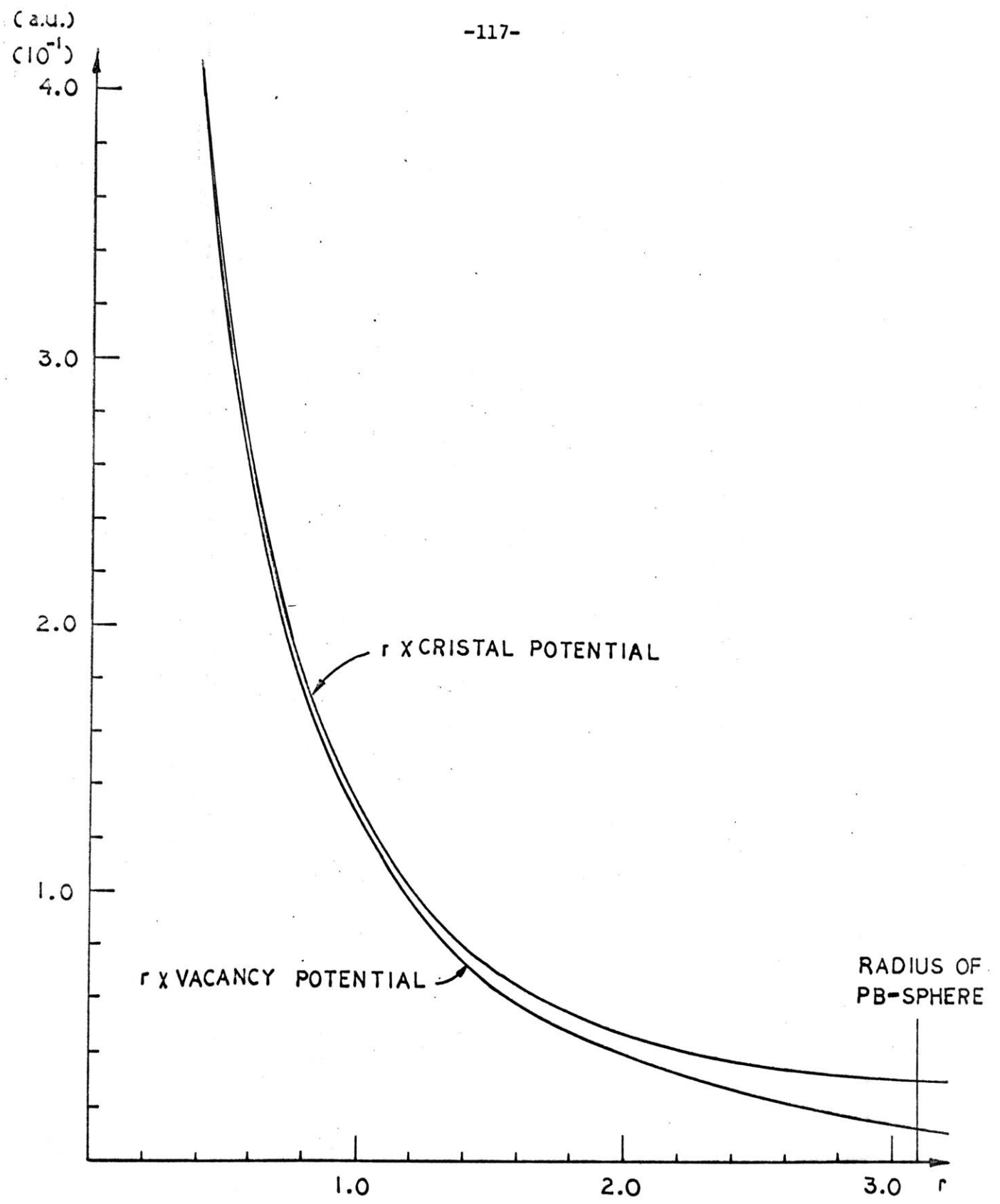


FIGURE 4.2 - Radius r times crystal and vacancy potentials in the sphere where the Pb-vacancy is located.

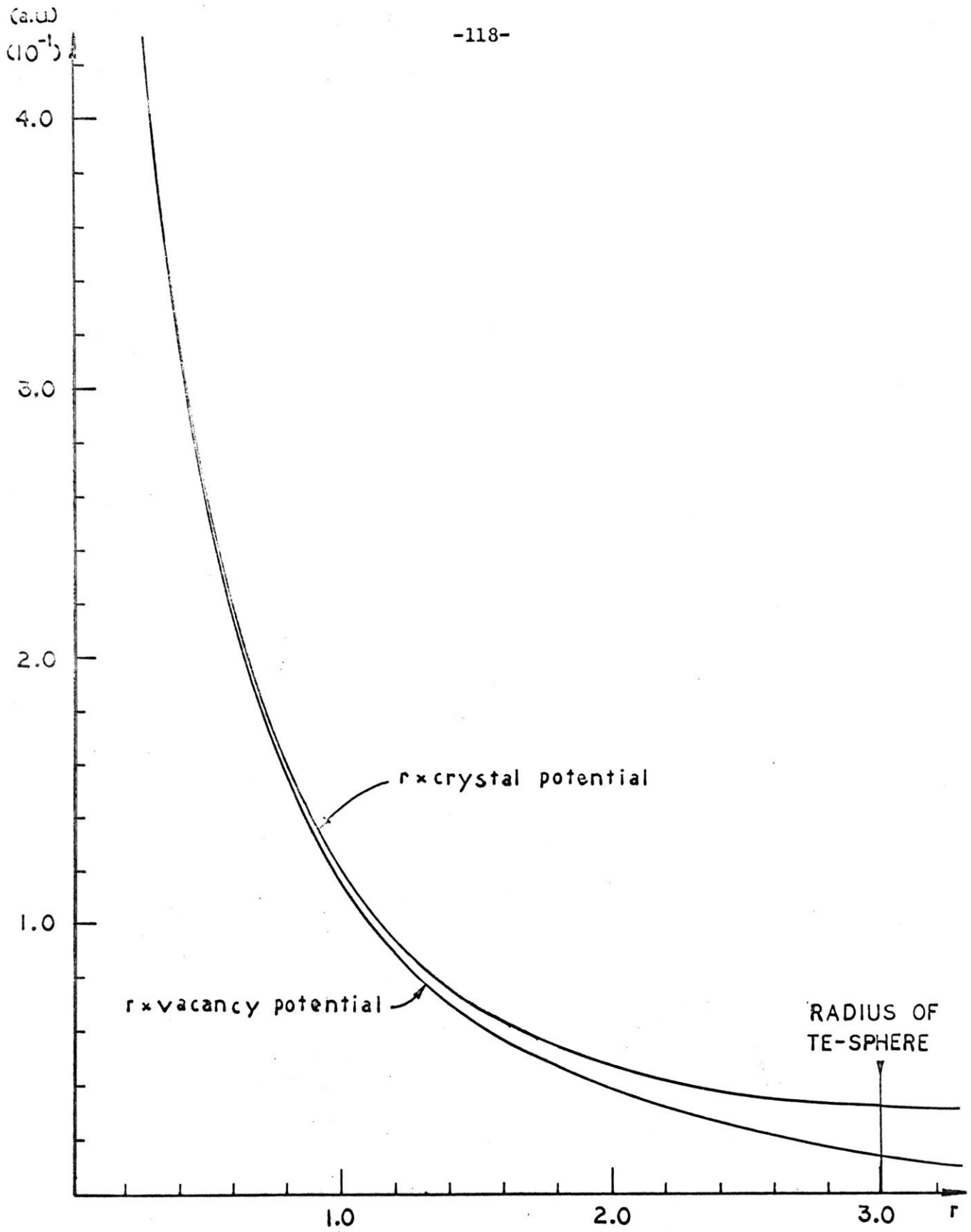


FIGURE 4.3 - Radius r times the crystal and vacancy potentials in the sphere where the Te-vacancy is located.

$N e^{-i(\vec{k}' - \vec{k}) \cdot \vec{r}} U(\vec{r})$ between the non-relativistic Bloch functions at Γ , i.e.

$$S_{m,m}^{j,j}(\Delta\vec{k}) = N \frac{\int_{\text{crystal}} d\vec{r} b_{m,j}^{\Gamma\beta'}(0,\vec{r})^* e^{+i\Delta\vec{k} \cdot \vec{r}} U(\vec{r}) b_{m,j}^{\Gamma\beta}(0,\vec{r})}{\int_{\text{crystal}} d\vec{r} |b_{m,j}^{\Gamma\beta'}(0,\vec{r})|^2 \cdot \int_{\text{crystal}} d\vec{r} |b_{m,j}^{\Gamma\beta}(0,\vec{r})|^2} \quad (4.53)$$

where N is, as before, the number of unit cells in the crystal and in Eq. (4.53), $\Delta\vec{k} = \vec{k} - \vec{k}'$. Because the perturbation $U(\vec{r})$ is important only in the cell where the vacancy occurs, Eq. (4.53) can be replaced

$$S_{m,m}^{j,j}(\Delta\vec{k}) = \frac{\int_{\text{cell}} d\vec{r} b_{m,j}^{\Gamma\beta'}(0,\vec{r})^* e^{+i\Delta\vec{k} \cdot \vec{r}} U(\vec{r}) b_{m,j}^{\Gamma\beta}(0,\vec{r})}{\int_{\text{cell}} d\vec{r} |b_{m,j}^{\Gamma\beta'}(0,\vec{r})|^2 \int_{\text{cell}} d\vec{r} |b_{m,j}^{\Gamma\beta}(0,\vec{r})|^2} \quad (4.54)$$

The expression for the numerator of Eq. (4.54) has been derived in the Appendix and the normalization integrals in the denominator may be obtained when performing the APW calculation at Γ . Both integrals are functions of the number of symmetrized APW's and the number of ℓ -terms used in the expansion of the APW's. Thus the same number of SAPW and ℓ -terms must be used in both calculations.

Table 4.2 presents the calculated values of $S_{m,m}^{j,j}(\Delta\vec{k})$ for a Pb- and Te-vacancy in the case where $\Delta\vec{k} = \vec{k} - \vec{k}' = \frac{\pi}{a}(t, 0, 0)$, a being the lattice parameter and t varying from 0.0 to its maximum value 4.0. When calculating these matrix elements the origin of the system of coordinates was assumed to be at the center of the sphere in which the vacancy occurs, and the change in the origin from the

TABLE 4.2 - Matrix elements of $e^{i\Delta\mathbf{k}\cdot\vec{r}} U(\vec{r})$ between non-relativistic single group wave-functions at Γ .

Band	Band	Pb vacancy					Te vacancy			Ref. No. on Fig. 4.3
		t					t			
		0.00	0.40	0.80	2.00	4.00	0.00	0.80	4.00	
$1\Gamma_1$	$1\Gamma_1$	2.397	2.396	2.393	2.372	2.302	0.468	0.467	0.453	1
$1\Gamma_1$	$2\Gamma_1$	-1.474	-1.474	-1.472	-1.461	-1.425	1.065	1.064	1.036	2
$1\Gamma_1$	$3\Gamma_1$	-1.239	-1.238	-1.236	-1.224	-1.184	-1.054	-1.052	-1.016	3
$2\Gamma_1$	$2\Gamma_1$	0.921	0.921	0.920	0.914	0.891	2.466	2.463	2.400	4
$2\Gamma_1$	$3\Gamma_1$	0.751	0.751	0.750	0.745	0.726	-2.364	-2.361	-2.299	5
$3\Gamma_1$	$3\Gamma_1$	0.648	0.648	0.647	0.639	0.615	2.413	2.408	2.308	6
$1\Gamma_{15,1}$	$1\Gamma_{15,1}$	0.752	0.751	0.749	0.733	0.683	4.085	4.071	3.773	7
$1\Gamma_{15,1}$	$2\Gamma_{15,1}$	1.768	1.766	1.762	1.728	1.618	-1.686	-1.681	-1.545	8
$2\Gamma_{15,1}$	$2\Gamma_{15,1}$	4.534	4.531	4.521	4.451	4.219	0.800	0.797	0.731	9
$1\Gamma_{15,2}$	$1\Gamma_{15,2}$	0.752	0.751	0.749	0.737	0.695	4.085	4.089	4.108	
$1\Gamma_{15,2}$	$1\Gamma_{15,2}$	1.768	1.767	1.765	1.747	1.686	-1.686	-1.698	-1.744	
$2\Gamma_{15,2}$	$2\Gamma_{15,2}$	4.534	4.532	4.524	4.469	4.288	0.800	0.798	0.742	
$\Gamma_{12,1}$	$\Gamma_{12,1}$	2.305	2.303	2.299	2.273	2.183	1.774	1.768	1.625	10
$\Gamma_{12,2}$	$\Gamma_{12,2}$	2.305	2.304	2.300	2.276	2.197	1.774	1.769	1.632	
Γ'_2	Γ'_2	0.160	0.159	0.158	0.148	0.115	0.143	0.142	0.103	11
$\Gamma'_{25,1}$	$\Gamma'_{25,1}$	1.575	1.574	1.572	1.556	1.502	1.190	1.186	1.097	12
$\Gamma'_{25,2}$	$\Gamma'_{25,2}$	1.575	1.575	1.574	1.567	1.535	1.190	1.188	1.124	
Band	Band	Pb vacancy					Te vacancy			Ref.No. on Fig. 4.3
		0.00	0.20	0.40	1.00	2.00	0.00	0.40	2.00	
$1\Gamma_1$	$1\Gamma_{15,1}$	0.000	0.002	0.003	0.008	0.014	0.000	-0.353	-1.648	13
$1\Gamma_1$	$2\Gamma_{15,1}$	0.000	0.003	0.006	0.014	0.026	0.000	0.143	0.685	14
$2\Gamma_1$	$1\Gamma_{15,1}$	0.000	-0.015	-0.030	-0.073	-0.134	0.000	0.044	0.206	15
$2\Gamma_1$	$2\Gamma_{15,1}$	0.000	-0.034	-0.069	-0.169	-0.321	0.000	-0.016	-0.077	16
$3\Gamma_1$	$1\Gamma_{15,1}$	0.000	-0.025	-0.049	-0.119	-0.218	0.000	0.160	0.736	17
$3\Gamma_1$	$2\Gamma_{15,1}$	0.000	-0.059	-0.117	-0.287	-0.536	0.000	-0.063	-0.300	18
$\Gamma_{12,1}$	$1\Gamma_{15,1}$	0.000	-0.018	-0.036	-0.089	-0.161	0.000	0.088	0.390	19
$\Gamma_{12,1}$	$2\Gamma_{15,1}$	0.000	-0.036	-0.071	-0.174	-0.318	0.000	-0.021	-0.089	20
$\Gamma'_{25,1}$	Γ'_2	0.000	-0.001	-0.002	-0.006	-0.010	0.000	-0.008	-0.039	21
$1\Gamma_1$	$\Gamma_{12,1}$	0.000	0.000	0.001	0.007	0.026	0.000	0.001	0.003	22
$2\Gamma_1$	$\Gamma_{12,1}$	0.000	-0.000	-0.000	-0.001	0.003	0.000	0.008	0.025	23
$3\Gamma_1$	$\Gamma_{12,1}$	0.000	0.000	0.001	0.006	0.020	0.000	0.009	0.029	24
$\Gamma'_{25,1}$	$1\Gamma_{15,1}$	0.000	0.010	0.020	0.050	0.091	0.000	+0.048	+0.240	25
$\Gamma'_{25,1}$	$2\Gamma_{15,1}$	0.000	0.026	0.052	0.128	0.236	0.000	0.023	0.095	26

Pb to the Te-sphere can be incorporated easily into the coefficients of the SAPW's. Let us consider the Γ -point and assume that the APW calculations was performed with the origin at the center of a Pb-sphere. The terms in the expression (2.6) for a particular SAPW with wave-vector \vec{k}_i will have $e^{i\alpha\vec{k}_i \cdot \vec{R}_{Pb}}$ and $e^{i\alpha\vec{k}_i \cdot \vec{R}_{Te}}$ at the Pb- and Te-spheres, respectively, where \vec{R}_{Pb} and \vec{R}_{Te} are positions of the centers of the spheres and α is an operation of the crystal point group. For the Γ -point, $\vec{k}_i = \vec{K}_i$, where \vec{K}_i is a reciprocal lattice vector. It is well known that for a face centered cubic lattice there are two kinds of reciprocal lattice vectors $\vec{K}_i = 2\pi/a (\ell m n)$, namely, ℓ, m, n are either all even or all odd. If the origin is at a Pb-sphere, then

$$\begin{cases} e^{i\alpha\vec{K}_i \cdot \vec{R}_{Pb}} = 1 \\ e^{i\alpha\vec{K}_i \cdot \vec{R}_{Te}} = \begin{cases} 1 & \text{if } \ell, m, n \text{ are even} \\ -1 & \text{if } \ell, m, n \text{ are odd} \end{cases} \end{cases} \quad (4.55)$$

for all operations α of the point group. Thus, if we have the coefficients of the SAPW's for a particular wave-function at Γ calculated with the origin at the Pb-sphere, we can obtain the coefficients of the SAPW's of the same wave-function when the origin is at the Te-sphere, by multiplying the former coefficients by $+1$ or -1 , depending upon whether the SAPW has ℓ, m, n even or odd.

The matrix elements in Table 4.2 were calculated with 10 SAPW's for each band and are plotted as a function of t in figure 4.4. The cutoff in the sums on the ℓ -parameters in Eq. (A.13) was taken as $\ell=10$. The convergence of the matrix elements, both in the number

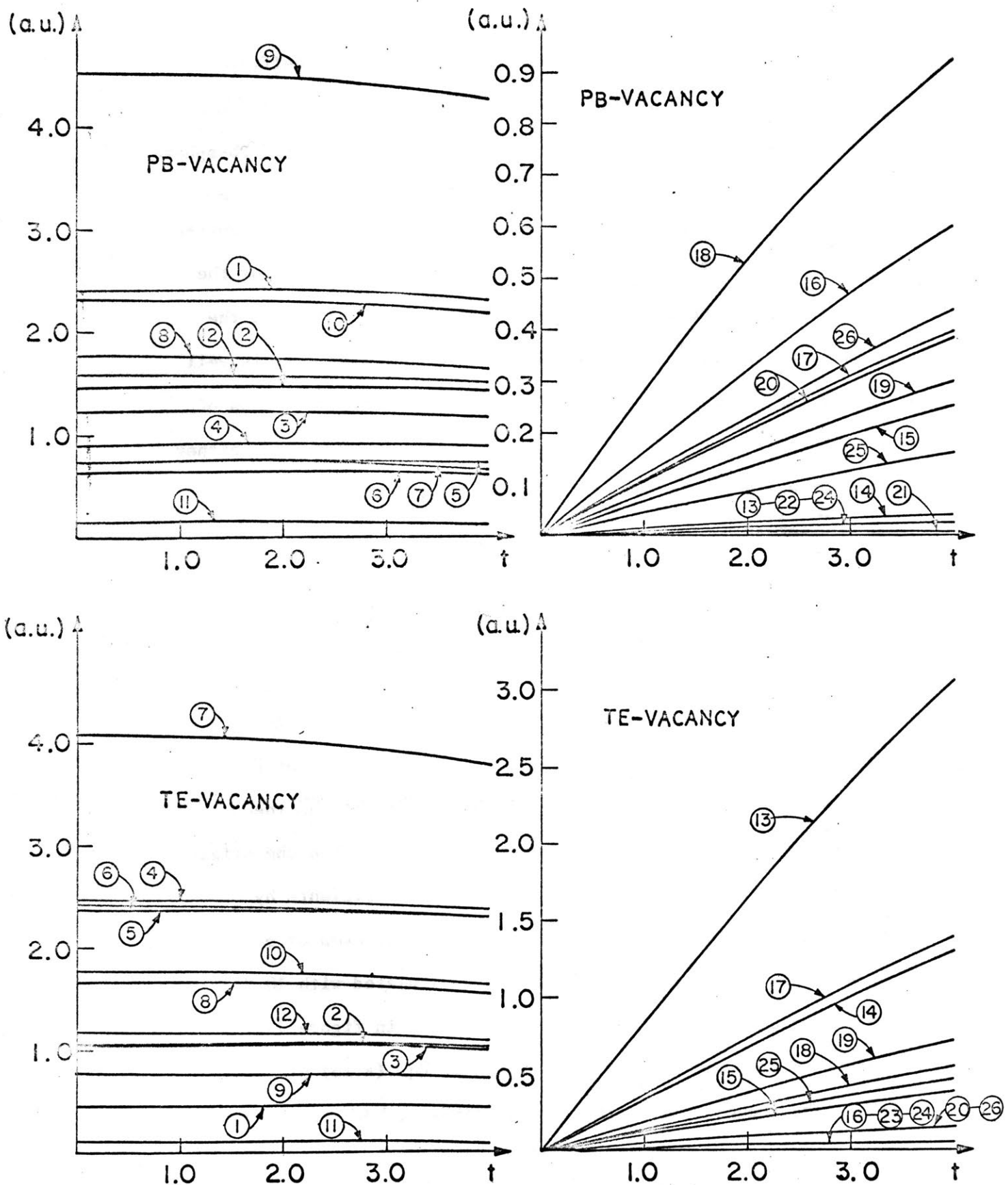


FIGURE 4.4 - Matrix elements of $e^{i\Delta\vec{k}\cdot\vec{r}} U(\vec{r})$ between non-relativistic single-group functions at Γ as function of t . (See also Table 4.2).

of SAPW's and ℓ -terms, was excellent and the results for $\ell=4$ and $\ell=10$ differ little (the difference was smaller than 10^{-4} Ry).

Two important conclusions can be deduced from Table 4.2 or figure 4.4. First, if the representations are the same the matrix elements are reasonably large and decrease slowly as $|\Delta\vec{k}|$ increases. Second, for different representations, the matrix elements are in general, small; if the representations have different parities, the matrix elements increase almost linearly with $|\Delta\vec{k}|$, and, if the representations have the same parities, the matrix elements increase quadratically with $|\Delta\vec{k}|$. This behavior of the matrix elements provides the important key in the solution of the vacancy problem in the $\vec{K}\cdot\vec{\pi}$ -APW scheme.

Let us expand the exponential in the numerator of Eq. (4.54) in Taylor's series near the origin (the impurity potential is assumed to be localized near the origin). Thus

$$\begin{aligned}
 & \int_{\text{cell}} d\vec{r} b_{m',j'}^{\Gamma_{\beta'}}(0,\vec{r})^* e^{i\Delta\vec{k}\cdot\vec{r}} U(\vec{r}) b_{m,j}^{\Gamma_{\beta}}(0,\vec{r}) \\
 &= \int_{\text{cell}} d\vec{r} b_{m',j'}^{\Gamma_{\beta'}}(0,\vec{r})^* U(\vec{r}) b_{m,j}^{\Gamma_{\beta}}(0,\vec{r}) \\
 &+ i\Delta\vec{k} \cdot \int_{\text{cell}} d\vec{r} b_{m',j'}^{\Gamma_{\beta'}}(0,\vec{r})^* \vec{r} U(\vec{r}) b_{m,j}^{\Gamma_{\beta}}(0,\vec{r}) + \dots \quad (4.56)
 \end{aligned}$$

If the representations Γ_{β} and $\Gamma_{\beta'}$ have the same parity, only terms with even powers in $(\Delta\vec{k}\cdot\vec{r})$ will contribute in Eq. (4.56), i.e., the second, fourth, etc. terms are zero. The k -independent term is different from zero only if $\Gamma_{\beta} = \Gamma_{\beta'}$, and $j=j'$, and the term propor-

tional to $|\Delta\vec{k}|^2$ is the leading term when Γ_β and $\Gamma_{\beta'}$, (which have the same parity) are different.

On the other hand, if the representation Γ_β and $\Gamma_{\beta'}$, have different parities, the first, third, etc. terms in Eq. (4.56) are zero and the first non-zero term is the term linear in Δk .

We can therefore conclude that it is a very good approximation to consider only the first two terms in Eq. (4.56). This is equivalent to saying that the vacancy potential is so localized that in the first Brillouin zone $e^{i\Delta\vec{k}\cdot\vec{r}}$ plays the role of a slowly-varying function of \vec{r} .

Table 4.3 presents the values obtained from table 4.2 and figure 4.4 of the matrix elements of $U(\vec{r})$ and $ixU(\vec{r})$ between the non-relativistic Bloch functions at Γ . These wave functions are such that the matrix elements are real numbers. With these matrix elements we can construct matrix T and tensor \vec{N} , defined by Eq. (4.40) and Eq. (4.41) respectively, observing that the operator $\vec{r}U(\vec{r})$ transforms in the same way as the momentum operator under the operations of the crystal point group. This means that when the matrix elements of $xU(\vec{r})$ between the non-relativistic wave-functions, table 3.5 can be used.

Next step in the calculations consists in obtaining for the important bands of PbTe the expressions for $C_{n,m}^{i,j}(\vec{R}_q)$ and $D_{n,m}^{i,j}(\vec{R}_q)$, given by Eq. (4.45) and Eq. (4.46).

Let us consider the three valence and three conduction bands which, at Γ , correspond to $1\Gamma_6^-$, $1\Gamma_8^-$, $2\Gamma_6^-$ and $2\Gamma_8^-$. They will

TABLE 4.3 - Matrix elements of $U(\vec{r})$ and $ixU(\vec{r})$ between non-relativistic bands at Γ , for Pb and Te-vacancies.

Band	Matrix element of $U(r)$		Matrix element of $ixU(r)$				
	Pb-vacancy (a.u.)	Te-vacancy (a.u.)	Pb-vacancy (a.u.)	Te-vacancy (a.u.)			
$1\Gamma_1$	$1\Gamma_1$	2.397	0.468	$1\Gamma_{15,1}$	0.0071	-0.824	
$1\Gamma_1$	$2\Gamma_1$	-1.474	1.065	$1\Gamma_1$	$2\Gamma_{15,1}$	0.0131	0.345
$1\Gamma_1$	$3\Gamma_1$	-1.239	-1.054	$2\Gamma_1$	$1\Gamma_{15,1}$	-0.0688	0.103
$2\Gamma_1$	$2\Gamma_1$	0.921	2.466	$2\Gamma_1$	$2\Gamma_{15,1}$	-0.162	-0.0386
$2\Gamma_1$	$3\Gamma_1$	0.751	-2.364	$3\Gamma_1$	$1\Gamma_{15,1}$	-0.113	0.370
$3\Gamma_1$	$3\Gamma_1$	0.648	2.413	$3\Gamma_1$	$2\Gamma_{15,1}$	-0.274	-0.152
$1\Gamma_{15,1}$	$1\Gamma_{15,1}$	0.752	4.085	$\Gamma_{12,1}$	$1\Gamma_{15,1}$	-0.084	0.121
$1\Gamma_{15,1}$	$2\Gamma_{15,1}$	1.768	-1.686	$\Gamma_{12,1}$	$2\Gamma_{15,1}$	-0.162	-0.029
$2\Gamma_{15,1}$	$2\Gamma_{15,1}$	4.534	0.800	$\Gamma'_{25,1}$	Γ'_2	-0.0053	-0.0186
$\Gamma_{12,1}$	$\Gamma_{12,1}$	2.305	1.774	Γ'_{25}	$1\Gamma_{15,1}$	0.0465	-0.124
Γ'_2	Γ'_2	0.160	0.143	Γ'_{25}	$\Gamma_{15,1}$	0.123	0.048
$\Gamma'_{25,1}$	$\Gamma'_{25,1}$	1.575	1.190				

be referred to as valence bands number 3,4 and 5 and conduction bands number 1, 2 and 3, in the order of increasing energy. Because these bands have, over almost the entire zone, a large contribution coming from the Kohn-Luttinger functions corresponding to the above Γ_6^- and Γ_8^- -bands, a reasonable choice for the phases $[\theta_n(\alpha, \vec{k}), \left\{ \begin{matrix} i=1,4,8 \\ \vec{k} \text{ in } 1/48 \text{ of} \end{matrix} \right.$ the zone] can be made.* The phases for the improper rotations are chosen such that

$$e^{i\theta_n(J\alpha\vec{k})} = e^{i\theta_n(\alpha\vec{k})}$$

where J is the inversion operator. Eq. (4.45) and Eq. (4.46) can now be written as

$$C_{n,m}^{i,j}(\vec{R}_q) = \frac{1}{N} \sum_k \frac{1}{t(\vec{k})} \sum_{\alpha} \sum_{\ell} C_{n,m}^{i,\ell}(\vec{K}) \Gamma_{\beta}(\vec{k}_o)(\alpha)_{j,\ell} e^{i\theta_n(\alpha\vec{k})} \times \begin{cases} 2 \cos(\alpha\vec{k} \cdot \vec{R}_q) & , \text{ if } \Gamma_{\beta}(\vec{k}_o) \text{ has odd-parity} \\ -2 i \sin(\alpha\vec{k} \cdot \vec{R}_q) & , \text{ if } \Gamma_{\beta}(\vec{k}_o) \text{ has even parity} \end{cases} \quad (4.57)$$

$$D_{n,m}^{i,j}(\vec{R}_q) = \frac{1}{N} \sum_k \frac{1}{t(\vec{k})} \sum_{\alpha} \sum_{\ell} C_{n,m}^{i,\ell}(\vec{K}) \Gamma_{\beta}(\vec{k}_o)(\alpha)_{j,\ell} e^{i\theta_n(\alpha\vec{k})} \alpha\vec{k} \cdot \begin{cases} -2i \sin(\alpha\vec{k} \cdot \vec{R}_q) & , \text{ if } \Gamma_{\beta}(\vec{k}_o) \text{ has odd-parity} \\ 2 \cos(\alpha\vec{k} \cdot \vec{R}_q) & , \text{ if } \Gamma_{\beta}(\vec{k}_o) \text{ has even-parity} \end{cases} \quad (4.58)$$

where the sum on α is restricted to only the 24 proper rotations.

For the valence bands, the important $\vec{K} \cdot \vec{\pi}$ -coefficients vary

* Near L, however, the contributions to the valence bands coming from the Luttinger-Kohn functions corresponding to the even-parity bands at Γ are reasonably large, as can be observed in figure 3.10.c, for the upper valence band.

reasonably slowly over 1/48 of the zone,* with the exception of a region near the point in the <100> axis where band crossing and quasidegeneracies exist. The contribution coming from $1\Gamma_6^-$ is the largest for the lowest valence band (number 3) and although the contribution coming from the even-parity Γ -bands is not small near the L-point, a reasonably localized Wannier function can be obtained, if the $1\Gamma_6^-$ -contribution is optimized, as explained in section 4.2. This optimization consists of defining $e^{i\theta_n(\alpha\mathbf{k})} = 1$ for all proper rotations.

Although throughout a large part of the 1/48 region of the B.Z. the valence bands number 4 and 5 consist primarily of the Kohn-Luttinger functions coming from the first and third partners of $1\Gamma_8^-$, reasonably large contributions also come from the other partners of $1\Gamma_8^-$, from the Γ_6^- -bands and from $2\Gamma_8^-$, besides the contribution from the even-parity Γ -bands. For both valence bands, the most localized Wannier functions were obtained not when the contribution coming from the first or third partners of $1\Gamma_8^-$ were optimized, but when all partners of $1\Gamma_8^-$ were optimized. With this procedure phase factors remain undefined and they are chosen in such a way that the contribution coming from the Γ_6^- -bands is optimal. In other words, the choice

$$e^{i\theta(\alpha)} = \begin{cases} 1 & , \text{ if } \chi_8^-(\alpha) > 0 \\ -1 & , \text{ if } \chi_8^-(\alpha) < 0 \end{cases}$$

* This does not mean that the coefficients are large in the entire region

where $\chi_8^-(\alpha)$ denotes the character of the matrix representing α in the Γ_8^- -irreducible representation, optimizes all partners of Γ_8^- . But, there are some α for which $\chi_8^-(\alpha) = 0$ and the corresponding phase-factors remain undefined. They can be chosen in order to optimize $\Gamma_{8,1}^-(\Gamma_{8,4}^-)$ or $\Gamma_{8,3}^-(\Gamma_{8,2}^-)$ or Γ_6^- . The optimization of Γ_6^- , which corresponds to the choice $e^{i\theta(\alpha)} = 1$ for all α , was the one that produced the best Wannier functions. Table 4.4 presents the choice of the phase factors in all these cases.

The conduction bands are also represented by reasonably slowly varying $\vec{k} \cdot \vec{\pi}$ -coefficients, except in regions near the points where accidental and quasi-degeneracies exist. Although the lowest conduction band (conduction band number 1) also has a large contribution coming from the Γ_8^- -bands, the optimization of the Γ_6^- -bands proved to give better results. The other two bands behaved in the same way as the two upper valence bands, as far as the choice of the phase factors is concerned.

Besides the three above mentioned valence bands, PbTe also has two other valence bands which are important in the vacancy problem. These bands will be called valence band number 1 and 2, and at Γ , they correspond to $3\Gamma_6^+$ and $1\Gamma_6^+$, respectively. Valence band number 1 has an average contribution of 0.897 coming from the Kohn-Luttinger function corresponding to $3\Gamma_6^+$ and valence band number 2 has an average contribution of 0.731 coming from $1\Gamma_6^+$. This means that very localized Wannier functions can be constructed for these bands if we choose the phase factors such that $e^{i\theta_n(\alpha\vec{k})} = 1$ for all rotations α .

TABLE 4.4 - Phase factors for the 24 proper rotations.

Rotation	Description	Contribution optimized			
		Γ_6	Γ_8	$\Gamma_{8,1}$	$\Gamma_{8,3}$
E	Identity	1	1	1	1
$8C_3$	$2\pi/3$ about $x=y=z$	1	-1	-1	-1
	$4\pi/3$ about $x=y=z$	1	-1	-1	-1
	$2\pi/3$ about $x=-y=z$	1	-1	-1	-1
	$4\pi/3$ about $x=-y=-z$	1	-1	-1	-1
	$2\pi/3$ about $x=-y=-z$	1	-1	-1	-1
	$4\pi/3$ about $x=-y=-z$	1	-1	-1	-1
	$2\pi/3$ about $x=y=-z$	1	-1	-1	-1
	$4\pi/3$ about $x=y=-z$	1	-1	-1	-1
$3C_2$ $4C_4$	π about z	1	1	1	1
	π about y	1	1	1	1
	π about x	1	1	1	1
$6C_4$	$3\pi/2$ about z	1	-	1	-1
	$\pi/2$ about y	1	-	-1	1
	$\pi/2$ about x	1	-	-1	1
	$3\pi/2$ about y	1	-	-1	1
	$3\pi/2$ about x	1	-	-1	1
	$\pi/2$ about z	1	-	1	-1
$6C_2$	π about $y=z$	1	-	-1	1
	π about $x=y$	1	-	1	-1
	π about $x=z$	1	-	1	-1
	π about $x=-y$	1	-	1	-1
	π about $x=-z$	1	-	-1	1
	π about $y=-z$	1	-	-1	1

In the determination of the vacancy energy levels, the conduction band that at Γ corresponds to $2\Gamma_6^+$ had to be included in the calculations, because it has an average contribution of 0.627 coming from the Kohn-Luttinger function corresponding to $2\Gamma_6^+$, and the matrix elements of the impurity potential connecting $2\Gamma_6^+$ and $3\Gamma_6^+$ and $1\Gamma_6^+$ are very large.

Once the coefficients $C_{n,m}^{i,j}(\vec{R}_q)$ and $D_{n,m}^{i,j}(\vec{R}_q)$ are known, the matrix elements of $U(\vec{r})$ between Wannier functions can be obtained. These matrix elements are calculated for the five valence bands and four conduction bands and for the site at the origin and twelve nearest neighbors of the type $\vec{R}_q = \frac{a}{2}(1,1,0)$. We have found that for all bands the matrix element connecting Wannier functions centered at the origin was 5 to 20 times larger than any other matrix element.

On the other hand, the matrix G can easily be obtained if Eq. (4.22) is used. According to this relation the matrix G is diagonal in both the band and partner indices and if $\Delta\vec{R}_q = \vec{R}_q - \vec{R}_q'$, where R_q and R_q' are two lattice sites, we obtain

$$G_{n,n}^{i,i}(\Delta\vec{R}_q, E) = \frac{1}{N} \sum_k \sum_\alpha \frac{2\cos(\alpha\vec{k} \cdot \Delta\vec{R}_q)}{E - E_n(\vec{k})} \quad (4.59)$$

where now the sum on \vec{k} is performed in 1/48 of the zone and the sum on α includes only the 24 proper rotations of the crystal point group. According to Eq. (4.59)

$$G_{n,n}^{i,i}(-\Delta\vec{R}_q, E) = G_{n,n}^{i,i}(\Delta\vec{R}_q, E) \quad (4.60)$$

and for $\Delta\vec{R}_q = 0$

$$G_{n,n}^{i,i}(0,E) \begin{cases} >0 & , \text{ if } E > E_n(\vec{k}) \\ <0 & , \text{ if } E < E_n(\vec{k}) \end{cases} \quad (4.61)$$

Due to the fact that, for values of E near the top or bottom of the energy band, the G-matrix depends strongly on the details of the band near these maxima, the number and distribution of points in the energy mesh are very important. We have calculated the elements of G for some values of E near and far from the extremum of the bands using both the regular and Conroy's³⁴ integration methods. For all bands very good convergence was obtained for a Conroy's mesh of 1000 points in 1/48 of the zone. Because continuous energy bands have been defined in k-space, $G_{n,n}^{i,i}(\Delta\vec{R}_q, E)$ properly approaches zero for large values of E, as can be observed in Fig. 4.5 where we present $G_{n,n}^{i,i}(0,E)$ for the valence bands number 3,4 and 5 and conduction band number 1. For the conduction band $G_{n,n}^{i,i}(0,E)$ is negative.

Let us now determine the bound states associated with vacancies in PbTe. Because the vacancy potential has the crystal point group symmetry, the wave-functions corresponding to the bound states will have to transform like the irreducible representations of the crystal point group. Thus, instead of diagonalizing the total matrix $[I_{NN} - G_{NN} U_{NN}]$, or $[G_{NN}^{-1} - U_{NN}]$, we factor it in block form, each block containing only states with wave-functions transforming as the same irreducible representation. This factorization can be accomplished

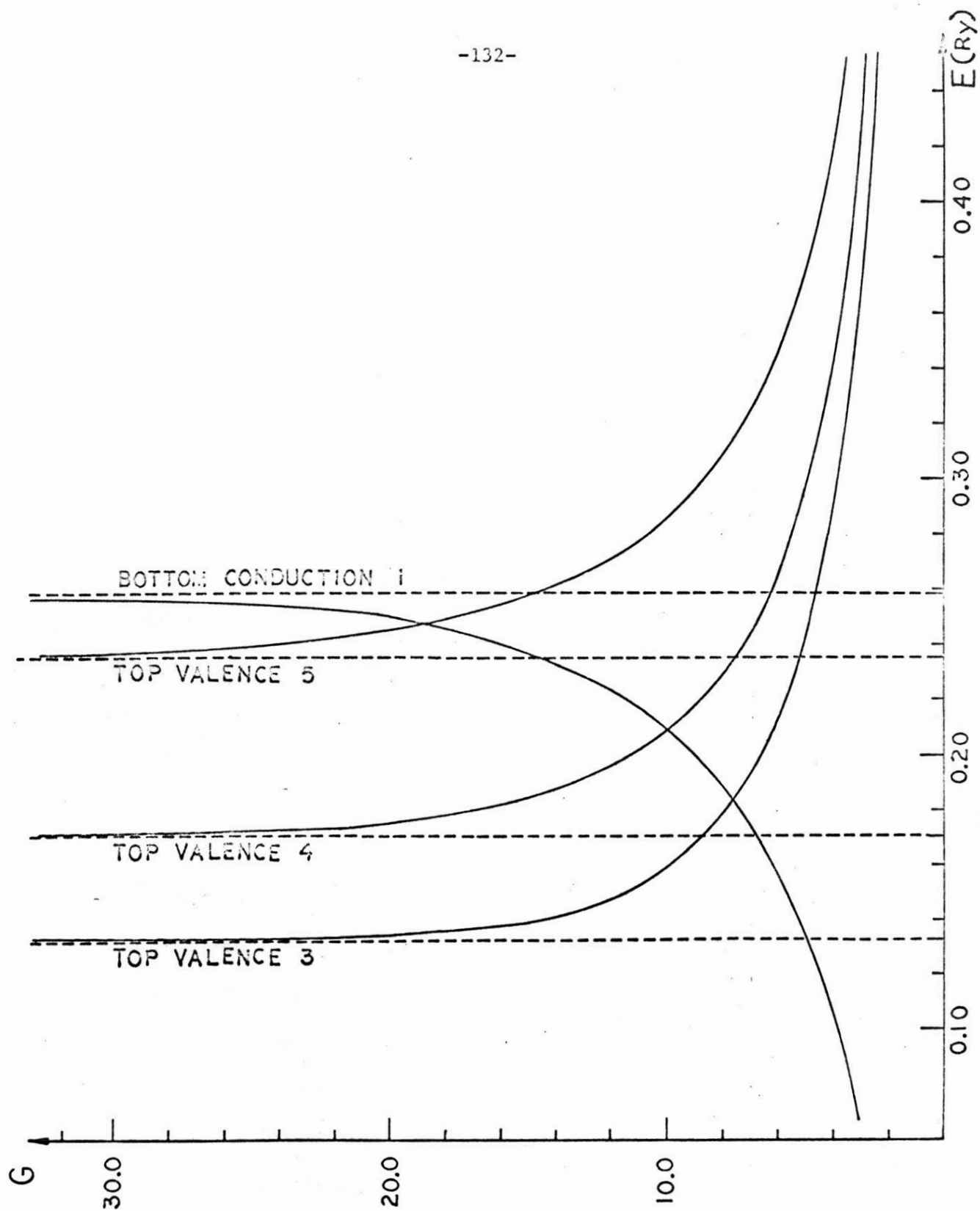


FIGURE 4.5 - $G_{n,n}^{i,i}(0,E)$ as a function of E for the valence bands number 3,4 and 5 and conduction band number 1.

using projection operators, if the transformation properties of the Wannier functions are known.

Although providing a proper G-matrix, our definition of Wannier functions do not produce functions with simple transformation properties. Let us consider Eq. (4.18) which defines a Wannier function. This equation can also be written as

$$a_{n,i}(\vec{r}-\vec{R}_q) = \sum_{m,j} C_{n,m}^{i,j}(\vec{R}_q) b_{m,j}^{\Gamma_Y(\vec{k}_o)}(\vec{k}_o, \vec{r}) \quad (4.62)$$

where $C_{n,m}^{i,j}(\vec{R}_q)$ is given by Eq. (4.45). If β is an operation of the crystal point group, then

$$\beta a_{n,i}(\vec{r}-\vec{R}_q) = \sum_{m,p} \frac{1}{N} \sum_{\vec{k}} \frac{1}{t(\vec{k})} \sum_{\alpha} \sum_{\ell} C_{n,m}^{i,\ell}(\vec{K}) \Gamma_Y(\vec{k}_o)(\beta\alpha)_{p,\ell} e^{-i\alpha\vec{k}\cdot\vec{R}_q} e^{i\theta_n(\alpha\vec{k})} b_{m,p}^{\Gamma_Y(\vec{k}_o)}(\vec{k}_o, \vec{r}) \quad (4.63)$$

If spin is not present, $\delta=\beta\alpha$ is one of the 48 operations contained in the sum on α . Then

$$\beta a_{n,i}(\vec{r}-\vec{R}_q) = \sum_{m,p} \frac{1}{N} \sum_{\vec{k}} \frac{1}{t(\vec{k})} \sum_{\delta} \sum_{\ell} C_{n,m}^{i,\ell}(\vec{K}) \Gamma_Y(\vec{k}_o)(\delta)_{p,\ell} e^{-i\delta\vec{k}\cdot\vec{R}_q} e^{i\theta_n(\beta^{-1}\alpha\vec{k})} b_{m,p}^{\Gamma_Y(\vec{k}_o)}(\vec{k}_o, \vec{r}) \quad (4.64)$$

and if for a given \vec{k} the same phase factor corresponds to all operations δ we obtain

$$\beta a_{n,i}(\vec{r}-\vec{R}_q) = \sum_{m,p} C_{n,m}^{i,p}(\beta\vec{R}_q) b_{m,p}^{\Gamma_Y(\vec{k}_o)}(\vec{k}_o, \vec{r}) = a_{n,i}(\vec{r}-\beta\vec{R}_q) \quad (4.65)$$

In the present calculation, however, we are dealing with double-group representations and $\delta=\beta\alpha$ is not necessarily* one of the 48 operations contained in the sum on α . Besides that, in order to produce localized Wannier functions the above choice of the phase factors is not always possible. For the inversion operator J, however, $\delta=\beta\alpha$ is always one of the 48 operations and

$$J a_{n,i}(\vec{r}-\vec{R}_q) = \pm a_{n,i}(\vec{r}+\vec{R}_q) \quad (4.66)$$

if we choose

$$e^{i\theta_n(J\delta\vec{k})} = \pm e^{i\theta_n(\delta\vec{k})} \quad (4.67)$$

But Eq. (4.67) is consistent with our present choices for the phase factors and this will allow us to factor the total matrix in two smaller matrices, one for the even-parity representations and the other for the odd-parity representations, as proved below.

We have that

$$\langle a_{m,i}(\vec{r}-\vec{R}_p) | U(\vec{r}) | a_{n,i}(\vec{r}-\vec{R}_q) \rangle = \pm \langle a_{m,i}(\vec{r}+\vec{R}_p) | U(\vec{r}) | a_{n,i}(\vec{r}+\vec{R}_p) \rangle \quad (4.68)$$

depending upon whether bands m and n have the same or different choices (4.67). If the symmetric and anti-symmetric linear combinations

$$\begin{aligned} \psi_{n,i}^s(\vec{r}, \vec{R}_p) &= \frac{a_{n,i}(\vec{r}-\vec{R}_p) + a_{n,i}(\vec{r}+\vec{R}_p)}{\sqrt{2}} \\ \psi_{n,i}^{as}(\vec{r}, \vec{R}_p) &= \frac{a_{n,i}(\vec{r}-\vec{R}_p) - a_{n,i}(\vec{r}+\vec{R}_p)}{\sqrt{2}} \end{aligned} \quad (4.64)$$

* The crystal point group has 96 operations.

are considered, then

$$\langle \psi_{n,i}^s(\vec{r}, \vec{R}_p) | U(\vec{r}) | \psi_{m,i}^{as}(\vec{r}, \vec{R}_q) \rangle = 0 \quad (4.65)$$

and U_{NN} can be written in the above block form.

It is easy to verify that the same is true for G_{NN} and G_{NN}^{-1} , and that the Wannier function centered at the origin has to enter the symmetric block as

$$\psi_{n,i}^s(\vec{r}, 0) = a_{n,i}(\vec{r}-0) \quad (4.66)$$

in order to be properly normalized.

In the present case we cannot further factor these two blocks into smaller blocks containing only one irreducible representation, but each block is totally diagonalized. In the following discussion we will call the energy levels obtained from the symmetric and anti-symmetric blocks, symmetric and antisymmetric levels, respectively.

Eq. (4.28) is solved first for the five valence bands in the single band approximation. The conduction bands are not considered in this calculation because of the following consideration. As we discussed before, the matrix element of the impurity potential between Wannier functions centered at the origin is larger than any other matrix element^{*}. Thus, the first order solution is obtained considering only the site at the origin and in this case only one perturbed energy level is possible for each band (symmetric solution). If the perturbation is very small this level stays in the band (virtual state), but if U is big enough, a bound state lying above the top of the band is obtained. It lies above the gap because the

^{*}The potential is assumed to be localized around the origin.

impurity potential is positive and, in order to satisfy Eq. (4.28), $G(0,E)$ has to be positive. However, as we in general are interested in energies smaller than the top of the lowest conduction band, the levels obtained for the conduction bands are not of interest. Now, if more sites are taken into account in the calculation, then not only will we change the energy level of the bound state which is obtained when only the site at the origin is considered, but also new bound states may appear above the top of the band.

The symmetric and antisymmetric energy levels obtained in the single-band approximation for the five valence bands are shown in Table 4.5 and figures 4.6 and 4.7. There we present the results for one site and for 13 sites. In the first case only one symmetric state is produced per band, while in the second case, seven symmetric and six antisymmetric levels exist for each band. For vacancy potentials in PbTe the perturbation is not strong enough to pull antisymmetric states out of the bands, and only symmetric bound states may occur. For a Pb-vacancy one symmetric bound state is produced both for valence band number 1 and 2.

The effect of considering more sites is to increase the energy of these states, as shown in figure 4.6. The perturbation, however, is not strong enough to produce symmetric bound states for valence bands number 3, 4 and 5. A different picture is produced when a Te-vacancy is present in PbTe. Now, besides valence bands 1 and 2, symmetric bound states are also pulled out of the valence bands 3, 4 and 5. All these bands, except valence band number 5, present

BAND	Pb-Vacancy						Te-Vacancy					
	Symmetric states				Antisymmetric states		Symmetric states				Antisymmetric states	
	1 site		13 sites		13 sites		1 site		13 sites		13 sites	
	States in the band	Energy of bound states (10^{-3} Ry)	States in the band	Energy of bound states (10^{-3} Ry)	States in the band	Energy of bound states (10^{-3} Ry)	States in the band	Energy of bound states (10^{-3} Ry)	States in the band	Energy of bound states (10^{-3} Ry)	States in the band	Energy of bound states (10^{-3} Ry)
VALENCE 1	0	52.027	6	94.221	6	-	0	1122.32	6	1278.27	6	-
VALENCE 2	0	631.182	6	758.366	6	-	0	43.216	6	75.132	6	-
VALENCE 3	1	-	7	-	6	-	0	123.813	6	137.845	6	-
VALENCE 4	1	-	7	-	6	-	0	38.752	6	57.695	6	-
VALENCE 5	1	-	7	-	6	-	0	16.427	5	39.010	6	-
										26.522		

TABLE 4.5 - Symmetric and antisymmetric states obtained in the single-band approximation for the valence bands of PbTe. The zero of energy is taken at the top of the band.

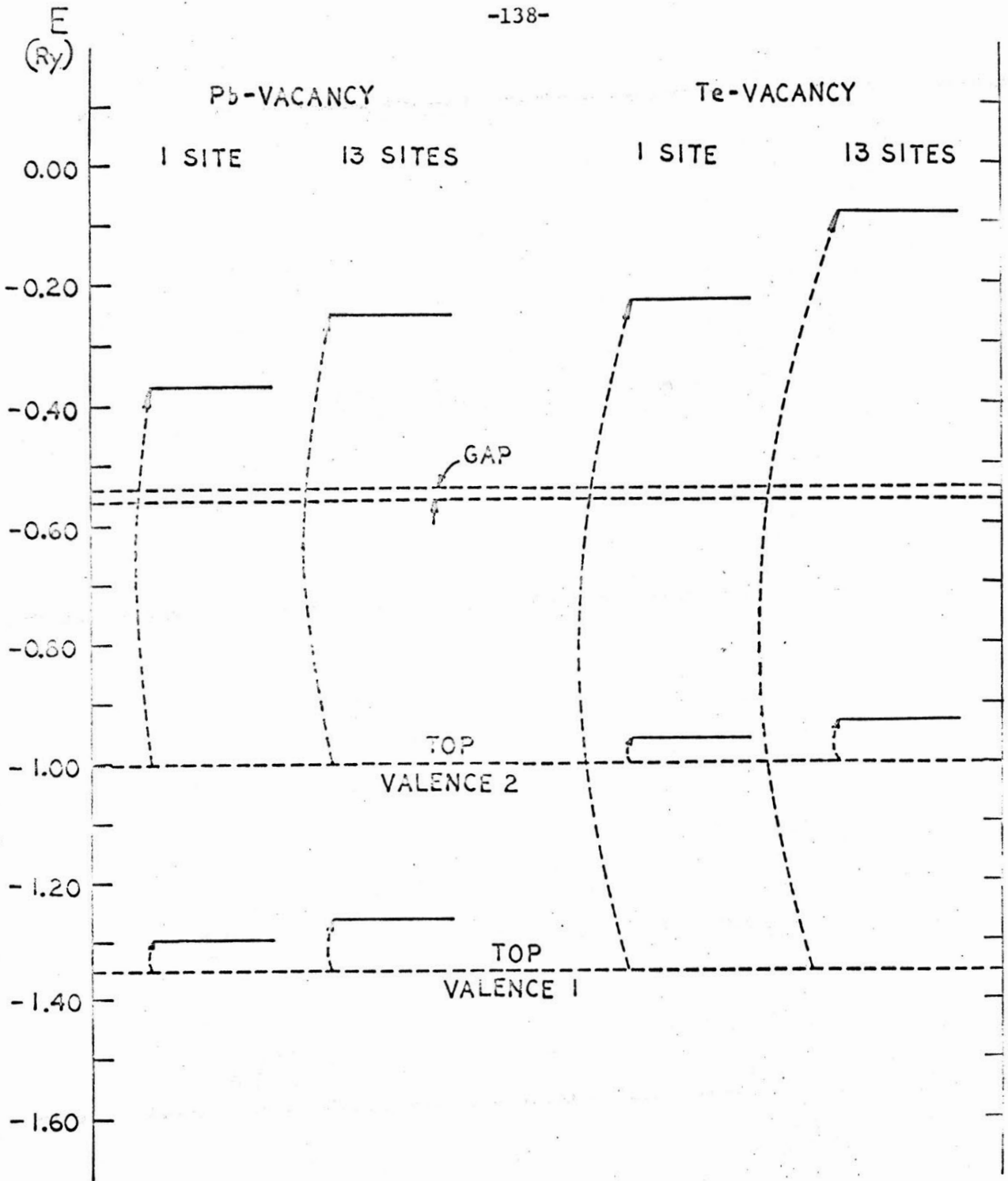


FIGURE 4.6 - Symmetric bound states produced by a Pb- and a Te-vacancy in the single band approximation for valence bands number 1 and 2 of PbTe.

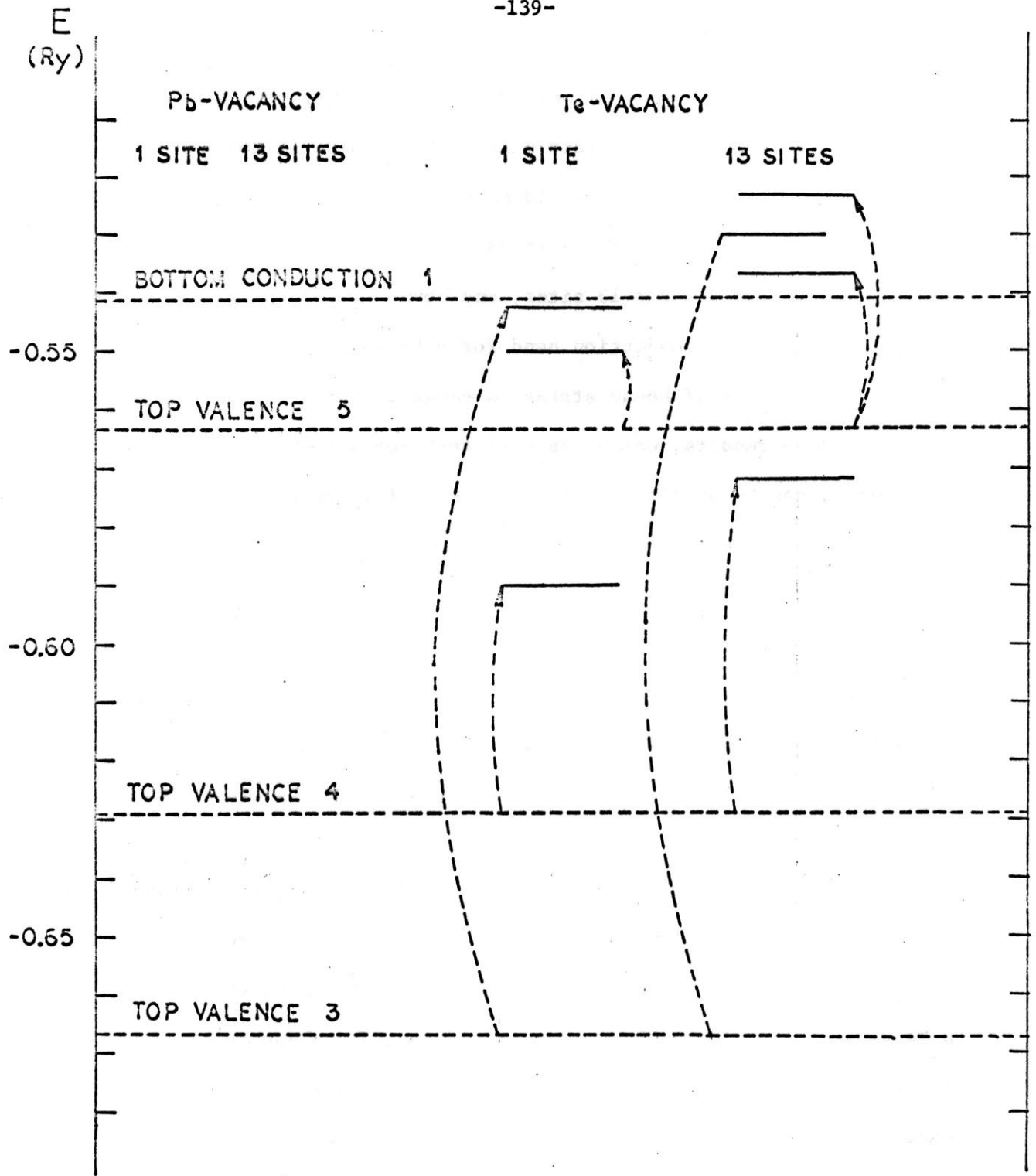


FIGURE 4.7 - Symmetric bound states produced by a Pb- and a Te-vacancy in the single band approximation for valence bands number 3,4 and 5.

only one symmetric bound state both for 1 and 13 sites. For valence band number 5, however, one state exists when 1 site is considered, but another one appears when all 13 sites are taken into account. From table 4.5 or figures 4.6 and 4.7 it can be observed that, in the single band approximation and for 13 sites, one bound state appears above the bottom of the lowest conduction band for a Pb-vacancy and, for a Te-vacancy, the number of bound states is equal to three.

The above results, which are different for a Pb-vacancy and a Te-vacancy, can be qualitatively explained using table 4.3. Valence band number 1 has a very large contribution coming from the Kohn-Luttinger function corresponding to Γ_6^+ ($^3\Gamma_1^+$) and, according to that table, the matrix element $\langle ^3\Gamma_1^+ | U(\vec{r}) | ^3\Gamma_1^+ \rangle$ is much larger for a Te-vacancy than for a Pb-vacancy. Valence band number 2, however, has a large contribution coming from Γ_6^+ ($^1\Gamma_1^+$) and $\langle ^1\Gamma_1^+ | U(\vec{r}) | ^1\Gamma_1^+ \rangle$ is much larger for a Pb-vacancy than a Te-vacancy. On the other hand, valence bands number 3, 4 and 5 have large contributions coming from Γ_6^- ($^1\Gamma_{15}$) and Γ_8^- ($^1\Gamma_{15}$) and $\langle ^1\Gamma_{15} | U(\vec{r}) | ^1\Gamma_{15} \rangle$ is much larger for a Te-vacancy than for a Pb-vacancy. Thus, we expect that, for valence band 1, 3, 4 and 5, the effect of the perturbation is stronger for a Te-vacancy than for a Pb-vacancy and, for valence band number 2, the opposite should occur. This is equivalent to saying that valence bands 1, 3, 4 and 5 have a large part of its charge density concentrated in the Te-sphere, while valence band 2 has its charge density in the Pb-sphere. This is in agreement with the LCAO or tight binding energy band calculation of PbTe performed by Schirf.⁵⁶

Finally, all the five valence bands and four conduction bands were considered together. For 13 sites the resulting symmetric and antisymmetric matrices have dimension 63 and 54, respectively. But, due to the fact that the valence bands number 1 and 2 and conduction band number 4 have a large contribution coming from the Γ_6^+ -levels and the other bands have a large contribution coming from the Γ_6^- and Γ_8^- -levels, these two groups can be considered separately. We are allowed to make this separation not only because the matrix elements $\langle \Gamma_6^+ | U(\vec{r}) | \Gamma_6^- \text{ or } \Gamma_8^- \rangle$ are smaller than $\langle \Gamma_6^+ | U(\vec{r}) | \Gamma_6^+ \rangle$ or $\langle \Gamma_6^- \text{ or } \Gamma_8^- | U(\vec{r}) | \Gamma_6^- \text{ or } \Gamma_8^- \rangle$ but also because they enter tensor \mathbb{N} which gives a second order contribution to the matrix element of U between Wannier functions.

When all bands are considered, we can only solve Eq. (4.28) for values of E outside the bands. This means that in the first group we look for solutions with energy between the top of valence band number 2 and bottom of conduction band number 4. In the second group, only energies in the gap can be considered. But, by investigating the dependence of the eigenvalues of the matrix $[G_{NN}^{-1} - U_{NN}]$ or energy E we can determine the number of states lying below and above a given energy E .

For the first group only one symmetric bound state was found at -0.43290Ry , for a Pb-vacancy, and at -0.23862Ry , for a Te-vacancy. In both cases, the effect of the interaction between the bands was to decrease the energy of the bound state obtained in the single band approximation, between the top of valence band 2 and bottom of

conduction band 4. This level, however, still lies well above the gap. For the second group, no bound state was found in the gap either for a Pb- or Te-vacancy. Comparing with the unperturbed case, no extra state appears or disappears above and below the gap, in the case of a Pb-vacancy, but, for a Te-vacancy, three extra states were found above the gap and, consequently, three states disappear below it.

If the results of the two groups are considered together, we conclude that both for a Pb- and a Te-vacancy no bound states are produced in the gap. For a Te-vacancy three states disappear below the energy gap and appear above it, while for a Pb-vacancy only one state disappears below the gap and appears above it.

A Pb-atom (configuration $6s^2 6p^2$) contributes 4 valence electrons, while a Te-atom (configuration $5s^2 5p^4$) contributes 6. If a Pb-vacancy is present in the crystal, then the perturbed crystal has 4 fewer electrons than the perfect crystal. But as only one state (which can accommodate two electrons) has moved from the valence to the conduction bands, there is still an empty state in the valence bands. Therefore, two holes are available in the valence band and we have a p-type semiconductor, in which the carriers can not be frozen out.

On the other hand, if a Te-vacancy exists, the perturbed crystal has 6 fewer electrons than the unperturbed crystal. But as four states have moved from the valence to the conduction bands, then there is one state filled in the conduction band, i.e., two

electrons are available there. An n-type semiconductor is produced and again the carriers cannot be frozen out. These results are shown schematically in figure 4.8.

It is interesting to note that the number of states pulled out the band depends on both the strength of the perturbation and on the shape of the energy bands. The first dependence is present in the U-matrix, while the second is present in the G-matrix. Because we are calculating the G-matrix using a Conroy's mesh of 1000 points a point corresponding to the top of the band probably does not occur in this mesh. Now, if we allow the energy to have values between the top of the band and the highest energy in the mesh, other bound states may occur, when more than one site is considered. This indeed happens in PbTe, for all valence bands both in the case of a Pb- and a Te-vacancy in a single band approximation. Let us consider, for example, valence band number 5. The top of the band occurs at L and corresponds to an energy E_{top} of -0.56395 Ry, while the maximum energy E_{max} in the mesh is -0.56218 Ry. When the energy was allowed to vary between these two values, 5 symmetric bound states and 3 antisymmetric bound states appeared very near E_{max} , in the case of a Pb-vacancy. For a Te-vacancy, 3 other symmetric bound states and 3 antisymmetric states were produced. The energies of these states are shown in Table 4.6.

When all bands were considered, these levels were shifted towards the E_{max} . For a Pb-vacancy, for example, the highest level is now at 3.5×10^{-5} instead of 1.037×10^{-3} in the single band

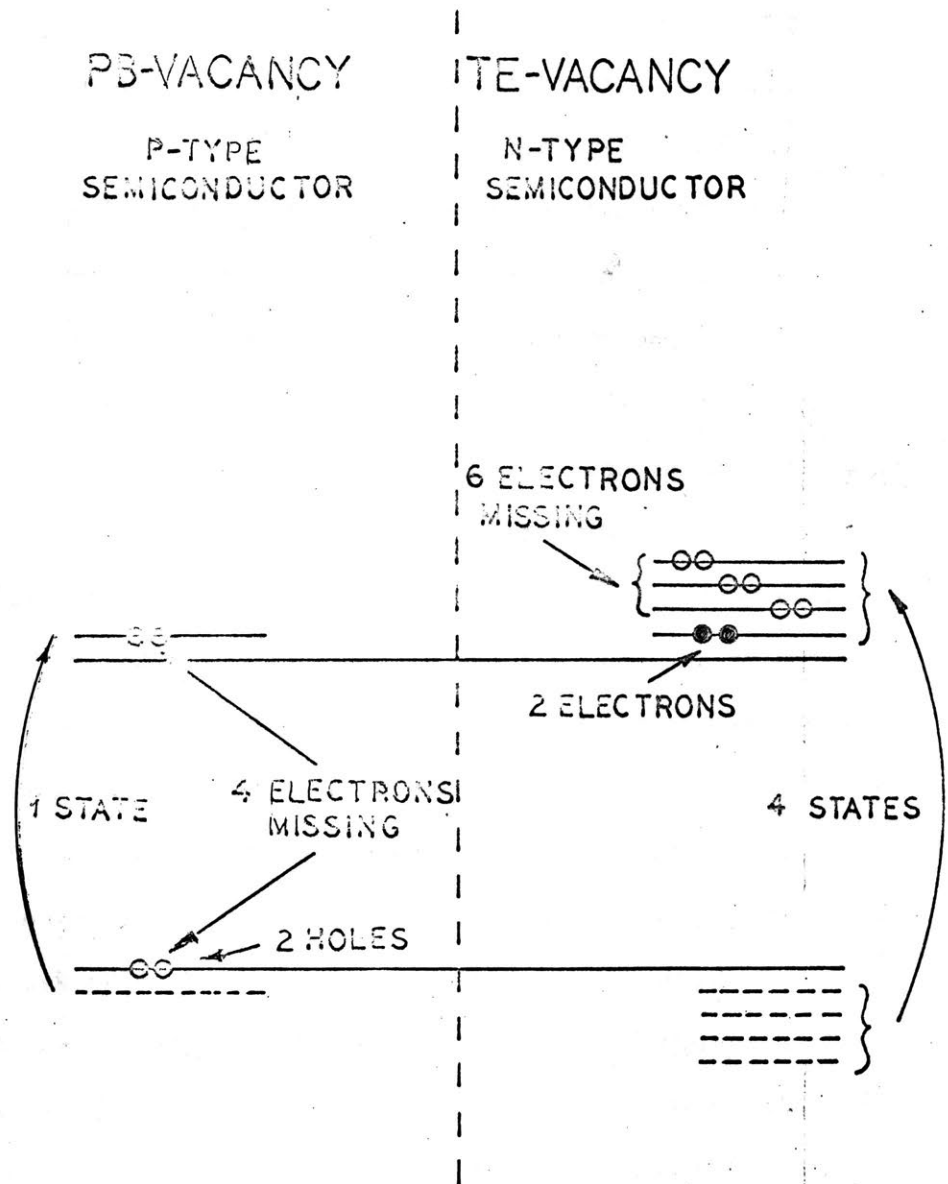


FIGURE 4.8 - Schematic representation of the effect of a Pb- and a Te-vacancy in PbTe.

TABLE 4.6 - Symmetric and antisymmetric states appearing between the top of valence band 5 ($E_{\text{top}} = -0.56395$ Ry) and the highest energy ($E_{\text{max}} = -0.56218$ Ry) in the Conroy's mesh of 1000 points corresponding to this band (single band approximation). The zero of energy in this table is taken at E_{max} .

Pb-vacancy		Te-vacancy	
Symmetric states (Ry)	Antisymmetric states (Ry)	Symmetric states (Ry)	Antisymmetric states (Ry)
0.2×10^{-5}	2.1×10^{-5}	0.8×10^{-5}	7.6×10^{-5}
1.2×10^{-5}	3.5×10^{-5}	9.27×10^{-4}	1.14×10^{-4}
4.0×10^{-5}	1.07×10^{-4}	1.572×10^{-3}	1.52×10^{-4}
6.0×10^{-5}			
1.037×10^{-3}			

approximation.

In order to decide whether these levels are bound states or not it is necessary to calculate the G -matrix for energies very near the top of the band using a very large mesh of points. However, we believe that these states are in the band because the comparison of the present mesh of 1000 points with the regular meshes of 152 and 916 points, which do include the top of the band, shows that the value obtained with Conroy's mesh is the convergent value. Even if some of these states are bound states, they are so close to the band that screening will be very important. But as the dielectric constant of PbTe is very large the effective perturbation potential will be much smaller than the potential we are using in the present calculation and, as a consequence, these states will be moved further towards the top of the band.

CHAPTER V

CONCLUSIONS

Two important results have been obtained in the preceding work. They are: the explanation of the effect of vacancies in PbTe from first principles and the calculation of the energy bands of that material using the $\vec{K} \cdot \vec{\pi}$ - APW scheme.

The vacancy problem is solved here using the method of Koster and Slater, which was used by Callaway and Hughes¹⁰ in the study of vacancies and divacancies in silicon. In the definition of the Wannier functions these authors considered non-degenerate non-relativistic bands and the regions of quasidegeneracies in k-space were disregarded in the calculations. Bloch functions for a particular band were chosen in such a way that their periodic part varied slowly in k-space. In this case, proper choices of the phase factors in the definition of the Wannier functions produces localized Wannier functions which transform like basis partners of the irreducible representations of the crystal point group. The U-matrix can be factored according to these representations thus decreasing the dimension of the secular equation to be diagonalized but the G-matrix, may not present the proper asymptotic behavior, for large values of the energy E.

In PbTe, however, relativistic corrections are very important and we have to deal with degenerate relativistic bands. Regions of quasidegeneracies are very important. They occur in a large part of the Brillouin zone, and cannot be disregarded. In PbTe therefore the

vacancy problem is somewhat different than in silicon. With the Bloch functions obtained by the $\vec{K} \cdot \vec{\pi}$ -APW calculation it is possible to choose phase factors in the definition of the Wannier functions in such a way as to produce localized functions. The bands were chosen in order of increasing energy and in this case proper G-matrices were obtained, but the U matrix can only be factored into two blocks, one for the even-parity representations and other for the odd-parity representations of the crystal point group. However as did Callaway and Hughes, we had to exclude from the definition of the Wannier functions symmetry points in k-space where degeneracies, other than spin or accidental occur, but we believe that the mesh of points used by us in the Brillouin zone contains all the peculiarities of the bands.

The results obtained here show that a Pb-vacancy produces a p-type material, while a Te-vacancy causes PbTe to be n-type and, in both cases, the carriers cannot be frozen out. Thus, if a Pb-vacancy is the major defect when excess tellurium is present in PbTe and if a Te-vacancy is the predominant defect when we have excess lead, the fact that a p-type material is produced in the first case and a n-type material in the second, with no carrier freeze-out in either case, can be well explained.

We have used 9 bands and 13 sites in our calculations and the energy convergence of the levels seems to be satisfactory. In the one-band approximation, the effect of considering more sites is to increase the energies of the levels already obtained, shifting them away from the bands. This increase, however, is not large and if

more sites are considered we expect the levels to be further shifted in the same direction, thus improving our results. Because all the bands that interact strongly with the five valence bands were taken into consideration, we expect that if more bands are considered, the results obtained will not differ much from ours, as far as the levels associated with the valence bands are concerned.

The one-electron energies and wave-functions used in the calculations were obtained by the $\vec{K} \cdot \vec{\pi}$ -APW method in a mesh of points in \vec{k} -space. In this method we start with the APW eigenvalues and eigenfunctions of the relativistic one electron Hamiltonian at Γ . The matrix elements of the operator $\vec{\pi}$ between the basis states at Γ are then used in the $\vec{K} \cdot \vec{\pi}$ secular equation to obtain the energies and wave-functions in a point \vec{k} of the Brillouin zone. For PbTe, we found that the relativistic contributions to $\vec{\pi}$ can be disregarded and only the matrix elements of momentum \vec{p} have to be considered. With 11 bands at Γ (corresponding to 30 partners) excellent results were obtained. It was necessary to change only one non-relativistic momentum matrix at Γ in order to fit the experimental gap at L and some experimental results, discussed at the end of Chapter III, can be well explained with these bands.

APPENDIX

MATRIX ELEMENT OF $U(\Delta\vec{k}, \vec{r}) = e^{i\Delta\vec{k} \cdot \vec{r}} U(\vec{r})$ BETWEEN NON-RELATIVISTIC BLOCH FUNCTIONS AT \vec{k}_0

The purpose of this Appendix is to derive an expression for the matrix element of the operator $U(\Delta\vec{k}, \vec{r}) = e^{i\Delta\vec{k} \cdot \vec{r}} U(\vec{r})$ between two non-relativistic Bloch functions. For simplicity we will use the notation

$$\langle b_{n,i}^{\Gamma_{\beta'}(\vec{k}_0)}(\vec{k}_0, \vec{r}) | U(\Delta\vec{k}, \vec{r}) | b_{n,i}^{\Gamma_{\beta}(\vec{k}_0)}(\vec{k}_0, \vec{r}) \rangle \quad (\text{A.1})$$

for the matrix element.

Since in the APW method, Bloch functions are expressed as linear combinations of symmetrized augmented plane waves we will have to calculate the matrix element of $U(\Delta\vec{k}, \vec{r})$ between two SAPW's, namely

$$\langle \psi_{n,i',j'}^{\Gamma_{\beta'}(\vec{k}_0)[\text{SAPW}]}(\vec{k}_i', \vec{r}) | U(\Delta\vec{k}, \vec{r}) | \psi_{n,i,j}^{\Gamma_{\beta}(\vec{k}_0)[\text{SAPW}]}(\vec{k}_i, \vec{r}) \rangle \quad (\text{A.2})$$

where $\vec{k}_i' = \vec{k}_0 + \vec{k}_i'$, $\vec{k}_i = \vec{k}_0 + \vec{k}_i$, \vec{k}_i' and \vec{k}_i being reciprocal lattice vectors, and j' and j are the column indices.

The group of the operator $U(\Delta\vec{k}, \vec{r})$ is the same as the group of $\Delta\vec{k}$, if $U(\vec{r})$ is assumed to have the symmetry of the group of \vec{k}_0 . In general, $U(\Delta\vec{k}, \vec{r})$ reduces* the group of the wave-vector \vec{k}_0 and breaks the representations of this group into sets of irreducible representations of the group of $U(\Delta\vec{k}, \vec{r})$. Observe that the representations $\Gamma_{\beta'}^{(\vec{k}_0)}$ and $\Gamma_{\beta}^{(\vec{k}_0)}$ might be different, since after reduction they might include equivalent irreducible representations of the group of $U(\Delta\vec{k}, \vec{r})$.

*The group of \vec{k}_0 has to be equal to or larger than the group of $U(\Delta\vec{k}, \vec{r})$.

But the basis used in the APW calculation might not be the proper basis for reduction, so that a unitary transformation is necessary before calculating the matrix elements. As Ferreira¹⁵ we reserve the name of transformed symmetrized augmented plane wave (TSAPW) for the new combination of APW's. Thus, in general we are interested in the calculation of

$$\begin{aligned}
 & \langle \psi_{n,i,j}^{\beta'}(\vec{k}_i, \vec{r}) | U(\Delta\vec{k}, \vec{r}) | \psi_{n,i,j}^{\beta}(\vec{k}_i, \vec{r}) \rangle \\
 &= \sum_{\alpha, \alpha'} \sum_{\ell, \ell'} V'_{i', \ell'}{}^* \Gamma_{\beta'}(\vec{k}_0)(\alpha')_{\ell', j'} V_{i, \ell} \Gamma_{\beta}(\vec{k}_0)(\alpha)_{\ell, j}^* \\
 & \times \langle \alpha' \psi^{\text{APW}}(\vec{k}_i, \vec{r}) | U(\Delta\vec{k}, \vec{r}) | \alpha \psi^{\text{APW}}(\vec{k}_i, \vec{r}) \rangle \tag{A.3}
 \end{aligned}$$

where V' and V are the unitary matrices and α and α' are operations of the group of \vec{k}_0 .

The expression for the matrix element of a general operator O between two TSAPW's is given by Ferreira¹⁵ and we present here the main steps in the calculation. It is important to mention that a TSAPW is not a SAPW made out of APW's and using the rotation matrices of the transformed basis, because the latter is

$$\sum_{\alpha} \sum_{\ell, m} V_{i, \ell} \Gamma_{\beta}(\vec{k}_0)(\alpha)_{\ell, m}^* V_{j, m}^* \alpha \psi^{\text{APW}}(\vec{k}_i, \vec{r})$$

while a TSAPW is

$$\sum_{\alpha} \sum_{\ell} V_{i, \ell} \Gamma_{\beta}(\vec{k}_0)(\alpha)_{\ell, j}^* \alpha \psi^{\text{APW}}(\vec{k}_i, \vec{r})$$

Any operation α' of the group of the wave-vector \vec{k}_0 can always

be written as $\gamma' \delta'$, where γ' is an operation of the subgroup that leaves $U(\Delta\vec{k}, \vec{r})$ invariant and δ' belongs to the Factor of the subgroup, which contains G/G_{sub} members, G and G_{sub} being the number of operations in the group of \vec{k}_0 and in the group of $U(\Delta\vec{k}, \vec{r})$, respectively. If we denote by $\Gamma_{\beta'}'(\vec{k}_0)$ and $\Gamma_{\beta}'(\vec{k}_0)$ the rotation matrices which are in the reduced form for the operations of the subgroup, i.e.,

$$\begin{aligned} \Gamma_{\beta'}'(\vec{k}_0) &= V^+ \Gamma_{\beta}(\vec{k}_0) V \text{ and } \Gamma_{\beta'}'(\vec{k}_0) = V'^+ \Gamma_{\beta'}(\vec{k}_0) V', \text{ then} \\ \sum_{\ell} V_{i,\ell} \Gamma_{\beta}(\vec{k}_0) (\alpha)_{\ell,j}^* &= \sum_q \Gamma_{\beta'}'(\vec{k}_0) (\alpha)_{i,q}^* V_{q,j} \\ \sum_{\ell'} V_{i',\ell'}^* \Gamma_{\beta'}(\vec{k}_0) (\alpha')_{\ell',j'} &= \sum_q \Gamma_{\beta'}(\vec{k}_0) (\alpha')_{i',q} V_{q,j'}^* \end{aligned} \quad (\text{A.4})$$

and since γ' commutes with $U(\Delta\vec{k}, \vec{r})$

$$\begin{aligned} &\langle \psi_{n,i',j'}^{\Gamma_{\beta'}'(\vec{k}_0)}[\text{TSAPW}] | U(\Delta\vec{k}, \vec{r}) | \psi_{n,i,j}^{\Gamma_{\beta}(\vec{k}_0)}[\text{TSAPW}] \rangle \\ &= \sum_{\gamma', \lambda} \sum_{q,q'} \sum_{\ell,\ell'} V_{q',j'}^* V_{q,j} [\sum_{\delta'} \Gamma_{\beta'}'(\vec{k}_0) (\delta')_{i',\ell'} \Gamma_{\beta}(\vec{k}_0) (\delta')_{i,\ell}^*] \\ &\times \Gamma_{\beta'}(\vec{k}_0) (\gamma')_{\ell',q'} \Gamma_{\beta}(\vec{k}_0) (\lambda)_{\ell,q}^* \langle \gamma' \psi^{\text{APW}}(\vec{k}_1', \vec{r}) | U(\Delta\vec{k}, \vec{r}) | \lambda \psi^{\text{APW}}(\vec{k}_1, \vec{r}) \rangle \end{aligned} \quad (\text{A.5})$$

where $\lambda = \delta'^{-1} \alpha$. The sum in δ' in Eq. (A.5) can be performed and a non-zero result is obtained only if

- a) the representations of the subgroup to which i' belongs are the same as the representation of the subgroup to which i belongs;
- b) the partner numbers of the irreducible representation of the subgroup to which the i' -th partner of $\Gamma_{\beta'}(\vec{k}_0)$ and the i -th partner of $\Gamma_{\beta}(\vec{k}_0)$ go are equivalent,

- c) the representations of the subgroup to which i' belongs is the same as the representation of the subgroup to which ℓ' belongs;
- d) the representation of the subgroup to which i belongs is the same as the representation of the subgroup to which ℓ belongs;
- e) the partner numbers of the irreducible representation of the subgroup to which the ℓ' -th partner of $\Gamma_{\beta}(\vec{k}_0)$ and the ℓ -th partner of $\Gamma_{\beta}(\vec{k}_0)$ go are equivalent.

If all the above conditions are satisfied the result of the sum on δ' is equal to G_{sub}/n_i , where n_i is the dimension of the common representation. Thus, we have to derive an expression for the matrix element of the operator $U(\Delta\vec{k}, \vec{r})$ between two APW's, i.e.

$$\langle \psi^{\text{APW}}(\vec{k}_i, \vec{r}) | U(\Delta\vec{k}, \vec{r}) | \psi^{\text{APW}}(\vec{k}_j, \vec{r}) \rangle \quad (\text{A.6})$$

But, in a sphere located at r_0 and having radius R

$$\begin{aligned} \psi^{\text{APW}}(\vec{k}_i, \vec{r}) = e^{i\vec{k}_i \cdot \vec{r}_0} & 4\pi \sum_{\ell_i=0}^{\infty} \sum_{m_i=-\ell_i}^{\ell_i} i^{\ell_i} \frac{j_{\ell_i}(k_i R)}{u_{\ell_i, E_i}(R)} u_{\ell_i, E_i}(r') \\ & \times Y_{\ell_i}^{m_i}(\theta'_{k_i}, \phi'_{k_i})^* Y_{\ell_i}^{m_i}(\theta', \phi') \end{aligned} \quad (\text{A.7})$$

A similar expression can be written for $\psi^{\text{APW}}(\vec{k}_j, \vec{r})$, and if the plane wave $e^{i\Delta\vec{k} \cdot \vec{r}}$ in $U(\Delta\vec{k}, \vec{r})$ is expressed in terms of spherical harmonics,

i.e., by

$$e^{i\Delta\vec{k} \cdot \vec{r}} = e^{i\Delta\vec{k} \cdot \vec{r}_0} 4\pi \sum_{\ell=0}^{\infty} \sum_{m=-\ell}^{\ell} i^{\ell} j_{\ell}(\Delta k r') Y_{\ell}^m(\theta'_{\Delta k}, \phi'_{\Delta k})^* Y_{\ell}^m(\theta', \phi') \quad (\text{A.8})$$

Eq. (A.6) can be written as

$$\begin{aligned}
 \langle \psi^{APW}(\vec{k}_i, \vec{r}) | U(\Delta\vec{k}, \vec{r}) | \psi^{APW}(\vec{k}_j, \vec{r}) \rangle &= e^{i\Delta\vec{k} \cdot \vec{r}} \sum_{\ell=0}^{\infty} \sum_{\ell_j=0}^{\infty} \sum_{\ell_i=|\ell-\ell_j|}^{\ell+\ell_j} \sum_{m'=-\ell_i}^{\ell_j} \\
 &\times (-)^{(L-\ell_i)} \frac{j_{\ell_i}(k_i R) j_{\ell_j}(k_j R)}{u_{\ell_i, E_i}(R) u_{\ell_j, E_j}(R)} \left[\int_0^R j_{\ell}(\Delta k r') u_{\ell_i, E_i}(r') u_{\ell_j, E_j}(r') \right. \\
 &\times r'^2 U(r') dr' \left. \right] (4\pi)^2 (2\ell+1) \left[\frac{2\ell_i+1}{2\ell_i+1} \right]^{1/2} Y_{\ell_i}^m(\theta'_{k_i}, \phi'_{k_i}) Y_{\ell_j}^{m'}(\theta'_{k_j}, \phi'_{k_j})^* \\
 &\times C(\ell \ell_j \ell_i ; 0 m' m') C(\ell \ell_j \ell_i ; 0 0 0) \tag{A.9}
 \end{aligned}$$

where $\ell_{ij}^<$ means the smallest between ℓ_i and ℓ_j and the C's are Clebsch-Gordon coefficients, which, in the Racah closed expression,

are given by

$$\begin{aligned}
 C(\ell \ell_j \ell_i ; 0 m' m') &= [(2\ell_i+1) \frac{(\ell+\ell_j-\ell_i)! (\ell_i+\ell-\ell_j)! (\ell_i+\ell_j-\ell)!}{(\ell+\ell_i+\ell_j+1)!} \\
 &\times (\ell)! (\ell)! (\ell_i-m')! (\ell_i+m')! (\ell_j-m')! (\ell_j+m')!]^{1/2} \\
 &\times \sum_{\nu} \frac{(-)^{\nu} \nu! (\ell+\ell_j-\ell_i-\nu)! (\ell-\nu)! (\ell_j+m'-\nu)! (\ell_i-\ell_j+\nu)! (\ell_i-\ell-m'+\nu)!}{\nu! (\ell+\ell_j-\ell_i-\nu)! (\ell-\nu)! (\ell_j+m'-\nu)! (\ell_i-\ell_j+\nu)! (\ell_i-\ell-m'+\nu)!} \tag{A.10}
 \end{aligned}$$

and

$$\begin{aligned}
 C(\ell \ell_j \ell_i ; 0 0 0) &= (-)^{\frac{\ell+\ell_j-\ell_i}{2}} \frac{L! (2\ell_i+1)^{1/2}}{(L-\ell)! (L-\ell_i)! (L-\ell_j)!} \\
 &\times \left[\frac{(\ell+\ell_j-\ell_i)! (\ell+\ell_i-\ell_j)! (\ell_i+\ell_j-\ell)!}{(\ell+\ell_i+\ell_j+1)!} \right]^{1/2} \tag{A.11}
 \end{aligned}$$

and in all these expressions $(\ell_i+\ell_j+\ell)$ must be equal to $2L$, where L is an integer.

When deriving Eq. (A.9) we made use of the following facts:

$$\begin{aligned}
 a) \int d\Omega' Y_{\ell_i}^{m_i}(\theta', \phi')^* Y_{\ell_j}^{m_j}(\theta', \phi') Y_{\ell}^m(\theta', \phi') \\
 = \left[\frac{(2\ell+1) (2\ell_j+1)}{4\pi(2\ell_i+1)} \right]^{1/2} C(\ell \ell_j \ell_i ; m_j m_i) C(\ell \ell_j \ell_i ; 0 0 0)
 \end{aligned}$$

b) that we must have $m_i = m + m_j$ and $l + l_i + l_j = 2L$, where L is an integer, in order for the Clebsh-Gordon coefficients to be different from zero.

c) the primed system of coordinates (inside the APW sphere) is chosen such that $\vec{\Delta k}$ is in the z' -direction. In this case $\theta'_{\Delta k} = 0$ and $\phi'_{\Delta k} = 0$ and $Y_l^m(\theta'_{\Delta k}; \phi'_{\Delta k})^* = \left[\frac{(2l+1)}{4\pi} \right]^{1/2} \delta_{m,0}$.

d) from b) and c) we obtain that $m=0$ and $m_i = m_j = m'$.

e) from the expressions (A.10) and (A.11) for the Clebsh Gordon coefficients we observe that

$$m' \leq l_i$$

$$m' \leq l_j$$

and if $l_{ij}^<$ means the smallest between l_i and l_j , then m' can only have values between $-l_{ij}^<$ and $+l_{ij}^<$; also

$$l \leq l_i + l_j$$

$$l_i \leq l + l_j$$

$$l_j \leq l + l_i$$

and then l_i can only have values between $|l - l_j|$ and $(l + l_j)$.

f) we have assumed that the potential $U(\vec{r})$ is spherically symmetric inside the APW sphere.

The sum on m' in Eq. (A.9) can also be written as

$$\sum_{m'=-l_{ij}^<}^{l_{ij}^<} Y_{l_i}^{m'}(\theta'_{k_i}, \phi'_{k_i}) Y_l^{m'}(\theta'_{k_j}, \phi'_{k_j})^* C(l, l_j, l_i; 0, m', m') C(l, l_j, l_i; 0, 0, 0)$$

$$= \sum_{m'=0}^{l_{ij}} \left[\frac{(2l_i+1)(2l_j+1)}{(4\pi)^2} \frac{(l_i-m')!(l_j-m')!}{(l_i+m')!(l_j+m')!} \right]^{1/2}$$

$$\begin{aligned}
 & \times P_{\ell_i}^{m'}(\cos\theta'_{k_i}) P_{\ell_j}^{m'}(\cos\theta'_{k_j}) C(\ell \ell_j \ell_i; 0 m' m') C(\ell \ell_j \ell_i; 0 0 0) \\
 & \times \begin{cases} 2 \cos [m'(\phi'_{k_j} - \phi'_{k_i})] & \text{for } m' > 0 \\ 1 & \text{for } m' = 0 \end{cases} \quad (A.12)
 \end{aligned}$$

Eq. (A.12) can easily be obtained if we expand the spherical harmonics in terms of the Legendre polynomials, i.e.,

$$Y_{\ell}^m(\theta', \phi') = (-)^m \left[\frac{(2\ell+1)}{4\pi} \frac{(\ell-m)!}{(\ell+m)!} \right]^{1/2} P_{\ell}^m(\cos\theta') e^{im\phi'} \quad \text{for } m > 0$$

$$Y_{\ell}^m(\theta', \phi') = (-)^m Y_{\ell}^{-m}(\theta', \phi')^* \quad \text{for } m < 0$$

and observe that

$$C(\ell \ell_j \ell_i; 0 -m' -m') = C(\ell \ell_j \ell_i; 0 m m)$$

Finally, if expressions (A.9) and (A.12) are used in Eq. (A.5)

we obtain

$$\begin{aligned}
 & \langle \psi_{n,i,j}^{\Gamma \beta'}(\vec{k}_i, \vec{r}) | U(\Delta\vec{k}, \vec{r}) | \psi_{n,i,j}^{\Gamma \beta}(\vec{k}_i, \vec{r}) \rangle \\
 & = \sum_{\ell=0}^{\infty} \sum_{\ell_i=1}^{\infty} \sum_{\ell_i'=|\ell-\ell_i|}^{\ell+\ell_i} I(\ell, \ell_i, \ell_i' | |\Delta\vec{k}|) F(\ell, \ell_i, \ell_i') H(\ell, \ell_i, \ell_i', \Delta\vec{k}) \quad (A.13)
 \end{aligned}$$

where

1) the radial integral $I(\ell, \ell_i, \ell_i' | |\Delta\vec{k}|)$ depends on $U(\vec{r})$ and $|\Delta\vec{k}|$ and is given by

$$\begin{aligned}
 I(\ell, \ell_i, \ell_i' | |\Delta\vec{k}|) & = \frac{1}{u_{\ell_i, E_i}(\ell, R) u_{\ell_i', E_i'}(\ell, R)} \left[\int_0^R dr' j_{\ell}(|\Delta\vec{k}| r') U(r') r'^2 \right. \\
 & \left. \times u_{\ell_i, E_i}(r') u_{\ell_i', E_i'}(r') \right]
 \end{aligned}$$

2) the function $F(\ell, \ell_1, \ell_1')$ does not depend on $U(\vec{r})$ or $\Delta\vec{k}$ and is given by

$$F(\ell, \ell_1, \ell_1') = (2\ell+1)(2\ell_1+1)(2\ell_1'+1) \frac{L!}{(L-\ell)!(L-\ell_1)!(L-\ell_1')!}$$

$$\times \frac{(\ell+\ell_1'-\ell_1)!(\ell+\ell_1-\ell_1')!(\ell_1+\ell_1'-\ell)!}{(\ell+\ell_1+\ell_1'+1)!}$$

3) the function $H(\ell, \ell_1, \ell_1')$ depends on the group of the operator $U(\Delta\vec{k}, \vec{r})$

$$H(\ell, \ell_1, \ell_1', \Delta\vec{k}) = \ell! 4\pi \sum_{m'=0}^{\ell_1} \sum_{j=0}^{\ell_1} (\ell_1'-m')!(\ell_1-m')! \sum_{\nu} \frac{(-)^{\nu}}{\nu!} [(\ell+\ell_1-\ell_1'-\nu)!]$$

$$\times (\ell-\nu)!(\ell_1+m'-\nu)!(\ell_1'-\ell_1+\nu)!(\ell_1'-\ell-m'+\nu)!]^{-1} j_{\ell_1'}(k_1'R)$$

$$\times j_{\ell_1}(k_1'R) \sum_{L_1, L_1'} \sum_{\gamma, \lambda} \frac{G_{\text{sub}}}{n_1} [U'^* \Gamma_{\beta'}^{(\vec{k}_0)}(\gamma')]_{L_1', j'}$$

$$\times [U \Gamma_{\beta}^{(\vec{k}_0)}(\lambda)]_{L_1, j} P_{\ell_1'}^{m'}(\cos\theta'_{\gamma, \vec{k}_1'}) P_{\ell_1}^{m'}(\cos\theta'_{\lambda, \vec{k}_1'}) e^{i(\lambda\vec{k}_1 - \gamma'\vec{k}_1') \cdot \vec{r}_0}$$

$$\times \begin{cases} 2 \cos [m'(\phi'_{\gamma, \vec{k}_1'} - \phi'_{\lambda, \vec{k}_1'})] & \text{for } m' > 0 \\ 1 & \text{for } m' = 0 \end{cases}$$

where $U(\vec{r})$ has the symmetry of the group of \vec{k}_0 , then $H(\ell, \ell_1, \ell_1', \Delta\vec{k})$ depends only on the group of $\Delta\vec{k}$.

BIBLIOGRAPHY

1. G.F. Koster and J.C. Slater, "Wave Functions for Impurity Levels", Phys. Rev. 95, 1167(1954);
Also, "Simplified Impurity Calculation", Phys. Rev. 96, 1208(1954).
2. Pearson, Handbook of Lattice Spacings and Structures of Metals and Alloys, (pergamon Press, 1958).
3. W.W. Scanlon, "Recent Advances in the Optical and Electronic Properties of PbS, PbSe, PbTe and their Alloys", J. Phys. Chem. Solids 8, 423 (1959).
4. V. Prakash, "The Optical Absorption Edge in the Lead Salts and its Variation with Temperature and Pressure", Ph.D. Thesis, Harvard Univ. (1967); and Div. Eng. and Appl. Phys. Tech. Rep. HP-13.
5. K.F. Cuff, M.R. Ellett, and C.D. Kuglin, "Band Structure and Transport Properties of PbTe", Proc. Intern. Conf. on Phys. of Semic., Exeter, 1962 (Inst. Phys. and Phys. Soc. London, 1962), p. 316.
Also, "Oscillatory Magnetoresistance in the Conduction Band of PbTe", J. Appl. Phys. Suppl. 32, 2179 (1961).
6. M.B. Seltzer and J.B. Wagner, Jr., "Self Diffusion of Lead-210 in Single Crystals of Lead Selenide", J. Chem. Phys. 36, 130 (1962).
7. H. Gobrecht and A. Richter, "Density Measurement and Disorder of Lead Selenide", J. Phys. Chem. Solids 26, 1889 (1965).
8. M.B. Seltzer and J.B. Wagner, Jr., "Diffusion in Lead Sulfide at 700°C", J. Phys. Chem. Solids 24, 1525 (1963).
9. A.J. Crocker, "The Role of Sodium in Lead Telluride", J. Phys. Chem. Solids 28, 1903 (1967).
10. J. Callaway and A.J. Hughes, "Localized Defects in Semiconductors", Phys. Rev. 156, 860 (1967);
Also, "Localized Defects in Semiconductors: The Divacancy in Silicon", Phys. Rev. 164, 1043 (1967).
11. For a review on impurities in metals see Chapter IV.
12. J.B. Conklin, Jr., "Relativistic Effects in Lead Telluride", Ph.D. Thesis, E. E. Dept. MIT (1964);
Also, J.B. Conklin, Jr., L.E. Johnson and G.W. Pratt, Jr., "Energy Bands in PbTe", Phys. Rev. 137, A1282 (1965).

13. P.J. Lin and L. Kleinman, "Energy Bands of PbTe, PbSe and PbS", Phys. Rev. 142, 478 (1966).
14. G.W. Pratt, Jr. and L.G. Ferreira, "Relativistic Effects and $\vec{K}\cdot\vec{P}$ Analysis of the Band Structure of PbTe", Proc. Int. Conf. on Phys. of Semic., Paris, 1964 (Academic Press, N.Y., 1965), p. 69.
15. L.G. Ferreira, "Calculation of Electronic Properties of Strained Lead Telluride", Ph.D. Thesis, E.E. Dept. MIT (1964); Also, "Deformation Potentials of Lead Telluride", Phys. Rev. 137 A1601 (1965).
16. G.W. Pratt, Jr. and N.J. Parada, "Interband Momentum Matrix Elements and a $\vec{K}\cdot\vec{P}$ -Interpolation Method Applied to PbTe", Intern. J. of Quant. Chem. I S, 589 (1967).
17. M. Cardona and F.H. Pollack, "Energy-Band Structure of Germanium and Silicon: the $\vec{K}\cdot\vec{P}$ Method", Phys. Rev. 142, 530 (1966).
18. F. Herman, "Recent Progress in Energy Band Theory", Proc. Int. Conf. on the Phys. Semic., Paris, 1964 (Academic Press, N.Y., 1965) p.3.
19. D. Brust, "Electronic Spectra of Crystalline Germanium and Silicon", Phys. Rev. 134, A1337 (1964).
20. L.L. Foldy and S.A. Wouthuysen, "On the Dirac Theory of Spin 1/2 Particles and Its Non-Relativistic Limit", Phys. Rev. 78 29 (1950).
21. T.L. Loucks, "Relativistic Electronic Structure in Crystals I. Theory", Phys. Rev. 139, A1333 (1965).
22. J.M. Luttinger and W.Kohn, "Motion of Electrons and Holes in Perturbed Periodic Fields", Phys. Rev. 97, 869 (1955).
23. L.M. Roth "g-Factor and Donor Spin-Lattice Relaxation for Electrons in Germanium and Silicon", Phys. Rev. 118, 1534 (1960).
24. J.Callaway, "Transformation Properties of Bloch Functions", Phys. Let. 26A, 114 (1968).
25. See, for example, J.S. Lomont, Applications of Finite Groups, (Academic Press Inc., N.Y., 1960).
26. See, for example, G.F. Koster, Space Groups and Their Representations, Solid State Phys., ed. F.Seitz and D. Turnbull (Academic Press, N.Y., 1957).

27. D.D. Buss, "Characterization of the Lattice Vibration Spectrum in PbTe", Ph.D. Thesis, E.E. Dept., MIT (1968).
28. M.Cardona and D.L. Greenaway, "Optical Properties and Band Structure of Group IV-VI and Group V Materials", Phys. Rev. 133, A1685 (1964).
29. E.N. Adams, "Motion of an Electron in a Perturbed Periodic Potential", Phys. Rev. 85, 41 (1952).
Also, "The Crystal Momentum as a Quantum Mechanical Operator", J. Chem. Phys. 21, 2013 (1953).
30. G. Wannier, Elements of Solid State Theory, Cambridge Univ. Press, Cambridge, 1959.
31. G.E. Kilby, "A Variational Approach to the Study of Strongly Bound Impurity States in Crystals", Proc. Phys. Soc. 90, 181 (1967).
32. G.F. Koster, "Theory of Scattering in Solids", Phys. Rev. 95, 1436 (1954).
33. J. Callaway, "Theory of Scattering in Solids", J. Math. Phys. 5, 783 (1964).
34. J. Friedel, "Metallic Alloys", Suppl. Nuovo Cimento 7, 287 (1958).
35. P.W. Anderson, "Localized Magnetic States in Metals", Phys. Rev. 124, 41 (1961).
36. P.A. Wolff, "Localized Moments in Metals", Phys. Rev. 124, 1030 (1961).
37. A.M. Clogston, "Impurity States in Metals", Phys. Rev. 125, 439 (1962).
38. A.M. Clogston, B.T. Matthias, M. Peter, H.J. Williams, E. Corenzwit, and R.C. Sherwood, "Local Magnetic Moments Associated with an Ion Atom Dissolved in Various Transition Metal Alloys", Phys. Rev. 125, 541 (1962).
39. A.M. Clogston, "Impurity States in Transition Metals", Phys. Rev. 136, A1417, (1964).
40. J. Sokoloff, "Electronic States of Magnetic Impurities in Non-Magnetic Metals", Phys. Rev. 161, 540 (1967).
41. See the review article by W.Kohn, "Shallow Impurity States in Silicon and Germanium", Solid State Phys., 5, 257 (1957).

42. W.Kohn, "Effective Mass Theory in Solids from a Many-Particle Standpoint", Phys. Rev. 105, 509 (1957).
Also, "Interaction of Charged Particles in a Dielectric", Phys. Rev. 110, 857 (1958).
43. G. Dresselhaus, "Effective Mass Approximation for Excitons", J. Phys. Chem. Solids 1, 14 (1956).
44. W. Kohn and J.M. Luttinger, "Theory of Donor States in Si", Phys. Rev. 98, 915 (1955).
45. H. Brooks, "Theory of the Electrical Properties of Ge and Si", Advan. Electronics Electron Phys. 7, 85 (1955).
46. L.J. Sham, "Theory of Shallow Impurities in Semiconductors", Phys. Rev. 150, 720 (1966).
47. J. Frenkel, "On the Transformation of Light into Heat in Solids I", Phys. Rev. 37, 17 (1931).
Also, "On the Transformation of Light into Heat in Solids II", Phys. Rev. 37, 1276 (1931).
48. For a list of references see reference 50.
49. G. Baldini, "Ultraviolet Absorption of Solid Argon, Krypton and Xenon", Phys. Rev. 128, 1562 (1962).
50. J. Hermanson and J.C. Phillips, "Pseudopotential Theory of Exciton and Impurity States", Phys. Rev. 150, 652 (1966).
51. J. Hermanson, "Exciton and Impurity States in Rare-Gas Solids", Phys. Rev. 150, 660 (1966).
52. K.H. Johnson, "Molecular Model for the Localized Electronic Structure of Imperfections in Crystals", Prog. Rep. Solid State and Molecular Theory Group, MIT, 67, 17 (1968).
53. K.H. Johnson, "Multiple-Scattering Model for Polyatomic Molecules", J. Chem. Phys. 45, 3085 (1966).
54. K.H. Johnson, "Scattering Model for the Bound Electronic States of an Impurity Complex in a Crystal", Int. J. Quantum Chem. (in press).
55. F. Herman and S. Skillman, Atomic Structure Calculations, (Prentice Hall, Inc. Englewood Cliffs, N.J., 1963).
56. V. Schirf, "Band Structure and Density of States of PbTe", M.S., Thesis, E.E. Dept. MIT, (1966).
57. Metallic Solid Solutions, edited by J. Friedel and A. Guinier (W.A. Benjamin, Inc. N.Y., 1963).

BIOGRAPHICAL NOTE

The author was born in August 5, 1939, in Campinas, Brazil, where he graduated from Colegio Estadual Culto a Cienica, in 1958. In March 1959, he entered Instituto Tecnologico de Aeronautica, Sao Jose dos Campos, Brazil, where he received S.B. degree "cum lauda", in December, 1963, and M.S. degree in August, 1965, both in Electrical Engineering. The following September, he entered Massachusetts Institute of Technology, where he has been a graduate student in the Department of Electrical Engineering.

The author has taught one year and a half at Instituto Tecnologico de Aeronautica, Brazil, and has been a research assistant at Massachusetts Institute of Technology, after receiving scholarship from Conselho Nacional de Pesquisas, Brazil.